UNIVERSITÀ DEGLI STUDI FIRENZE

Dottorato di Ricerca in Scienze Biomediche

Ciclo XXVIII

Coordinatore Prof. Persio dello Sbarba

Novel strategies to overcome Cisplatin resistance in colorectal cancer.

Settore Scientifico Disciplinare: MED/04

Tutor: Prof.ssa Annarosa Arcangeli **Dottorando: Dr. Gianluca Bartoli**

_____ _____

Coordinatore: Prof. Persio Dello Sbarba

_____

Anni 2012/2015

INDEX

1. INTRODUCTION

1.1 Chemotherapy and chemoresistance

1.1.1 Chemotherapeutic drugs

Chemotherapeutic drugs are antineoplastic drugs given with the purpose of inhibiting tumor proliferation. Clinical experience has shown that in many cases the use of a single agent for the treatment of cancer does not provide long-term responses (He et al,.2015). Many improvements in cancer therapy have risen from the use of drug combinations, where the inhibition of parallel pathways with non-cross-resistant drugs improves treatment efficacy and reduces the occurrence of drug resistance (Bozic et al,.2013).

1.1.2 Chemoresistance

Tumor resistance to chemotherapy is a complex clinical problem, hard to resolve for the intrinsic properties which define it. Innate or acquired resistance is a multi-factorial event which leads to the failure of various therapeutic approaches. Administration of a chemotherapeutic drug can be seen, in darwinian model of population study, as an artificial selection which acts on a group of heterogeneous, both in terms of genotype and phenotype, neoplastic clones (Gerlinger and Swanton. 2010). Some of them can be selected by pharmacological treatment, survive and produce a new tumoral mass not-responsive to the therapy. There are many factors which can modulate chemotherapy sensibility, such as (1) the actual drug quantity which can reach the tumour mass, (2) a decrease of the levels of drug for improving excretion and/or reduction of cell membrane permeability, (3) possible inactivation or modification by

detoxification enzymes (at cellular, hepatic and kidney level), (4) target alteration in terms of its metabolic pathway and/or tumour microenvironment (Figure I).

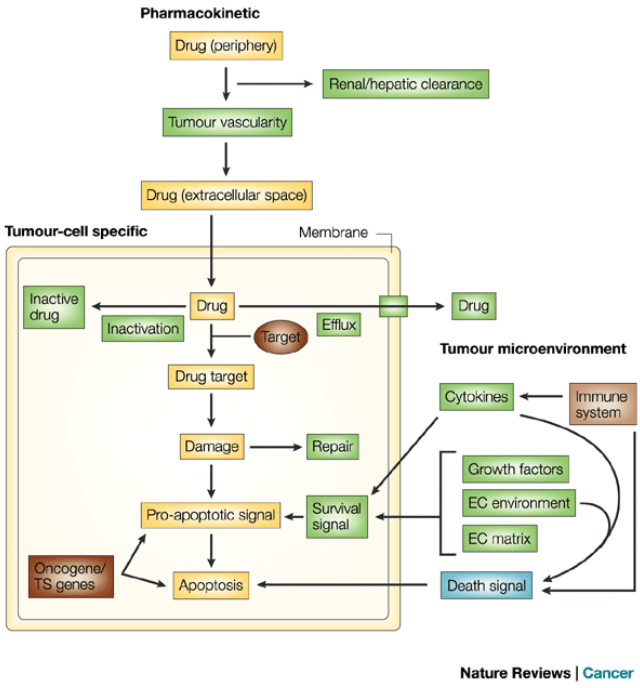

Figure I. Drug metabolism in cancer cells

1.1.2.1 Alterations of membrane mechanism of transports

One of the critical elements for a drug to be effective is its ability to reach the target organ at an efficacious concentration. The dynamic interactions among drug absorption, distribution, metabolism and excretion determine the plasma concentration of a drug, and dictate the amount of free drug that reaches the target site, and therefore, influence the ultimate outcome the drug may provide. Normal tissue morphology is altered in cancer tissues, limiting drug penetration and accumulation (Marcucci et al,. 2013). In the majority of cancers, vessel growth is not

only stimulated, but these vessels are also abnormal in almost all aspects of their structure and function (Shi et al,. 2013). This results in a hostile tumor microenvironment, characterized by hypoxia, low pH and high interstitial hostile fluid pressure that can alter the intrinsic characteristics of tumor cells and lead to selection of more malignant clones (Jain. 2005). Abnormal tumor vessels can also impede the function of immune cells in tumors, as well as the transport and/or distribution of chemotherapeutics and oxygen. As a result, the abnormal tumor vasculature can lead to a resistance of tumor cells to radiation therapy and many chemotherapeutics.

One of the main forms of resistance against chemotherapeutic drugs is carried out, at a cellular level, by plasma membrane; given their lipophilicity, many drugs enter the cell by passive diffusion and the slow kinetics of this mechanism of transport is a first obstacle to the reach of their intended target. There are also active extrusion mechanisms, mediated by specific families of proteins, which limit the accumulation of a drug inside the cell. Among these there are ABC (ATP-binding cassette) transmembrane proteins, which carry out this efflux against gradient of concentration. There are seven subfamilies of codifying genes for ABCs: ABC1, MDR/TAP, MRP, ALD, OABP, GCN20, White. The members of these subfamilies, as P-glycoprotein, codified by MDR1 (multidrug resistance 1) gene (Hodges et al,. 2011) are involved in the extrusion of many kind of drugs as: etoposide, doxorubicin, vinblastine. An overexpression of P-glycoprotein can lead to chemoresistance by a decrease of concentration of drug at intracellular level (Videira et al. 2014). The mechanism of action of this class of transporters is duplex, they are both associated to an ATP-mediated extrusion of drug molecules from cells into biological fluids and, controlling ion balancing in kidney tissue, in the excretion of drugs from the body (Videira et al. 2014).

Another class of extrusion proteins, involved in the excretion of chemotherapeutic drugs is MATE (Multidrug And Toxic Compound Extrusion) family. There were originally discovered in bacteria, where they mediate antibiotic resistance, but there were recently found human variants involved in the transport of numerous xenobiotic molecules, including several chemotherapy agents (Kuroda et Tsuchiya. 2009).

1.1.2.2 Drug inactivation

Mechanisms which inactivate a drug limit the active quantity that can actually bind to its intracellular target. At hepatic level the presence of several families of cytochrome proteins plays a crucial role, in particular P-450 family. These classes of proteins metabolize drugs usually by inserting an atom of oxygen on the non-activated carbon atoms by hydrolysis, oxidation and reduction. At the end of these modifications the drug molecule is often conjugated to glutathione, sulphates, glycine or glucuronic acid and excreted from the organism with one of the already described transporters.

Platinum based drugs bind covalently to GSH and the resulting complex is extruded form the cell by ABC proteins (Liu et al,. 2012). High levels of GSH have been found in Cisplatin-resistant tumor cells and its variation during passage of time after exposure is also significant (Jamali et al,. 2015). This process of conjugation is catalyzed by the family of glutathione-S-transferase enzymes and an increase in the expression of certain their subtypes has been correlated with Cisplatin resistance in ovarian cancer (Sawers et al,. 2014).

1.1.2.3 Modification of drug targets

It’s possible that during therapy the original target of a chemotherapeutic drug can undergo several modifications or a reduction of its expression level, so to be no longer a useful target to block tumor development. For example, tamoxifen, an estrogen inhibitor used for the treatment of breast cancer, can be inactivated by a reduction of estrogen receptors expression; beside that several tumoral clones can also become completely homone-independent for their development and invasiveness (Jiang et al,. 2013).

Another characteristic which can induce chemoresistance is the genetic instability of tumoral clones that lead to an accumulation of genetic mutations; this can alter the native structure of an oncogene or a tumor suppressor gene, inhibiting the actions of chemotherapeutic drugs if these mutations modify their target sequence. In CRC the occurrence of tumor somatic mutations in the RAS/RAF/MAPK and PI3K/PTEN/AKT pathways remains the main challenge for treatment with the new biological agents. It has been recently proposed to consider a quadruple negative profile for CRC, based on the status of KRAS, BRAF, PI3KCA and PTEN, as tumor markers of sensitivity to anti-EGFR treatment (De Mattia et al,. 2015).

Genetic instability may lead to the loss of an entire gene, a chromosome or to genomic alterations; this can induce acquired resistance not only for the disappearance of therapeutic targets but also because these processes can produce a chromosomic reshuffle capable of altering metabolic pathways and targets of other drugs as well (Kuznetsova et al,. 2015).

1.1.2.4 DNA-damage repair

The DNA-damage repair capability of a tumoral cell is strictly linked to its resistance towards those chemotherapeutic drugs which have DNA as main target of their action. Following DNA-damage, a cell can proceed to its repair or, if it's too severe and/or not repairable, to induce the activation of apoptosis.

There are specific mechanisms to arrest cell cycle until the damaged is repaired, among which there are the nucleotide excision repair (NER), which removes the adducts DNA-drug and the mismatch repair (MMR), which check the new DNA strands and remove single mismatch bases inserted during DNA replication.

NER is a mechanism which involves 17 different proteins among which is ERCC1; ERCC1-XPF nuclease complex is crucial to repair double-strand breaks and crosslink damages; recently polymorphisms to this complex have been related to CRC risk (Yang et al,. 2015) and to Cisplatin resistance (McNeil et al,. 2015) as well. Mutations in MMR genes as hMLH1 and hMLH2 are common in ovary (Xiao et al,. 2014), breast (Alkam et al, 2013) and colon cancer (Wang et al,. 2014). A common characteristic in Cisplatin chemoresistance in head and neck squamous cell carcinoma (HNSCC) is linked to hMLH1 hypermethylation, while decitabine (DAC) was seen to restore Cisplatin sensitivity in *in vitro* and *in vivo* models of HNSCC (Viet et al,. 2014).

1.1.2.5 Cell cycle arrest and apoptosis induction

There is a critical balance between cell cycle arrest and programmed cell death; numerous proteins are involved as main actors of this equilibrium among which p53 has a central role, inducing cell cycle arrest, senescence and apoptosis under cellular stress. The progression of cell cycle is tightly controlled by cyclins and cyclin-dependent

kinases (CDK). p21(WAF1) is one member of CDK inhibitor family, which hinder cell cycle transition from G1 to S phase. p21(WAF1) is a well-characterized p53-downstream gene and its promoter contains consensus p53-binding sequences. It has been shown that p21(WAF1) is one of the major mediator of p53-induced growth arrest. In response to DNA damage, p53 induces not only cell cycle G1 phase arrest, but also G2/M checkpoint arrest and at the same time activates DNA repairing mechanisms. Activation of p53 can trigger both the mitochondrial (intrinsic) and the death-receptor-induced (extrinsic) apoptotic pathways (Ryan et al,. 2001). p53 induces the expression of pro-apoptotic Bcl-2 (B-cell lymphoma-2) family of proteins, mainly Bax, Noxa and PUMA, but downregulates the pro-survival Bcl-2, leading to permeabilization of outer mitochondrial membrane. Then cytochrome c releases from the mitochondria binds to Apaf-1, and induces the activation of the initiator caspase-9, eventually resulting in the activation of executioner caspase-3, -6 and -7. On the other hand, activated p53 also upregulates the expression of some DRs (death receptors), such as Fas (CD95/APO-1), DR5 (TRAIL-R2), and PIDD (p53-induced protein with death domain). Together with caspase-8, they form the death-inducing signaling complex, subsequently activating caspase-3 and inducing apoptosis (Ryan et al,. 2001). Different types of p53 mutations play a pivotal role in determining the biologic behavior of CRC, such as invasive depth, metastatic site and even the prognosis of patients. p53 mutations are associated with lymphatic invasion in proximal colon cancer, and show significant correlation with both lymphatic and vascular invasion in distal CRC (Russo et al,. 2005). p53 activity can be compromised by inactivation of its positive modulators as p14ARF, or for hyperexpression of its negative regulators as AKT. In combination with another tumor suppressor gene BRCA1, implicated in DNA repair, apoptosis and cell cycle control, p53 mutations, in breast cancer, contribute to resistance to chemo and radiotherapy, while BRCA1 dysfunction leads to enhanced sensitivity to DNA damaging therapeutic

agents (Scata et El-Deiry. 2007). BRCA1 is a part of a complex involved in DNA double strand breaks repair; its overexpression in ovarian cancer and NSCLC leads to an acquired resistance towards platium-based compounds (Cisplatin, oxaliplatin and carboplatin) which often exert this kind of lesions (Papadaki et al., 2012).

Cancer can be viewed as the result of a succession of genetic changes during which a normal cell is transformed into a malignant one; evasion of cell death is one of the essential changes in a cell that cause this malignant transformation. The mechanisms by which evasion of apoptosis occurs can be broadly dividend into: 1) disrupted balance of pro-apoptotic and anti-apoptotic proteins, 2) reduced caspase function and 3) impaired death receptor signaling.

The Bcl-2 family is comprised of pro-apoptotic and anti-apoptotic proteins which play a pivotal role in the regulation of apoptosis, especially via the intrinsic pathway as they reside upstream of irreversible cellular damage and act mainly at the mitochondria level. When there is disruption in the balance of anti-apoptotic and pro-apoptotic members of the Bcl-2 family, the result is dysregulated apoptosis in the affected cells. This can be due to an overexpression of one or more anti-apoptotic proteins or an underexpression of one or more pro-apoptotic proteins or a combination of both. In colorectal cancers with microsatellite instability, mutations in the BAX gene are quite common. Miquel et al. demonstrated that impaired apoptosis resulting from BAX frameshift mutations could contribute to resistance of colorectal cancer cells to anticancer treatments (Miquel et al,. 2005).

Except for p53, there are other proteins inhibitor of apoptosis; IAPs are a group of structurally and functionally similar proteins that regulate apoptosis, cytokinesis and signal transduction. They are characterized by the presence of a baculovirus IAP repeat (BIR) protein domain. Eight IAPs have been identified, NAIP (BIRC1), c-IAP1

(BIRC2), c-IAP2 (BIRC3), X-linked IAP (XIAP, BIRC4), Survivin (BIRC5), Apollon (BRUCE, BIRC6), Livin/ML-IAP (BIRC7) and IAP-like protein 2 (BIRC8). IAPs are endogenous inhibitors of caspases and they can inhibit them by binding their conserved BIR domains to the active sites of caspases, by promoting degradation of active caspases or by keeping the caspases away from their substrates. Dysregulated IAP expression has been reported in many cancers (Fulda et Vucic. 2012). Livin was demonstrated to be highly expressed in melanoma and lymphoma while XIAP was found to be upregulated in osteosarcomas and was linked to Cisplatin resistance (Qu et al., 2015).

1.1.2.6 Survival signals

Tyrosine kinase proteins (PTK) can have a relevant effect on chemotherapy resistance, by the regulation of apoptotic balance. Among different protein kinases, RTKs comprise a well-known group and consist of a transmembrane receptor linked to the intracellular kinase domain. These proteins have emerged as key pharmacological targets in oncology (Choura et Rebaï. 2011). Among them we find the epidermal growth factor receptor (EGFR and HER2); in vitro experiments have demonstrated that overexpression of EGFR and HER2 increase tumor resistance to the therapy (Pegram et al,. 1998). In breast cancer this oncogene has become an important biomarker both for classification and target therapy; 15-30% of all breast cancers cases overexpress this gene (Mitri et al. 2012) and patients in this category usually receive monoclonal antibody therapy with trastuzumab, a monoclonal antibody directed against HER2; this is the mainstay of the treatment for early and metastatic HER2-positive breast cancers (Vogel et al,. 2002). His overexpression was found also in endometrial cancer (Santin et al., 2008). Trastuzumab binds to domain IV of the extracellular segment of the

HER2/neu receptor; cells treated with this monoclonal antibody (mAb) undergo arrest during the G1 phase of the cell cycle. In addition to that, trastuzumab suppresses angiogenesis both by induction of antiangiogenic factors and repression of proangiogenic ones. One of the most relevant proteins that is activated by it is tumor suppressor protein p27 by simultaneously inhibiting PI3K/AKT, Mirk and hKIS pathways.

Tumor kinases (TK) targets can modulate AKT/PKB pathway and produce important effects on PI3K, mTOR and STAT pathways. Indeed, activated AKT phosphorylates and inhibits tuberous sclerosis 2 (TSC2), allowing Ras homolog enriched in brain (Rheb) to accumulate in the GTP-bound state and trigger activation of the mTOR complex1 (mTORC1) pathway.

Although mTOR is frequently activated in human cancers, mutation of the mTOR gene has been found only occasionally (Robbins et al., 2011). This means that over-activation of the mTOR pathway is mostly due to signaling defects upstream of mTOR in the phosphatidylinositol-3-kinase (PI3K)/AKT/mTOR pathway. Mutations in PI3K alpha catalytic subunit kinase domain (PIK3CA) generally arise late in tumorigenesis, and can be identified in 32% of CRC tumors (Samuels et al., 2004). Loss of heterozygosity (LOH) and mutations in Phosphatase and tensin homolog (PTEN), a negative regulator of PI3K activity, have also been reported in CRC (Zhou et al., 2002). Both PIK3CA mutations and PTEN loss lead to mTOR over-activation.

AKT is one of the downstream targets of PI3K. It is a serine/threonine kinase that is activated due to the formation of PIP3 by PI3K. PIP3 binds the PH domains of AKT and aids in the recruitment of AKT to the plasma membrane, which alters the conformation of AKT to allow for subsequent phosphorylation by PDK1. AKT regulates many cellular processes, including differentiation, proliferation and

transformation by phosphorylating GSK-3 (Kim et Kimmel. 2000). Through the upregulation of the transcription repressor Snail, AKT modultes the induction of the epithelial-mesenchymal transition and tumor cell invasion. AKT/mTORC1 induces the expression of HIF-1 and VEGF, which are key elements involved in tumoral neoangiogenesis.

STAT proteins are another class of proteins important in modulating tumorigenesis, they become activated by JAKs through phosphorylation of specific tyrosine residues; the receptors to which JAKs bound are cytokine receptors and their ligands include a series of extracellular proteins such as interferon (INF) and other cytokines, growth factors, hormones, and other polypeptides. The JAK/STAT signal transduction pathway plays key roles in normal physiological processes; however, during the multistep process of carcinogenesis, various pathological events result in constitutive activation of this pathway. This, during oncogenesis, up-regulates specific genes encoding functional proteins that are responsible for specific processes such as cell cycle regulation (cyclins D1/D2 and c-Myc), apoptosis inhibition (Bcl-xL and Mcl-1), and neoangiogenesis (VEGF) (Arumuggam et al., 2015).

1.2 Cisplatin chemoresistance

Cisplatin or cis-diamminedichloroplatinum(II) is currently part of many therapeutic approaches against numerous types of cancer (Non-small cell lung cancer, ovarian cancer, squamous cell carcinoma of the head and neck, bladder cancer, testicular cancer and cervical cancer and malignant mesothelioma) (NCI, 2015).

Cisplatin undergoes aquation to form $[Pt(NH_3)_2Cl(OH_2)]+$ and $[Pt(NH_3)2(OH_2)_2]_2+$ once inside the cell, while the low cellular concentration of chloride ions facilitates this

process; the aquated form is more reactive to the cellular targets. Although many cellular components interact with Cisplatin, DNA is the primary biological target of the drug (Jamieson et Lippard. 1999). The platinum atom of Cisplatin forms covalent bonds to the N_7 positions of purine bases to afford primarily 1,2- or 1,3-intrastrand crosslinks and a lower number of interstrand crosslinks.

Cisplatin modifications distort the structure of the DNA duplex. Intrastrand 1,2-crosslinks bend it significantly towards the major groove, exposing a wide, shallow minor groove surface to which several classes of proteins bind. These include high-mobility group (HMG) box proteins, repair proteins, transcription factors and other proteins such as histone H1 that preferentially recognize 1,2-intrastrand crosslinked platinum–DNA adducts (Jamieson et Lippard. 1999).

DNA damage caused by Cisplatin modulates several signal transduction pathways already outlined, among which: AKT (v-AKT murine thymoma viral oncogene homologue), c-ABL (v-abl Abelson murine leukemia viral oncogene homologue 1), p53 and MAPK (mitogen-activated protein kinase)/JNK (c-Jun NH2-terminal kinase)/ERK (extracellular signal-regulated kinase) (Wang et Lippard. 2005).

Several mechanisms can limit Cisplatin efficacy in chemotherapy, leading to resistance as reported in Figure II:

- Pre-target resistance (decrease of Cisplatin binding to its transporters);
- On-target resistance (increase of efficacy and expression levels of DNA repairing mechanisms and related proteins);
- Post-target resistance (disruption of apoptotic signaling pathways);
- Off-target resistance (stimulation of survival signals which antagonize Cisplatin cytotoxicity).

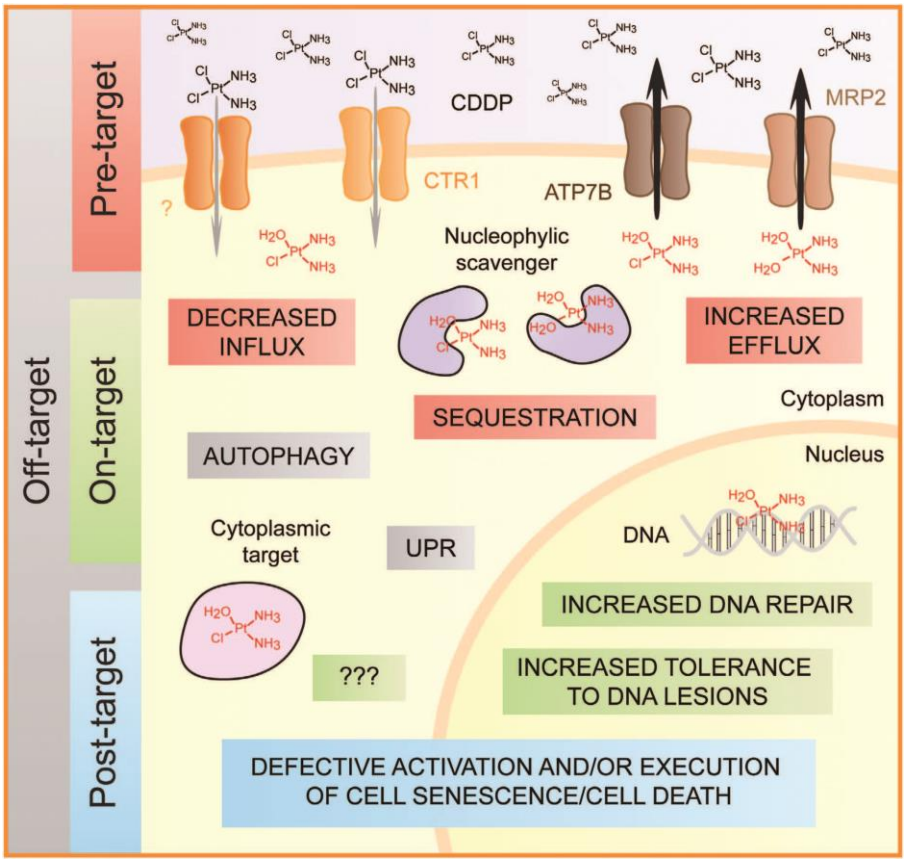

Figure II. Molecular mechanisms of Cisplatin resistance

1.2.1 Pre-target resistance

There are two mechanisms by which cancer cells can elude Cisplatin cytotoxicity before it binds to cytoplasmic targets and DNA: (1) a reduced intracellular accumulation and (2) an increased sequestration by GSH, metallothioneins and other cytoplasmic proteins with nucleophilic properties.

For a long time, Cisplatin was believed to enter cells prominently by passive diffusion across the plasma membrane, mainly because the uptake of Cisplatin, which is highly polar, is relatively slow when compared with that of chemically similar anticancer agents that are actively transported; however several transporter were discovered to mediate Cisplatin influx and efflux from the cell. The two most important transporters involved in this process are the copper transporters CTR1 and CTR2 (encoded by the SLC31A gene, 1 and 2, respectively), whose altered levels of expression or functionality are associated with Cisplatin resistance (Katano et al,. 2002, Huang et al,. 2014). Other transporters, involved in either the uptake or extrusion of Cisplatin from cells, have been indicated as possible mediators of Cisplatin resistance. They include members of ABC proteins (Cui Y. et al. 1999, Ohishi et al., 2002, Korita et al., 2010), solute carriers, such as members of the SLC22 family (Koepsell et Endou, 2004), or MATE (SLC47) transporters (Moriyama et al., 2008, Yonezawa et al., 2006; Yokoo et al., 2007). Particular attention also deserve two P-type ATPases, ATP7A and ATP7B, whose altered expression and localization has been linked to the occurrence of Cisplatin resistance in ovarian cancer (Kalayda et al., 2008).

1.2.2 On-target resistance

The sensitivity of cancer cells to the genomic cytotoxic effects of Cisplatin is limited in the presence of a proficient DNA repair apparatus. In particular, the nucleotide excision repair (NER) system is believed to resolve the majority of DNA lesions provoked by Cisplatin although components of the mismatch repair (MMR) machinery have also been implicated in this process (Kunkel et Eire. 2005; Furuta et al., 2002).

Cisplatin DNA adducts can engender double-strand breaks (DSBs), which are normally repaired along with DNA synthesis via homologous recombination (HR) (Smith et al., 2010). Accordingly, HR-deficient neoplasms, such as those bearing loss-of-function mutations in the genes encoding breast cancer 1, early onset (BRCA1) or breast cancer 2, early onset (BRCA2), are generally more susceptible to the genotoxic effects of Cisplatin than HR-proficient cancers of the same kind (Farmer et al,. 2005).

It's important to remember that Cisplatin exert important effect on cytoplasmic components (mitochondria, ER and lysosomes) that account for its extranuclear toxicity, these molecules, as well as the enzymatic systems that regulate their preservation/turnover, may also be involved in the development of on-target resistance (Sancho-Martínez et al,. 2012).

While Cisplatin forms more stable adducts with DNA than with RNA (Nafisi et Norouzi. 2009), aquated Cisplatin was shown to react faster with hairpin RNA molecules than with analogous DNA hairpins or ssDNA *in vitro* (Papsai et al,. 2008). Still, Cisplatin-induced damage to the translational machinery appears to be more complex than simple platination of rRNAs. The results of in vitro experiments demonstrated that Cisplatin inhibited translation via its interaction with mRNA and formation of high-molecular weight adducts from cross-linked mRNA and rRNA species (Heminger et al,. 1997). These Cisplatin-RNA interactions are likely responsible for the inhibition of translation in its initiation and/or elongation phases (Heminger et al,. 1997).

Due to their reactivity with sulfur-containing nucleophiles, Cisplatin and its aquated species form Pt-S adducts with various sulfur-containing amino acids, peptides and proteins, including glutathione and metallothioneins (Alderden et al., 2006), in which

the most relevant binding sites are represented by sulfur atoms of cysteine or methionine residues (Zimmermann et al,. 2009). High reactivity of thiol- and thioether-containing amino acids, peptides and proteins combined with their high cellular abundance is responsible for the fact that Cisplatin-protein interactions account for the majority of adducts formed in Cisplatin-treated cells. Moreover, available evidence points out that these Cisplatin-protein interactions may be significantly involved in Cisplatin toxicity and resistance of cancer cells against this anticancer agent (Mezencev. 2015).

Exposure of cells to Cisplatin causes characteristic mitochondrial alterations leading to the activation of the intrinsic pathway of apoptosis and other signals leading to cell death (Servais et al., 2008). When mitochondria are appropriately primed by Cisplatin, the outer transmembrane potential is dissipated and the permeability of the outer membrane is increased. As a result cytochrome c, which then binds apoptosis protease-activating factor-1 (apaf-1) and other proteins to form the complex known as apoptosome, is release into the cytosol and can activate apoptosis (Yuan et al., 2010). In addition to that, Cisplatin has also been linked to ROS over-production. Treatment with Cisplatin inhibits antioxidant enzymes, including superoxide dismutase (SOD), catalase, glutathione peroxidase, glutathione S-transferase and glutathione reductase (Kadikoylu et al., 2004) in kidney tissues, which may explain the depletion of GSH observed. Excessive ROS production leads to mitochondrial and cellular oxidative stress. Through the cell, ROS damage many macromolecules including DNA, proteins and lipids, which are associated to cell death (Masgras et al,. 2012).

Lysosomes seem to play a significant role in Cisplatin cytotoxicity. This is supported by the relationship between lysosomal and endosomal trafficking, lysosomal handling of Cisplatin and Cisplatin cytotoxicity. This central role might be due to 1) primary deadly

signaling that originated in the lysosomes as a consequence of Cisplatin accumulation or targeting; or 2) delivery of Cisplatin to other subcellular structures or organelles from which deadly signaling starts. In this sense, it has been shown that Cisplatin causes lysosomal membrane permeabilization accompanied by apoptosis (Appelqvist et al., 2011), and that cathepsin D is involved in this process (Emert-Sedlak et al., 2005).

ER stress seems to be an important mechanism of Cisplatin cytotoxicity, at least in many cell types. Treatment with Cisplatin activates ER stress markers (Grp78, GADD153/CHOP, calpain, caspase 12/human caspase 4, cytosolic Ca2+ increase, etc.) in cultured cancer cells (Kim et al., 2011). Aquated forms of Cisplatin react with nucleophilic sites of macromolecules including proteins; it has been shown that Cisplatin can bind and disrupt the proper folding of many proteins, including albumin (Ahmed-Ouameur et al., 2006) by attacking disulphide bonds. Because Cisplatin accumulates in the ER, it is conceivable to think that some direct ER stress might arise from disturbing protein folding.

1.2.3 Post-target resistance

Intracellular stress conditions, such as those induced by Cisplatin, promote the rapid activation of an integrated adaptive response aimed at the re-establishment of cellular homeostasis. This is generally accompanied by the emission of anti-apoptotic signals and only when homeostasis cannot be restored (when stress conditions are excessive in intensity or duration) lethal signals are transmitted, leading to cell death. For Cisplatin, these signals consist in the switch of the DNA damage response from a cytoprotective to a cytotoxic mode, followed by the activation of BAX and BAK1163 or the accumulation of ROS and consequent permeability transition pore complex

opening (Mandic et al,. 2001). Both these processes eventually promote the functional and physical breakdown of mitochondria followed by the activation of caspase-dependent and independent mechanisms of cell death. Thus, post-target Cisplatin resistance has been associated not only with genetic and epigenetic alterations that impair p53 signaling but also with defects in several other pro-apoptotic signal transducers, including mitogen-activated protein kinase 14 (MAPK14, known as p38MAPK) and c-Jun N-terminal kinase 1 (JNK1) (Brozovic et al., 2004). Along similar lines, post-target Cisplatin resistance appears to be significantly influenced by the expression levels and functional status of BCL-2 family members and caspases which have a major role in the execution of apoptotic cell death (Tajeddine et al., 2008).

1.2.4 Off-target resistance

The susceptibility of cancer cells to Cisplatin can also be limited by molecular circuitries that deliver compensatory survival signals even though they are not directly activated by the drug. For example, the overexpression of v-erb-b2 avian erythroblastic leukemia viral oncogene homolog 2 (ERBB2) has been suggested to promote Cisplatin resistance not only by delivering pro-survival signals via AKT signaling axis, but also by finely regulating the transitory cell cycle arrest that is required for the repair of Cisplatin-induced DNA lesions (Fijołek et al,. 2006).

Various components of the autophagic machinery and several chaperones of the heat-shock protein (HSP) family are reported to impair the cytotoxic response of cultured cancer cells to Cisplatin (Yu et al,. 2011). Moreover, the expression levels of HSP27 may constitute predictive biomarkers of clinical responses to Cisplatin in esophageal squamous cell carcinoma patients (Miyazaki et al,. 2005).

1.2.5 Role of ion channels in Cisplatin chemoresistance

Ion channels are integral membrane proteins that mediate the influx/efflux of essential signaling ions into/from the cell or intracellular organelles, thereby controlling cytoplasmic/intraorganellar ion concentrations, membrane potential and cell volume. Numerous studies have demonstrated the involvement of different ion channels in the regulation of fundamental cellular processes, such as proliferation and apoptosis (Lang et al., 2005 ; Bortner et Cidlowski. 2014)

Changes in cell volume and ion gradients across the plasma membrane play a pivotal role in the initiation of apoptosis. In Ehrlich ascites tumor cells (EATC) Poulsen and colleagues found that in wild type cells the induction of apoptosis after Cisplatin treatment leads to an apoptotic volume decrease (Poulsen et al., 2010). This phenomenon was coupled to net loss of Cl^{-}, K^{+}, Na^{+}, and aminoacids. Comparing these results with EATC Cisplatin resistant cells, the authors found an increase cell viability, less caspase 3 activation, less pronounced AVD connected to a decrease in Cl^{-} loss and an increase NaCl uptake. All these data can be linked to a Cisplatin-induced malfunctioning of Na/K ATP-ase (Panayiotidis et al. 2006). A reduction of anion currents, like chloride channels, has proven to be a common characteristic of chemoresistance to Cisplatin and beyond, in various tumor cell lines (Poulsen et al,. 2010; Hoffmann et Lambert. 2014). This volume reduction seems to play an important role in human epidermoid cancer KB cells while, in Cisplatin resistant KCP-4, which lack the expression of Cl^{-} channels, after a specific treatment with histone deacetilases, Cisplatin resistance can be reduced (Shimizu et al., 2008).

Na^{+}-dependent transporters for organic osmolytes contribute to the volume reduction connected to Cisplatin response, while overexpression of the taurine transporter TauT protects kidney cells against Cisplatin-induced apoptosis (Han et Chesney. 2009).

Recently also calcium modulated potassium channels like KCa3.1 have been correlated to modulating Cisplatin resistance; Lee and colleagues demonstrated that its block with clotrimazole and TRAM-34, or its suppression with a dominant-negative construct, is linked to a reduction in Cisplatin sensitivity in epidermoid cancer cell line KB-3-1 while, in multi-drug resistant KCP-4, KCa3.1 presence was greatly reduced both as level of protein expressed and the related I_K current (Lee et al. 2008).

Another potassium channel, hERG1, has been correlated to Cisplatin induced apoptosis in gastric cancer; Cisplatin activity seem to induce an overexpression of this channel and its silencing promotes a reduction of Cisplatin effect of apoptotic proteins Bcl-2, Bax and on caspase-3 activation, reducing apoptosis (Zhang et al. 2012).

Cisplatin has been correlated to an induction of apoptosis also by increasing mitochondrial membrane permeability, modulating the expression level of MTP protein in cervical and colorectal human cell lines. This has been correlated with dissipation of mitochondrial electron membrane potential, with production of reactive oxygen species (ROS), with Bax translocation, with the release of apoptotic signals (ex. cytochrome C) and by caspase activation (Sharaf el dein O. et al., 2012).

Aquaporin role in modulating Cisplatin resistance is still controversial, Shi and colleagues point out that AQP5 knockdown in HT-29 colorectal cell line, is linked to an increase in MAP-kinase p38 activation and an acquired resistance (Shi et al,. 2014). However Trigueros-Motos and colleagues, examining AQP3 gene, (linked to a compensatory response to a volume decrease following doxifluridine and gemcitabine treatment) found an increase expression of this gene but this effect was not linked to Cisplatin treatment (Trigueros-Motos et al., 2012). Acquaporins seems to be affected by Cisplatin treatment in ovarian carcinoma: Xuejun and colleagues found that aquaporin 1 levels were diminished after Cisplatin treatment while aquaporins 3 and 8 were upregulated in SKOV3 cell (Xuejun et al,. 2014).

TRP channels also seem to be involved in modulating chemoresistance; they normally mediate a flux of calcium and magnesium, but also of metallic bivalent cations as zinc, copper, cadmium and iron. Many studies found that they can mediate a relevant Cisplatin uptake and that this drug is even able to influence their expression levels (Bouron et al., 2015).

Progressive understanding of the molecular mechanisms which regulate the establishment and progression of different tumors is leading to ever more specific and efficacious pharmacological approaches. In this picture, ion channels represent many unexpected, but very promising, different players even in understanding chemoresistance mechanisms in cancer and they can be efficacious players in overcoming this phenomenon.

1.3 Cisplatin analogues

Cisplatin is a very effective cancer drug and it's still use in treatment of bladder cancer, cervical cancer, malignant mesothelioma, non-small cell lung cancer, ovarian cancer, testicular cancer and squamous cell carcinoma of the head and neck (NCI, 2015). However it presents non only problems of resistance but of toxicity to kidney (nephrotoxicity), nervous system (neurotoxicity), to the ear (ototoxicity) and to bone marrow (myelotoxicity). Several analogues have been developed during the last 30 years to overcome Cisplatin resistance, increase efficacy and to lower side effects, among which carboplatin, oxaliplatin, satraplatin and picoplatin have been identified as the most effective (Kelland. 2007).

Carboplatin is a chemotherapeutic drug used for cancers of ovaries, lung, head and neck. In terms of its structure, carboplatin differs from Cisplatin because it has a

bidentate dicarboxylate ligand in place of the two chloride ligands, which are the leaving groups in Cisplatin. It exhibits lower reactivity and slower DNA binding kinetics, although it forms the same reaction products in vitro at equivalent doses with Cisplatin (Wheate et al,. 2010). Compared to Cisplatin, the greatest benefit of carboplatin is its reduced side effects, particularly the elimination of nephrotoxic effects; the main drawback of carboplatin is its myelo-suppressive effect which is very strong (Dasari et Tchounwou. 2014).

Oxaliplatin is currently approved for the treatment of adjuvant and metastatic colorectal cancers when used in combination with 5-FU and folinic acid (FOLFOX regimen). Recent clinical trials have tried to extend its spectrum of activity to include the treatment of metastatic gastric and oesophago-gastric adenocarcinoma, and improve its effectiveness against colorectal cancers through its administration with different drugs such as irinotecan and capecitabine. Oxaliplatin has proven less ototoxicity and nephrotoxicity than Cisplatin and carboplatin (Passetto et al., 2006).

Satraplatin is an orally active platinum drug that has shown anti-cancer activity against several platinum sensitive and resistant cell lines including human lung, ovary, cervix and prostate and is undergoing a variety of Phase I, II and III clinical trials in conjunction with various drugs such as docetaxel in the treatment of prostate cancer, paclitaxel in the treatment of NSCLC and capecitabine to treat advanced solid tumors (http://www. clinicaltrials.gov).

Picoplatin was designed primarily to circumvent glutathione-mediated drug resistance mechanism. In vitro studies demonstrated picoplatin ability to overcome platinum drug resistance, showing anticancer activity in Cisplatin, carboplatin and oxaliplatin resistant cell lines (Wheate et al., 2010). Picoplatin is currently undergoing various Phase I and Phase II studies as a treatment for colorectal cancer in combination

with 5-FU and leucovorin, in combination with docetaxel for prostate cancer and as a treatment for patients with progressive or relapsed NSCLC (Wheate et al., 2010).

While thousands of analogues of Cisplatin have been prepared and tested so far, quite surprisingly the immediate parent Pt compounds that are obtained through simple replacement of the two chlorides with different halides as metal ligands (in particular the diiodido and dibromido derivatives) have been poorly investigated. Most likely, this situation arises from the early misconception and/or generalization that chloride replacement with other halides will result into substantial loss of the anticancer activity (Wilson et Lippard. 2014). These arguments led us to explore this kind of modification in a more systematic way and analyze its chemical and biological consequences.

1.4 Chemotherapeutic drugs used for CRC treatment

The most used chemotherapeutic drugs for treatment of colorectal cancer are:

- *5-Fluorouracil (5-FU):* is an analogue of pirimidine, classified as an antimetabolite. It can alter DNA synthesis inhibiting thymidylate synthase. Interrupting the action of this enzyme blocks synthesis of thymidine, required for DNA replication. Thymidylate synthase methylates deoxyuridine monophosphate (dUMP) to form thymidine monophosphate (dTMP) Administration of 5-FU causes a scarcity in dTMP, so rapidly dividing cancerous cells undergo cell death (Longley et al,. 2003). The overproduction of the enzyme itself, the changings in the sequence of its target as well as the reduction of activating enzymes are the principle mechanisms of resistance

(Longley et al., 2003). The main collateral effect of 5-FU are: nausea, vomit, diarrhea, photosensitivity, headache, cardiotoxicity, mucositis and hear loss (Hwang, 2004). 5-FU is metabolized by the liver and excreted by the kidney; its half-life is very short, several minutes. It's usually administrated in therapeutic combinations with folic acid.

- *Capecitabine:* it's a pro-drug which is converted in 5-FU and acts in the same way by inhibiting DNA synthesis; it's used in combination with other chemotherapeutic drugs including Cisplatin and oxaliplatin (Gustavsson et al., 2015).
- *Folinic acid (leucovorin):* it's a drug used in chemotherapy with methotrexate, otherwise in combination with 5-FU for treatment of CRC because of its pro-inhibition effects of thymidylate synthase. It can be administrated by mouth, intravenous or intramuscular injection. In 2004, the Multicenter International Study of Oxaliplatin/5-FU/Leucovorin in the Adjuvant Treatment of Colon Cancer (MOSAIC) trial demonstrated that the addition of oxaliplatin to 5-FU/Leucovorin improved both DFS and OS in patients with stage III colon cancer (André et al., 2004).
- *Irinotecan:* it's a chemotherapeutic pro-drug and it's converted by the liver by hydrolysis in SN-38, the active form. Once activated, SN-38 inhibits the topoisomerase I and DNA replication, inducing apoptosis. it's used in combination with 5-FU and irinotecan in the regimen FOLFIRI in CRC therapy (Gustavsson et al., 2015).
- *Oxaliplatin:* it's capable of interfering with all cell cycle phases and, being an alkylating antineoplastic agent, to bind to DNA and induce apoptosis. Cisplatin forms covalent adduct with purine DNA bases and induce double strand breaks of DNA stands; this interaction is the root cause for its cytotoxic effect (Yousef

et al., 2009). It can induce acute and delayed toxic effects as: myelotoxicity, nephrotoxicity, nephrotoxicity, nausea, vomit and hear loss (Tsang et al,. 2009).

In CRC 5-FU, capecitabin, leucovorin are used in stages II, III e IV (TNM), while oxaliplatin, the most common Cisplatin analogue with carboplatin, only in stages III and IV and the irinotecan only in stage IV (Ragnhammar et al,. 2001) (Table I).

TNM Stage	Chemotherapeutic drugs
0	None
I	None
II	5-FU, leucovorin and capecitabin
III	5-FU, leucovorin and capecitabin, **oxaliplatin**
IV	5-FU, leucovorin and capecitabin, **oxaliplatin**, irinotecan

Table I. Chemotherapeutic drugs used in CRC cancer divided for TNM stages.

1.5 Ion channels

Ion channels are proteins formed by different transmembrane subunits assembled to form a pore for the selective entrance of a specific ion. They are involved in determining the cellular rest potential and have a crucial role in the insurgence of action potentials, in secretion of various neurotransmitters or specific proteins (hormones, mucins, enzymes, sebum), in regulating cell volume and in many other cellular processes.

They are located on cell membranes of all cellular types and, with ion transporters (e.g. sodium-potassium pump, sodium-calcium exchanger, etc), of the two classes of ionophore proteins.

The play a crucial role for cancer cells in regulating cell volume, migration, cell cycle progression and apoptosis (Figure III). They can be regulated by many factors among which growth factors and hormones; their expression is in many cases altered in cancer, so they can be exploited as promising therapeutic targets.

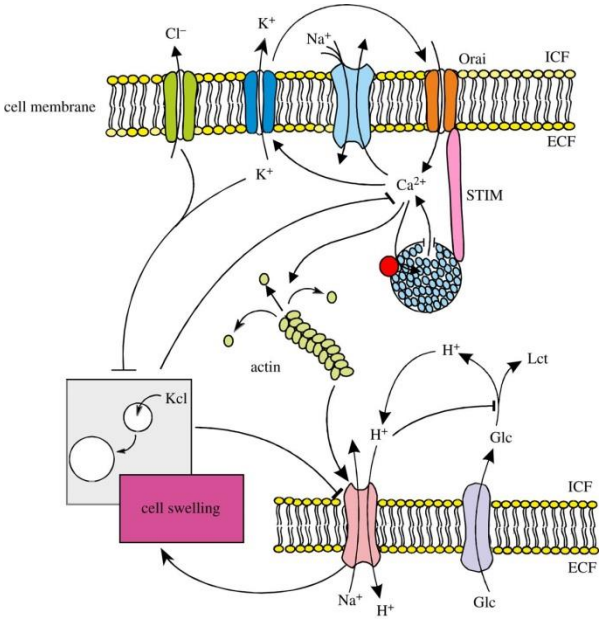

Figure III. Ion channels in regulating cellular homoeostasis

1.5.1 Structure and classes of ion channels

Ion channels are composed of different subunits that are organized to form a central pore in the cell membranes; inside it there are several amino acids which, thanks to their charge and spatial conformation, give to pore of the channel its selectivity to a specific ion. On the basis of what modulates the opening probability of an ion channel,

two different superfamilies are distinguished: voltage-gated and ligand-gated ion channels; the first type is modulated by changes in membrane potential, while the other opens after binding a specific molecule, which constitutes its ligand (Kunzelmann. 2005). Another possibility is to classify ion channels by the ion which fluxes inside them; they can be distinguished: chloride channels, sodium channels, potassium channels, calcium channels, proton channels and non-selective cation channels.

1.5.1.1 Ca^{2+}channels

Voltage gated Ca^{2+} channels are tetrameters formed by four subunits: α1, α2, β, γ. Channel pore is located between the four homologous membrane-spanning domains (I–IV) of α subunit bridged intracellular loops (Van Petegem et Minor. 2006).

Ca^{2+} is a ubiquitous second messenger, and is an important signalling molecule for several fundamental cell processes including cell cycle control, migration, and apoptosis. Regulation of intracellular Ca^{2+} involves both Ca^{2+} entry from the extracellular space and Ca^{2+} release from intracellular stores in the endoplasmic reticulum (ER) or mitochondria. Ca^{2+} signalling is fundamental in wide range of cellular and tissue functions as cardiac potential, muscular contraction, secretion, learning processes and long term memory, depolymerization of actin filaments, inhibition of Na+/ H+ exchanger or co-transport of Na+, K+, 2Cl- with the consequential regulation of cell volume, fundamental in regulating cellular proliferation (Berridge et al. 2003).

In cancer, not only the proliferation of tumour cells stops depending solely on external growth signals via development of significant growth autonomy (Prevarskaya et al., 2010), but Ca^{2+}-signalling undergoes profound remodelling to favour activation of Ca^{2+}-dependent transcription factors, such as the nuclear factor of activated T cells (NFAT),

c-Myc, c-Jun, c-Fos which promote hypertrophic growth via induction of the expression of the G1 and G1/S phase transition cyclins (D and E) and associated cyclin-dependent kinases (CDK4 and CDK2) (Roderick et Cook. 2008). Calcium is also important in cancer cells in regulating apoptosis, cell migration and invasion as well as in promoting tumoral neo-vascularization.

Many Ca^{2+}-transporters have been implicated in all these processes, including SERCA, the Golgi network secretory pathway and plasma membrane PMCA Ca^{2+}-ATPases, the inositol 1,4,5-trisphosphate receptor (IP3R) and ryanodine receptor (RyR) as well as Ca^{2+} release channels of the endoplasmic reticulum as STIM and ORAI, T-type voltage-gated calcium channels (VGCCs), various TRP-members, such as TRPV6, TRPC1, TRPC3 and TRPC6, TRPM2, TRPM7 and TRPM8 (Prevarskaya et al,. 2014).

1.5.1.2 Na^+ channels

Voltage-gated sodium channels (VGSCs) are trimers formed by 3 subunits: α, β1 and β2. The core of the channel is constituted by the α subunit, while the others have regulatory functions. VGSCs are responsible for the rising phase of the action potential in the majority of electrically excitable cells and are therefore important in impulse generation and propagation; they comprise a multi-gene family of at least nine different functional members ($Na_V1.1$–1.9) coding for the pore-forming α-subunits. There are also four auxiliary β-subunits, of which one or two at a time can associate with an α-subunit and modulate channel expression and activity in the plasma membrane. Several individual Na_V isoforms are differentially expressed in different human cancers; these include $Na_V1.5$ in astrocytoma, breast and colon cancers (Chioni et al., 2010; Brisson et al., 2013; Driffort et al., 2014), $Na_V1.6$ in cervical cancer, and $Na_V1.7$ in breast, prostate

and non-small cell lung cancers (Fraser et al., 2014).

1.5.1.3 K^+Channels

Potassium channels are formed by four α subunits, each of them composed by six transmembrane segments, assembled to form the tetrameric structure of the pore of the channel. Several β subunits can be associated with alpha subunits, sometimes in a α4β4 stoichiometry with regulatory functions. They can be classified according to several criteria, including the stimulus to which they respond and their biophysical and structural properties, into four main families: voltage-gated K^+ channels, calcium-activated K^+ channels, inward-rectifier K^+ channels and two-pore-domain K^+ channels. Potassium currents play a key role in multiple cellular functions such as the maintenance of resting membrane potential and the active repolarization of the action potential, the regulation of cell volume, differentiation, proliferation, migration and apoptosis. Therefore, K^+ channels control the electrical excitability of nerves and muscles, affect neurotransmitter and insulin release, and modulate the immune response and other physiological processes (Niemeyer et al., 2001). Potassium channels are widely distributed in a variety of healthy and cancer cells. They are involved in physiological cell proliferation and neoplastic growth as well as tumor progression and malignancy.

Overexpression of $K_V1.1$ has been reported in medulloblastoma (Northcott et al., 2012), elevated $K_V1.3$ can be detected in multiple solid tumors as breast, colon, and prostate cancer (Comes et al., 2013). Altered expression of the intermediate-conductance calcium activated channel $K_{Ca}3.1$ has also been shown in glioblastoma (Catacuzzeno et

al., 2012). $K_V1.5$ channels are dysregulated in different types of cancers including lymphomas, astrocytomas, oligodendrogliomas and glioblastomas (Comes et al., 2013). Expression levels of $K_V10.1$ (EAG1, voltage gated eag related subfamily H, member 1) are lower in glioblastoma multiforme and in malignant brain tumors and its expression is inversely related to cancer malignancy (Patt et al., 2004). Human ether-a-go-go related gene (hERG) K^+ channel, also known as $K_V11.1$, is constitutively expressed in neuroblastoma, and a molecular complex between β1-integrins and hERG channels regulates adhesion-dependent differentiation of neuroblastoma cells (Cherubini et al., 2005).

1.5.1.4 Chloride channels

Chloride channels are ubiquitously expressed, being localized both in plasma membrane and in intracellular organelles. They have many different functions as the regulation of electrical excitability, trans-epithelial fluid transport, ion homeostasis, pH levels, and cell volume regulation, the latter being particularly important for cancer cells migration and infiltration (Jentsch et al.,2002).

ClC-3 is a member of the ClC chloride channels and transporters family and it has been suggested to be a molecular component involved in activation of volume-sensitive Cl^- currents and to be closely related to cell proliferation, migration, apoptosis, and acidification of synaptic vesicles (Zhang et al., 2013). Volume-activated chloride channels play a crucial role in the process of regulatory volume decrease (RVD) induced by hypotonic stresses. RVD is a phenomenon that contributes to cell shape and volume changes required for cell migration, and so it also has an important role in

cancer progression (Lang. 2007) as well as in the neoangiogenic process (Manulopolos et al., 2000).

Calcium-activated chloride channels (CaCCs) play several important roles including epithelial secretion, olfactory transduction, membrane excitability, regulation of vascular tone, and photoreception (Hartzell et al., 2009). Calcium-activated chloride channel regulator 2 (CLCA2) is normally expressed in trachea and lungs and it has been shown that loss of CLCA2 expression in human breast cancer appears to be closely associated with tumorigenicity and that the expression of CLCA2 was down-regulated in colon cancer (Peretti et al., 2015).

Volume-regulated anion channel VRAC (also known as VSOR or VSOAC) seems to play an important effect in modulating Cisplatin resistance as well. Especially VRAC subunits, LRRC8A or LRRC8D, were found to increase resistance against carboplatin and Cisplatin. This finding can be explained by an unsuspected role of VRAC in drug transport. This transport required the obligatory channel subunit LRRC8A and also depended on LRRC8D, a subunit that strongly increased VRAC's permeability to Cisplatin/carboplatin (Planells-Cases et al., 2015).

1.5.1.5 Ion channels as drug targets

There are many approved K^+ channel blockers used in the clinic for various indications. Imipramine, for example, was initially known for its major inhibitory effect on serotonin reuptake, norepinephrine reuptake and acetylcholine at the neural synapses in central nervous system. In preclinical studies imipramine inhibited proliferation of melanoma cells (Gavrilova-Ruch et al., 2002) and induced apoptosis in ovarian cancer

cells (Asher et al., 2011). By using bioinformatics-based drug repositioning, Jahchan and colleagues re-proposed imipramine to treat incurable Cisplatin-resistant small-cell lung cancer (SCLC), moving the drug into clinical studies for this new indication (Jahchan et al.,2013). Antiarrhythmic verapamil is effective against prostate cancer (Rybalchenko et al., 2001) and neuroblastoma (Chen et al., 2014). As verapamil is also a calcium channel inhibitor, the anticancer effects of verapamil can be attributed to its combined inhibitory activity against potassium and calcium channels. The major concern for repurposing such anti-psychotic drugs for cancer is that they modulate one or more than one neurotransmitters like serotonin, histamine, norepinephrine and acetylcholine with high potency. Hence, such drugs need to be screened for their higher anti-cancer potency over antipsychotic use or if they can be prescribed cautiously to cancer patients.

Another case is nifedipine, a potent blocker of L-type Ca^{2+} channels, which is one of the drugs indicated for the management of angina and hypertension. In vitro studies indicated that nifedipine reduces mitogenic effect of endothelin 1 (ET1) by blocking Ca^{2+} channels in lung cancer (Zhang et al., 2008). However, its anticancer activity is disputed (Largent et al., 2010), and since primary indication of nifedipine is hypertension, it cannot be used in hypotensive cancer patients as it may cause hypotensive shock.

In general, in order to target ion channels it is important to understand the expression pattern and significance of expression of each of those variants in a specific cancer type as well as in normal tissue to avoid dangerous adverse effects.

1.5.2 hERG: structure and expression

Among the ion channels which are part of Eag-related potassium channels, hERG (Human ether-à-go-go-related channel) is the most studied. This ion channel is best known for the repolarizing I_{Kr} current in the cardiac action potential. When this channel's ability to conduct electrical current across the cell membrane is inhibited or compromised, either by application of drugs or by rare genetic mutations, it can result in the so called long QT syndrome, a potentially fatal aritmic disorder which has made hERG1 inhibition an important antitarget which must be avoided during drug development (Sanguinetti et Tristani-Firouzi. 2006).

hERG potassium channel, encoded by KCNH2 gene, comprises four alpha subunits, which form the channel's pore through the plasma membrane. Each hERG subunit consists of 6 transmembrane alpha helices, numbered S1-S6, a pore helix situated between S5 and S6, and cytoplasmically located N- and C-termini. The S4 helix contains a positively charged arginine or lysine amino acid residue at every 3rd position and act as a voltage-sensitive sensor. Between the S5 and S6 helices, there is an extracellular loop and “the pore loop”, which begins and ends extracellularly but loops into the plasma membrane; the pore loop for each of the hERG subunits in one channel face into the ion-conducting pore and is adjacent to the corresponding loops of the other three subunits; together they form the selectivity filter region of the channel pore. Near N-terminus a PAS domain is located which slow the kinetic of inactivation of the channel. (Morais Cabral et al., 1998) (Figure IV).

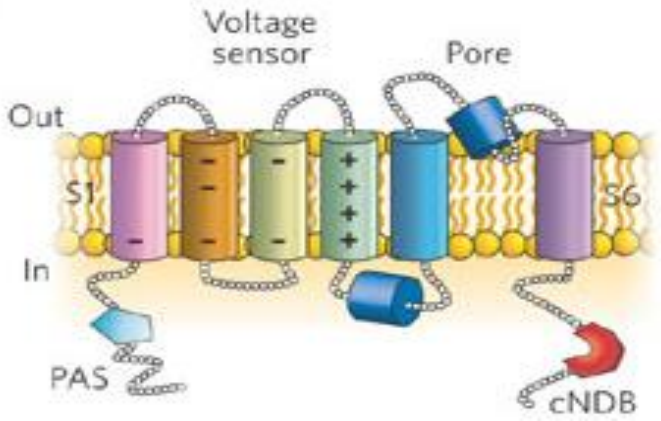

Figure IV. Structure of hERG1 channel.

KCNH2 gene expresses at least two alternative transcripts, KCNH2a and KCNH2b, coding for hERG1a and hERG1b proteins, respectively. hERG1b presents a shortened and distinct N terminus, of 34 amino acid residues. This domain determines the faster deactivation gating typically observed in hERG1b (Larsen et al., 2008). The relative abundance of these isoforms determines the kinetic properties of the rapid delayed rectifying K1 current (Larsen et Olesen, 2010). In cardiac myocytes both isoforms contribute to the rapid delayed rectifying K1 current although hERG1a tends to predominate (Larsen et Olesen, 2010).

1.5.2.1 hERG and cancer

hERG may be utilized as a potential tumor marker, given its expression in a variety of tumor cells and its absence from most non-cancerous human tissues. Specifically, hERG was detected in endometrial cancer and in colon carcinomas and hERG mRNA was sensitive and specific indicator for tumor malignancy. The prognostic value of hERG expression in tumors has been evaluated in several tissues; in

acute myeloid leukemia (AML) blasts, hERG K^+ channel expression is associated with a 50% reduction of relapse-free and overall survival time compared with patients with hERG-negative AML (Pillozzi et al., 2007). Patients with esophageal squamous cell carcinomas similarly exhibit reduced survival when hERG is detected (Ding et al., 2008) and in colon adenocarcinomas, there is a significant correlation between hERG K^+ channel expression and invasiveness or dissemination. hERG is not detected in normal colonic mucosa while substantial hERG was found in patients with non-metastatic and metastatic adenocarcinoma (Lastraioli et al., 2004).

1.5.2.2 hERG inhibitors

Many drugs have the ability to block hERG channel as cyclosporin a, used in bone-marrow transplantation and to prevent rejection of kidney, heart, and liver transplants (Lee et al., 2011), endoxifen, the active metabolite of tamoxifen (Chae et al., 2015), paroxetine, an antidepressant drug of the selective serotonin reuptake inhibitor (SSRI), blocks the hERG by binding to the open and inactivated states of the channels (Lee et al., 2014) as well as many others (Durdagi et al., 2010). A selective block after treatment with E4031 has been related to a decrease in tumor proliferation in many types of cancer (Smith et al. 2002). This mechanism is induced by a cell cycle arrest and was proven in the cell line model of FLG 29.1 which went in a permanent block in G0/G1 phase after a prolonged treatment with hERG1 inhibitors (Pillozzi et al. 2002). Other drugs which exhibited a comparable effect in several *vitro* models are: astemizole, eritromicyn e vincrastine (blockers of G2 phase), terazosine, WAY 123398 and cesium chloride (Jehle J. et al. 2011). Interestingly a novel pyrimido-indole compound, CD-160130, seems to block hERG1 channels with a higher efficacy for the

isoform b, with less effect on cardiac repolarization and could be a promising target to study the effect of hERG1 block without incurring in the long QT syndrome (Gasparoli et al., 2015).

1.5.3 K_{Ca}3.1: structure and expression

In human genome there are eight voltage-independent calcium activated potassium channels, one of large conductance (K_{Ca}1.1), three of low conductance (K_{Ca}2.1, K_{Ca}2.2 and K_{Ca} 2.3), one of intermediate conductance (K_{Ca}3.1, whose structure is reported in Figure 9) and four others K_{Ca}4.1, K_{Ca}4.2 and K_{Ca}5.1. They are operated by intracellular calcium levels, through calmodulin binding; identical to K_{Ca}2.x channels, K_{Ca}3.1 is composed of six transmembrane domains (S1–S6), with the pore loop located between S5 and S6, as well as cytoplasmic N- and C-termini (Jensen et al., 1998). Another mechanism was shown by Gerlach et al., who demonstrated the role of kinases in the regulation of K_{Ca}3.1 by showing that hydrolyzable ATP analogues, but not other nucleoside triphosphates, activated the channel via an increase in PoMAX without changing the apparent Ca^{2+} sensitivity (Gerlach et al., 2000).

K_{Ca}3.1 was originally identified in epithelial and endothelial tissues, including colon, lung, kidney, prostate, placenta and salivary gland, as well, as in the immune system where it is expressed in thymus, spleen, lymphocytes, mast cells, macrophages and bone marrow (Jensen et al., 1998; Bradding et Wulff 2009). More recently, K_{Ca}3.1 has also been identified within sensory neurons and microglia, leading to the proposal that this channel may constitute a therapeutic target in the central nervous system for acute and chronic neurodegenerative disorders and for treatment of secondary damage after spinal cord injury (Bouhy et al., 2011).

$K_{Ca}3.1$ plays a key role in red blood cells volume regulation as the loss of K^+ and Cl^- allows erythrocytes to shrink as it moves through the capillaries (Hoffman et al., 2003); it is also co-expressed in vascular endothelia with $K_{Ca}2.3$ where these two channels play a key role in the endothelial derived hyperpolarizing factor (EDHF) response (Félétou. 2009).

Another of its crucial role is the regulation of T- lymphocytes during their activation: along with $K_v1.3$ channel it plays an important role in cell activation, migration, and proliferation through the regulation of membrane potential and calcium signaling (Bradding et Wulff 2009). In tumor cells its higly expressed in clear cell renal carcinoma (Rabjerg et al., 2015), malignant glioma (Turner et al., 2014), prostate cancer, hepatocellular carcinoma and endometrial and mammary carcinoma (Rabjerg et al. 2015).

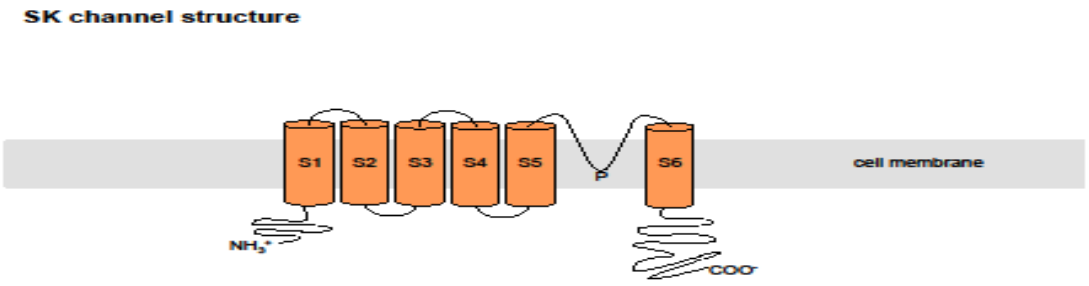

Figure V. Structure of $K_{Ca}3.1$.

1.5.3.1 K_{Ca}3.1 modulators

Among K_{Ca}3.1 activators we found NS309, potent and selective for this channels compared to other members of the family (EC_{50} for K_{Ca}3.1 =20 nM; EC_{50} for KCa2.3 =600 nM); unfortunately it has a low *in vivo* half-life, and it has a strong effect on hERG inhibition at 1μM (Strøbaek et al. 2004). Riluzole is another activator of K_{Ca}3.1 (EC_{50}= 1.49 μM) widely in use from 1995 for ASL treatment which not only has a relevant effect on all K_{Ca} channels but is able to block hERG (IC_{50}= 50μM) and several Na_v channels (Bellingham. 2011). From Riluzole template several other K_{Ca}3.1 activators have been developed with a higher specificity for this channel and less unwanted effects on others; one of these compounds is SKA-31, which is 10 times more potent than Riluzole and activates KCa2.1 with EC_{50}= of 2.9 μM, KCa2.2 with an EC_{50}=1.9 μM, KCa2.3 with EC_{50} = 2.9 μM, and KCa3.1 with EC_{50} = 260 nM (Sankaranarayanan et al. 2009).

K_{Ca}2.3 and 3.1 are important players in regulating arterial blood pressure, they are both expressed by endothelial cells and by associated smooth muscular tissue; activators like SKA-31 have therefore demonstrated a relevant decrease on systemic arterial blood pressure with vasodilatation and bradycardic effects with potential role in hypertension treatment (Sankaranarayanan et al. 2009; Radtke et al. 2013).

K_{Ca}3.1 can be the target of several inhibitor compounds; in KB tumoral epidermoid Cisplatin-sensitive cells this channels, activated after ipotonic stress, can be inhibited by drugs as clotrimazole and TRAM-34. This inhibition has not been reported in KCP4 cells a KB-derived Cisplatin resistant cell line (Lee et al. 2008).

1.6 Colorectal cancer

1.6.1 Epidemiology

Colorectal cancer (CRC) is the third most common malignant neoplasm worldwide and the second leading cause of cancer deaths (irrespective of gender) in the United States (American Cancer Society, 2015). It is the second most common cause of cancer in women (9.2%) and the third most common in men (10.0%) with it being the fourth most common cause of cancer death after lung, stomach, and liver cancer (World Health Organization, 2014). The highest incidence is reported in countries of Europe, North America, and Oceania, whereas incidence is lowest in some countries of south and central Asia and Africa (MM Center et al, 2009).

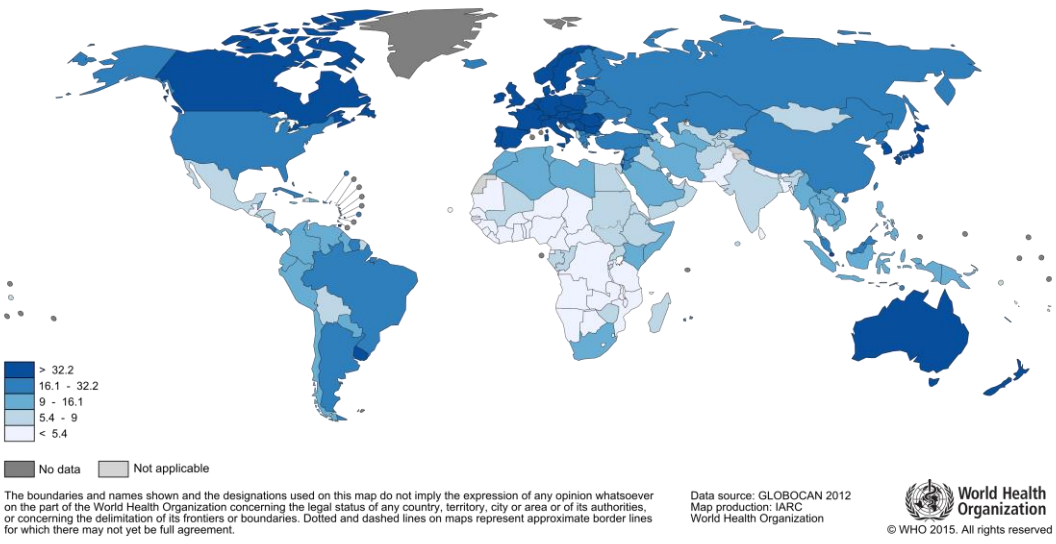

Figure VI. Estimated age-standardized colorectal cancer incidence for men in 2012 (Ferlay et al., 2012).

In Italy there are almost 40 new cases every 100.000 inhabitants every year and with a stronger incidence among the population between 50 and 70 years; it arises more frequently in proximal colon (38,8%), distal colon (29,6%) and rectum (28,5%) (Robbins and Cotran 9th edition). The CNESP (Centro Nazionale di Epidemiologia, Sorveglianza e Promozione della Salute) has registered from the 2008 a constant reduction of mortality in both sexes and a constant reduction in mortality rates; despite that CRC remains the second cause for tumor death in 2014 with almost 19.000 deaths in Italy (Airtum et Aoim, 2014). For incidence rates, 52.000 new diagnoses have been estimated in 2014 with a prevalence of 350.000 units and a cure fraction of 30% in men and of 44% in women (Airtum et Aoim, 2014).

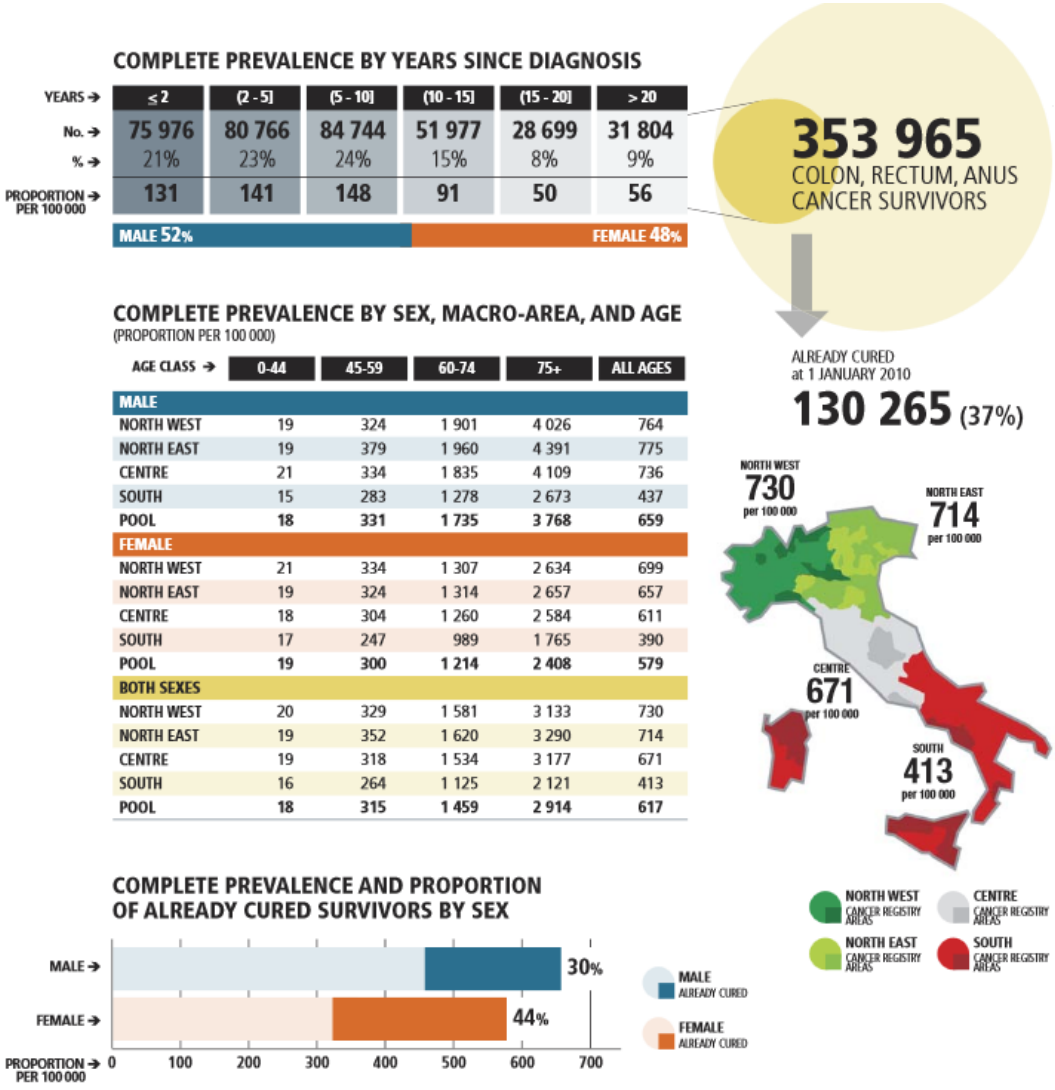

Figure VII. Summary of prevalence data of colorectal tumor in Italy. (Airtum et Aoim 2014).

1.6.2 Etiology

Colorectal cancer is the result of a complex interaction of genetic and environmental factors; about 75% of patients with CRC have sporadic disease with no apparent evidence of having inherited the disorder. The remaining 25% of patients have a family history of CRC that suggests a hereditary contribution, common exposures among family members, or a combination of both (National Cancer Institute, 2015)

1.6.2.1 Risk factors

- *Alimentary:* the main hexogen risk factor is diet; recently the World Cancer Research Fund and the American Institute for Cancer Research reported that an excessive intake of red meat and meat-based preparations (Oostindjer et al., 2014) together with obesity are contributory causes for developing colon cancer (National Cancer Institute, 2015); on the other hand a high consume of dietary fibers could be associated with a reduced risk of colorectal cancer (Kunzmann et al., 2015).
- *Not alimentary:* Based on solid evidence, tobacco smoke is associated with increased incidence and mortality from CRC (National Cancer Institute, 2015), as long term high alcohol consumption (more than 50 g/day) (Wang et al, 2015; National Cancer Institute, 2015), while regular physical activity is associated with a decreased incidence.
- Other intestinal inflammatory diseases like Crohn's disease or ulcerative colitis (Freeman. 2008; Lindström et al., 2011) seems to have also an impact on CRC development.

- As for nonsteroidal anti-inflammatory drugs (NSAIDs), there are evidences which indicate that they have a positive role in preventing the development of CRC (Cuzick et al,. 2009; Flossmann et Rothwell, 2007) although there is also proof of the harm of their use which includes: upper gastrointestinal bleeding, chronic kidney disease and serious cardiovascular events such as myocardial infarction, heart failure, and hemorrhagic stroke (National Cancer Institute, 2015). Despite that, Burn and colleagues found that in the CAPP2 randomized trial, 600 mg aspirin per day for a mean of 25 months substantially reduced cancer incidence after 55.7 months in carriers of hereditary colorectal cancer (Burn et al., 2011).

- *Genetic:* hereditary forms of CRC have been associated with polyposic and non-polyposic syndromes and specific related tumor suppressor and stability genes among which the familial adenomatous polyposis (APC), Lynch syndrome (MLH1, MSH2, MSH6, PMS2 and EPCAM), Junior polyposis syndrome, (BMPR1A, SMAD4, MUTYH-associated polyposis (MHY) and Peutz-Jeger syndrome (STK11) are the most relevant (Jasperson et Burt. 2015; National Cancer Institute, 2015).

- *Hormonal:* administration of estrogens and progesterone/progestins in postmenopausal women seems to induce a decrease of CRC risk (Barzi et al., 2013). For this reason hormone replacement therapies (HRT) have been developed and they proved, in Women's Health Initiative Trial, to reduce colon cancer risk of 56%. Furthermore the length of HRT intake and the combined effect of progesterone/progestins and estrogens has been related to a reduction of

adenoma recurrence and to the improve of the survival rates of CRC patients (Schindler, 2007).

1.6.3 Pathogenesis

Colorectal cancer develops by a series of sequential modifications which precede the developing of a real neoplasia which are: hyperplasia, metaplasia, low-grade dysplasia and high-grade dysplasia (Figure VIII).

The probability that a polyp could evolve towards and invasive form of cancer depends on its histology type (tubulous or villous) and its dimensions. The risk is low (less than 2%) for polyps inferior of 1.5 cm of diameter, intermediate for polyps of 1.5-2.5 (2-10%) cm and high (>10%) for polyps larger than 2.5 cm of diameter (http://www.airc.it/tumori/tumore-al-colon-retto.asp).

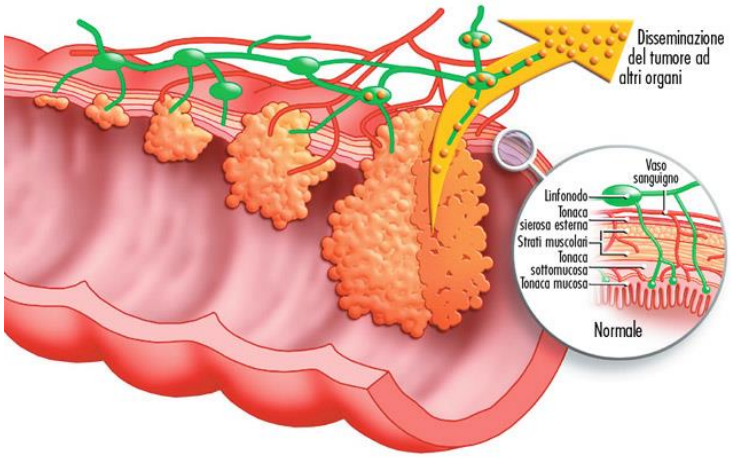

Figure VIII. Sequential modifications of colorectal mucosa which preceded the develop of CRC.

The most common histologic type of CRC is the adenocarcinoma (>90%) (Hamilton et al., 2010) and its invasiveness follow four different non consequential step:

- *Local invasion:* from the mucosa the cancer can infiltrate connective and muscular tissue and then adjacent organs;
- *Lymphatic diffusion:* Lymph node metastases are common when the primary tumor penetrates the *muscolaris propria*;
- *Hematic diffusion:* the most affected organ is liver along with lungs, bones, adrenal glands, ovaries and brain;
- *Peritoneum:* the second most frequent site of metastasis after the liver.

1.6.4 Diagnosis

The initial symptomatology of CRC is often aspecific, with modest alterations in bowel movements, followed by abdominal pains and sporadic intestinal bleeding. Right colon may increase its diameter and acquire a higher distensibility, while the faeces can have a more fluid consistency. Before giving clear signs of its presence, the tumor may grow very much in diameter with a continuous but not conspicuous bleeding; other symptoms may include, pain, anemia, bowel obstruction (less frequent unless the tumor arises near the ileocecal valve), and the presence of an abdominal mass. In left colon, which has a smaller diameter and contains more solid faeces, an eventual obstruction is more frequent and precocious, while a tumor which develops in the rectum produced a much more conspicuous bleeding and alterations of normal intestinal motility.

1.6.5 Prevention and staging

An effective prevention is strongly suggested, especially after the age of 50, with a first level exam like the fecal occult blood test. According to the guidelines of the American College of Gastroenterology, the annual fecal immunochemical testing is the preferred colorectal cancer detection test (Lieberman et al,. 2012). If this exam will turn out to be positive the patients will undergo a colonoscopy as a second level examination.

The main second level diagnostic exams for prevention of CRC are:

- *Endoscopy:* may be executed for different segments of colorectal tract, with either a sigmoidoscopy or a colonoscopy. It's the most reliable exam for CRC prevention, diagnosis and follow-up. With early detection and removal of intestinal polyps (benignus adenomas), it reduces the risk of developing colorectal cancer by up to 90 percent. In addition, early detection of cancer that is already present in the colon or rectum lead to better treatment outcomes and reduced chance of metastasis (Ro et al., 2015).
- *lower gastrointestinal series:* also called barium enema, is a medical procedure used to examine and diagnose problems with the human colon. X-ray pictures are taken while barium sulfate fills the colon via the rectum.
- *computed tomography (CT):* CT has high diagnostic value for the diagnosis of sporadic colon cancer using either water or carbon dioxide as intraluminal contrast agent, with sensitivity comprised between 82% and 96% (Ridereau-Zins, 2014, Sibileau et al., 2014 and Soyer et al., 2012). It may be used to provide important information on tumor dimensions, diffusion to nearby tissues

and lymphnodes status and it's equally used also to evaluate presence of a metastasis.

- *Nuclear magnetic resonance (NMR):* NMR imaging has a major role for the local staging of rectal cancer (Hoeffel et al., 2014, Torkzad et al., 2014) although its use is not recommended to search for and to detect rectal cancer that has not been proven by rectoscopy.

- *Ecography:* Abdominal ultrasound presents high sensitivity, specificity in the diagnosis of colon cancer and it's used in combination with colonoscopy and rectoscopy to help the diagnosis (Martínez-Ares et al,. 2009).

Correct staging is critical because treatment (particularly the need for pre-operative therapy and/or for adjuvant treatment, the extent of surgery) is generally based on this parameter. For colorectal cancer Duke's classification, modified by Aster-Coller, is often used; it consist of six different stages:

- *A:* tumor mass confined within the mucosa;
- *B1:* tumor mass invading the *muscolaris mucosae* but not the *muscolaris propria*;
- *B2:* tumor mass invading the *muscolaris propria*;
- *C1:* as B1 stage but with positives regional lymph nodes;
- *C2:* as B2 stage but with positives regional lymph nodes;
- *D:* presence of metastasis

The most used tumor staging classification system however is TNM Classification of Malignant Tumors, a cancer staging notation system that gives codes to describe the stage of a person's cancer, when this originates with a solid tumor. For every kind of tumor four different stages exist (with the stage 0, referred to the “carcinoma in situ” phase), indicated with numbers from 1 to 4, in increasing level of graveness.

The “T” parameter can vary from 1 to 4, depending on the extension of the primary tumor mass. It comprehends the “Tis” for an in situ carcinoma.

The “N” parameter describes the regional lymph nodes status, if 0 they are free of neoplastic cells, otherwise the parameter may vary from 1 to 3 with an increasing invasiveness of tumoral cells.

The “M” parameter indicates the presence (1) or the absence (0) of a distant metastasis.

The following table compare the two systems and their stages.

TNM Classification (American Joint Commission on Cancer)				**Dukes' Classification**
Stages	**T**	**N**	**M**	**Stages**
Stage 0	Tis	N0	M0	
Stage I	T1	N0	M0	A
	T2	N0	M0	B1
Stage II	T3	N0	M0	B2
	T4	N0	M0	B2
Stage III	T1, T2	N1 or N2	M0	C1
	T3, T4	N1 or N2	M0	C2
Stage IV	Any T	Any N	M1	D

Table II. Principal methods of tumoral staging and their parameters

1.6.6 Therapy

In the last ten years colon cancer therapy significantly improved and the median survival rates are nearly doubled as standard therapeutic options have been strictly linked to the stage of the carcinoma (National Cancer Institute, 2015).

1.6.6.1 Surgery

Therapy for treatment of colorectal cancer always include a surgery intervention with the excision of the trait where the tumor has developed with or without anastomosis. Differently to what happened in the past, the surgery treatment nowadays tends to be a lot more conservative, with the preservation of bowel functionality (except for either older or high risk patients) and the OS rates are increased as well thanks to a more prompt diagnosis and the implementation of screening programs.

In colon cancer, surgery is based on colectomy and resection of lymph nodes (West et al,. 2010) and in most cases, a laparoscopic intervention is possible (Lee et al., 2012). The evaluation of a minimum of 12 lymph nodes is considered a measure of surgery quality (Madoff, 2012). Resection must be complete to be curative, so other atypical nodes or ganglions outside the resection field should be biopsied or resected whenever possible (Binefa et al.,2014).

1.6.6.2 Radiotherapy

Radiation therapy uses high-energy radiation to shrink tumors and kill cancer cells. X-rays, gamma rays, and charged particles are types of radiation used for cancer treatment. The radiation may be delivered by a machine outside the body (external-

beam radiation therapy), or it may come from radioactive material placed in the body near cancer cells (internal radiation therapy, also called brachytherapy). Systemic radiation therapy uses radioactive substances, such as radioactive iodine, that travel in the blood to kill cancer cells. It's usually used in combination with chemotherapy with an adjuvant or neoadjuvant approach (Lawrence et al,. 2008).

1.6.6.3 Chemotherapy

Surgery is the main treatment for CRC cure, but in cases of stage III and IV, the administration of chemotherapy is often used for optimizing the chances of healing. Chemotherapy can be administrated prior to a surgery intervention to reduce the tumor mass (adjuvant therapy) or after to increase the survival rate by killing those cells could still be present and be undetected (neoadjuvant therapy).

2. AIM OF THE THESIS

The aim of the present work was that of study two strategies to overcome Cisplatin chemoresistance in colorectal cancer: (1) to exploit K^+ ion channels modulating agents as new therapeutic tools in order to increase Cisplatin therapeutic potential in colorectal cancer cells (2) to test two new Cisplatin-analogues, cis-Pt-I_2 and cis-Pt-Br_2, with increased selectivity in order to overcome resistance in a panel of tumor cell lines.

3. MATERIALS AND METHODS

3.1 Cell culture

Colorectal cancer (CRC) cell lines HCT-116, H630, HCT-8, HT29 and HCT-116 p53-/- were cultured in RPMI-1640 medium (Euroclone; Milan, Italy), supplemented with 2mM L-Glut, 10% fetal bovine serum (FBS) and 1% penicillin/streptomycin (complete medium). PANC-1, IGROV-1 and A549 were cultured in DMEM high glucose medium (Euroclone; Milan, Italy), supplemented with 4mM L-Glut, 10% fetal bovine serum (FBS) and 1% penicillin/streptomycin (complete medium). HCT-116 and HT29 cells were kindly provided by Dr. R. Falcioni (Regina Elena Cancer Insitute, Roma). Cells were cultured at 37°C in a humidified atmosphere in 5% CO_2 in air.

3.2 Cell viability assay

To evaluate the IC_{50} of each drug, cell viability was assessed through either the Trypan Blue exclusion test (Sigma-Aldrich) or the WST-1 cell viability assay (Roche Diagnostics, Mannheim, Germany). In any case, cells were seeded at $1x10^4$/well in 96-well plates (Costar Corning) in complete medium and incubated for 24h before drug addiction. Following drug addition, cells were further incubated for different times. When the Trypan Blue exclusion test was applied, cells were harvested and counted using a hemocytometer. For WST-1 assay, at the end of incubation the WST-1 reagent was added and absorbance was measured at 450 nm. All experiments were performed at least in duplicate. The IC_{50} values were calculated using Origin Software (Microcal

Origin 8.0 software; OriginLab Corporation, Nothampton, MA). To assess drug combinations, experiments were conducted following the diagonal constant ratio combination design, proposed by Chou and Talalay (Chou et Talalay. 1984).

Briefly, cells were treated with mixtures of two drugs at their IC_{50} concentrations with a 2-fold serial dilution (1/1, 1/2, 1/4, 1/8, 1/16, 1/32, 1/64) of the IC_{50}s for 24h. Following incubation, cells were harvested and counted using a Bürker hemocytometer. All experiments were repeated at least in duplicate.

3.3 Cell cycle analysis

Cell cycle distribution was assessed by flow cytometry after staining the cells with propidium iodide (PI). Cells were seeded and treated with different drugs at their IC_{50} for 24h. At the end of incubation, cells were harvested, washed with PBS and resuspended (5×10^5 cells/ml) in 300 µl Propidium Iodide staining solution and incubated at 4°C in the dark for 20 minutes. The DNA content of the cells was measured by BD FACSCanto (Becton Dickinson, Franklin Lakes, NJ, USA) and the percentage of cells in each cell cycle phase was determined using ModFit LT 3.0 analysis software (Verity Software House, Topsham, ME USA).

3.4 Cell transfection

HCT-116 cells were cultured as previously described. Twenty-four hours before transfection cells have been plated to be 50-70% confluent at the time of the experiment. Transfection has been performed using Lipofectamine 2000 reagent according to the manufacturer's instruction with 1) KCNH2-siRNAs (44858 anti-herg1 siRNA1 and 44762 anti-herg1 siRNA3, Ambion; Austin TX, USA) (100 nM final

concentration in total) 2) KCNN4-siRNAs (7801 anti-kcnn4 siRNA1 and 7803 anti-kcnn4 siRNA3, Ambion; Austin TX, USA) (5 nM final concentration in total). As negative control cell lines has been transfected only with lipofectamine. 16 hours after transfection medium was changed and after 48 hours cells were collected for cell viability assay and proteins extraction as previously described.

3.5 Annexin/PI assay

Apoptosis was quantified using the Annexin V/propidium iodide test (Annexin-VFLUOS staining kit; Roche Diagnostics, Mennheim, Germany). Cells, treated as above, were harvested after 24 hours of treatment with the different drugs (at their IC_{50} value), washed with PBS, re-suspended in 100 µl of binding buffer and incubated with FITC-conjugated annexin V and propidium iodide for 15 min. Flow cytometry was performed using the BD FACSCanto (Becton Dickinson, Franklin Lakes, NJ, USA). Data were analyzed through the BD FACSDiva Software 6.1.3. Only for experiments concerning Cis-Pt-I_2 the experiments were performed in the same conditions explained above, using Muse Annexin V and Dead Cell Assay (Merk Millipore, Billerica, MA) according to the manufacturer instructions and data were collected and analyzed with Muse Cell Analyzer (Merk Millipore, Billerica, MA).

3.6 Immunofluorescence

Immunofluorescence was performed applying the procedures detailed in Lastraioli et al., 2015, using the following primary antibodies: anti-hERG1 (DivalToscana.Srl, dilution 1:1000), anti-KCa3.1 (Sigma –Aldrich AV35098, dilution 1:1000), anti-KCa2.3 (Sigma –Aldrich P4747, dilution 1:1000). The secondary

antibodies used were the anti-mouse-Alexa-488 (Sigma –Aldrich, dilution 1:500) and anti-rabbit-Alexa-488 (Sigma –Aldrich, dilution 1:500).

3.7 Total RNA extraction and Real time PCR

Total RNA was extracted following the TRIzol® Reagent protocol. *ATP7A*, *ATP7B*, *KCNA3*, *KCNH1*, *KCNH2*, *KCNMA1*, *KCNN3*, *KCNN4*, *SLC31A1* and *SLC31A2* mRNAs were quantified by real-time quantitative polymerase chain reaction (RQ-PCR), using the PRISM 7700 sequence detection system (Applied Biosystems, Life Technologies, Carlsbad, CA, USA) and the SYBR Green PCR Master Mix Kit (Applied Biosystems) as in Pillozzi et al., 2007.

Primers used are the following:

ATP7A-F GCCTGCGTACGTGGATTTAT

ATP7A-R TGGATCCATTTTGATTTCCTC

ATP7B-F TCCAGACCACCTTCATAGCC

ATP7B-R AGATCACAGCCAGAGAAGGG

KCNA3-F TTGTCCTAGCAAAGCCACCT

KCNA3-R CTCAGGATGGCCAGAGACAT

KCNH1-F CCTGGAGGTGATCCAAGATG

KCNH1-R CCAAACACGTCTCCTTTTCC;

KCNH2-F ACGTCTCTCCCAACACCAAC

KCNH2-R GAGTACAGCCGCTGGATGAT

KCNMA1-F TCTTTGCTCTCAGCATCGGTG;

KCNMA1-R CCGCAAGCCGAAGTAGAGAAG;

KCNN3-F AAGCGGAGAAGCACGTTCATA

KCNN3-R CTGGTGGATAGCTTGGAGGAA

KCNN4-F GCCTGTGCACTGGAGTCAT

KCNN4-R CGTGCTTCTCTGCCTTGTTA

SLC31A1-F GTGACGGGTTAAGATTCGGA

SLC31A1-R TGGTGGGAATGATCCATTTT

SLC31A2-F CAAACAGAAGCACCGCTGTA

SLC31A2-R GAGGAGACCCGAGAGCAGAC

3.8 Protein extraction and western blot (WB)

Protein extraction and western blot (WB) were performed as described in Crociani et al., 2013. For the experiments 50 μg of total lysates were used. For hERG1 and KCa3.1 detection, the anti-hERG1 (DivalToscana.srl, dilution 1:1000), anti-KCa3.1 (Sigma -Aldrich AV35098, dilution 1:1000) and anti-KCa2.3 (Sigma -Aldrich P4747, dilution 1:1000) primary antibodies were used. Anti-rabbit peroxidase-conjugate (Sigma-Aldrich, dilution 1:10000) was used as secondary antibody. WB images were acquired with an Epson 3200 scanner, and the relative bands analyzed with ImageJ 1.47v free software (developed at the National Institutes of Health).

3.9 Patch-clamp experiments

Membrane currents were recorded using the patch-clamp technique in the whole-cell configuration, at room temperature (25°C). Electrodes were pulled from borosilicate glass capillaries (i.d 0.86 mm, o.d. 1.5 mm; Harvard Apparatus, Holliston, MA, USA), using a PC-10 pipette puller (Narishige, Tokio, Japan). Electrodes typically had a resistance of 3-5 MΩ. Series resistance was always compensated up to 80%. Currents were amplified and filtered using a Axopatch-1D (Molecular Devices,

Sunnyvale, CA) equipped with pClamp hardware and software (pClamp 10.3). Currents were low-pass filtered at 5 kHz and digitized online at 10 kHz with pClamp (Axon Instruments) hardware and software. Data were subsequently analyzed with pClamp and Origin (Microcal Inc., Northhampton, MA, USA) software.

For hERG1 currents recording pipettes contained (in mM): K^+ aspartate 130, NaCl 10, $MgCl_2$ 2, $CaCl_2$ 2, Hepes-KOH 10, EGTA-KOH 10, pH 7.3. The extracellular solution contained (in mM): NaCl 95, KCl 40, $CaCl_2$ 2, $MgCl_2$ 2, Hepes-NaOH 10, Glucose 5, pH 7.4. High extracellular [K^+] allows to increase the amplitude of inward hERG1 currents, thus avoiding the necessity of applying excessively negative test potentials. The K^+ equilibrium potential was -30mV. For Vrest measurement the extracellular solution contained (in mM): NaCl 130, KCl 5, $CaCl_2$ 2, $MgCl_2$ 2, Hepes-NaOH 10, Glucose 5, pH 7.4.

For measurements of KCa3.1 channel currents, we used an internal pipette solution containing (in mM): K^+aspartate 145, $MgCl_2$ 2, HEPES 10, K_2EGTA 10, and $CaCl_2$ 5.96 (250 nM free Ca^{2+}) or 8.55 (1 μM free Ca^{2+}), pH 7.2. Na^+ aspartate Ringer was used as an external solution: 160 mM Na^+aspartate, 4.5 mMKCl, 2 mM $CaCl_2$, 1 mM $MgCl_2$, and 5 mM HEPES, pH 7.4 (as reported in Sankaranarayanan et al. 2009).

KCa3.1 currents (250 nM free Ca^{2+}) were elicited by 200-ms voltage ramps from -120 to +40 mV applied every 10 s, and the fold increase of slope conductance by drug was taken as an indication of channel activation, as reported in Sankaranarayanan et al. 2009. hERG1 currents were elicited by a two-step protocol, pre-conditioning the cell for 8 s at membrane potentials of 0 mV and -70 mV and then testing the tail current at -120 mV (for 450 ms). The effect of Riluzole was determined on maximal hERG1 tail currents (i.e. after conditioning at 0 mV). The current-voltage relationship for hERG1 was determined from peak tail currents at 2120 mV (for 1.1 second), following 15

second conditioning potentials from 0 to270mV (10mVsteps). The time between consecutive trials in the same stimulating protocol was 4 seconds. The holding potential (VH) was 0 mV. The same stimulation protocol was used to determine the concentration-response relationships for Cisplatin, Riluzole and SKA-31. For clarity, in Figure 12 and 13, we only reported the drug effect on the tail currents elicited after conditioning at 0 mV.

3.10 Cisplatin uptake measurement

The determination of platinum concentration in the cellular pellets was performed in triplicate by a Varian 720-ES Inductively Coupled Plasma Atomic Emission Spectrometer (ICP-AES) equipped with a CETAC U5000 AT+ ultrasonic nebulizer, in order to increase the method sensitivity.

Before the analysis, samples were weighted in PE vials and digested in a thermoreactor at 80 °C for 24 h with 2 mL of aqua regia (HCl suprapure grade and HNO_3 suprapure grade in 3:1 ratio) and 0.2 mL of H2O2 suprapure grade. After digestion, the samples were diluted to about 5 mL with ultrapure water (≤18 M) and accurately weighed; 5.0 mL of each sample were spiked with 1 ppm of Ge used as an internal standard, and analysed. Calibration standards were prepared by gravimetric serial dilution from a commercial standard solution of Pt at 1000 mg L−1. The wavelength used for Pt determination was 214.424 nm whereas for Ge was used the line at 209.426 nm. The operating conditions were optimized to obtain maximum signal intensity, and between each sample, a rinse solution constituted by HCl suprapure grade and HNO_3 suprapure grade in 3:1 ratio was used in order to avoid any “memory effect”.

3.11 Patients

The study cohort included 223 untreated patients who underwent radical surgery with curative intent for colorectal adenocarcinomas at the Department of General Surgery and Surgical Oncology, Azienda Ospedaliero-Universitaria, Careggi, Florence. This cohort represents a subgroup of the patients operated on at the Department in the period September 2001 to January 2015 who were selected without any bias. Patients affected by hepatitis C viral infection or who had undergone preoperative radiotherapy or chemotherapy for rectal cancer were excluded. Samples of tumor were collected during surgery, after obtaining

an informed written consent, and immediately processed for the sample storing. The samples were classified as adenocarcinomas or adenomas and staged according to the American Joint Committee on Cancer classification by experienced pathologists.

3.12 Immunohistochemical Staining

IHC for $K_{Ca}3.1$ was carried out on 7-μm sections on positively charged slides. After dewaxing and dehydrating the sections, endogenous peroxidases were blocked with a 1% H_2O_2 solution in phosphate-buffered saline. Subsequently, antigen retrieval was performed by heating the samples in a microwave oven at 600 W in citrate buffer pH 6.0 for 20 minutes. The primary antibody used was anti-$K_{Ca}3.1$Sigma-Aldrich AV35098, dilution 1:2000. Incubation with the primary antibody was carried out overnight at 4°C and immunostaining was performed with a commercially available kit (Picture-MAX Polymer Kit, DAB, broad spectrum, Thermo Fisher Scientific, Waltham, MA, USA) according to the manufacturer's instructions. Specimens were evaluated

using a quantitative assessment, using a scoring systems based on the determination of the percentage of positive cells (Score 0: 0% of positive cells, Score 1: 1-25% of positive cells, Score 2: 26-49% of positive cells, Score 3: ≥50% of positive cells). For all the other antigens we carried out the same protocols and applied the same scoring systems as reported in Lastraioli et al., 2012.

3.13 Chemicals

Riluzole, SKA-31 and TRAM-34 (Sigma-Aldrich) were dissolved in DMSO at a concentration of 5 mM while E4031, Cisplatin and Oxaliplatin (Sigma-Aldrich) were dissolved in bidistilled water at the concentration of 5 mM. cisPtI_2 and cis$PtBr_2$ were dissolved in bidistilled water at the concentration of 1mM. All stock solutions were stored at -20°C. The effect of DMSO was subtracted from the effect of the relative drug in each experiment performed.

3.14 Chemistry of *cis*-$PtBr_2(NH_3)_2$ and *cis*-$PtBr_2(NH_3)_2$: synthesis and characterisation.

The synthesis of this Pt complex was performed through a slight modification of Dhara's synthesis for Cisplatin (Dhara. 1970). A solution of 400 mg (2.4 mmol) of KI in 3 mL of water was added to an aqueous solution (5 mL) of 250 mg of $K_2[PtCl_4]$ (0.6 mmol) which was quantitatively converted into a dark solution containing $K_2[PtI_4]$ after five minutes of stirring at room temperature. Then the addition of two equivalents of ammonium hydroxide as a 40% solution results in the separation of cis-$PtI_2(NH_3)_2$ as a

bright yellow compound, leaving behind a colorless solution. The solid was filtered off and thoroughly washed with water (Yield 90%).

A suspension of 200 mg of cis-$PtI_2(NH_3)_2$ (0.41 mmol) in water (5mL) was mixed with a solution of $AgNO_3$ (0.82 mmol) in water (1,5 mL) and stirred in the dark (40ºC) until a pale yellow solution was formed over the suspension. The AgI formed was then filter off using neutral celite over a solution of two equivalents of KBr in 7 mL of water. The colorless solution was stored until orange crystalline precipitation was observed. The bright orange crystals of *cis*-$PtBr_2(NH_3)_2$ are filtered off and washed with water and dried in air. Yield was 25%. Purity of the product was assessed through elemental analysis of C, N and H [calculated C: 0%, H: 1.45%, N: 7.20%, experimental: C: 0,54%, H: 1.45%, N: 7.18%], ^{1}H, ^{195}Pt NMR and IR analysis (see SI). Cis geometry checked as describe in the literature (Infrared and Raman Spectra of Inorganic and Coordination Compounds, 6th Edition). Solution behaviour of cis-$PtBr_2(NH_3)_2$ and *cis*-$PtI_2(NH_3)_2$ was assessed through spectrophotometric experiments performed with a Varian Cary 50 Bio UV-Vis spectrophotometer in buffered solutions without the use of DMSO and of NaCl. A solution of the complex (10^{-4} M) was prepared in 50 mM phosphate buffer at pH = 7.4. The absorbance was monitored in the wavelength range between 200 and 800 nm for 72 h at 25° C.

3.15 Log P determination

The octanol–water partition coefficients for *cis*-$PtBr_2(NH_3)_2$ and *cis*-$PtI_2(NH_3)_2$ was determined by modification of the reported shake flask method (Marzo et al., 2015). Water (50 mL, distilled after Milli-Q purification) and n-octanol (50 mL) were shaken together for 72 h to allow saturation of both phases. Solution of the complex was prepared in the aqueous phase (3×10^{-3} M) and an equal volume of octanol was added.

Biphasic solutions were mixed for ten minutes and then centrifuged for five minutes at 6000 rpm to allow separation. Concentration in both phases was determined by UV-VIS. Reported log P is defined as log[complex]oct/[complex]wat. Final value was reported as the mean of three determinations.

3.16 Circular Dichroism experiments, interaction with ctDNA

CD spectra were measured with a Jasco J-715 spectropolarimeter with the following conditions: scan speed 50 nm/min; response 1 sec; data pitch 0.1 nm; bandwidth 2.0 nm; 8 accumulations. Calf thymus DNA (ctDNA) 52.0 μM in phosphate buffer 50 mM, pH=7.4 was additioned with *cis*-$PtBr_2(NH_3)_2$ 2.3 mM in H_2O or Cisplatin 1.0 mM in H_2O, to 0.5:1 and 1:1 molar ratio directly in a 1-cm quartz cylindrical cell, volume 2.5 ml. Concentrations and molar ratios are indicated per base. All samples (except one, see results) were incubated at room temperature (22°C) for 72h before measurement. The ctDNA had a base-pair length of ca. 800, obtained with a standardized procedure by sonication. The DNA concentration was checked by absorbance measurement at 260 nm (0.34 u.A., 1 cm cell). Phosphate buffer was used in all case to measure the blank spectrum.

3.17 Quantitative evaluation of binding of cis-$PtI_2(NH_3)_2$ and Cisplatin to mammalian DNA in a cell-free medium.

Solutions of double-helical calf thymus (CT) DNA (42% G + C, mean molecular mass approximately 2 × 107) at a concentration of 0.032 mg mL−1 (1 × 10−4 M related to the phosphorus content) were incubated with cisPtI2 (8 μM) or Cisplatin (8 μM) at a value of rf = 0.08 in 0.1 mM KI or KCl, respectively, at 37 °C (rf is defined as the molar ratio of free platinum complex to nucleotide phosphates at the onset of incubation with DNA). Two different stock solutions of cisPtI2 (0.1 mM) or Cisplatin (0.1 mM) were prepared. One contained the PtII complex incubated for 7 days in unbuffered KI or KCl, respectively (0.01 M, pH 6) at 37 °C in the dark, whereas the other contained PtII complexes incubated for 7 days in double distilled water at 37 °C in the dark. Fifty microliters of the PtII complex aged in KI/KCl (0.01 M) or in water were quickly mixed with 4950 μL of DNA dissolved in NaClO4 (10 mM), and the reaction mixture was maintained at 37 °C. In the experiments in which the PtII complex aged in water was used, the final reaction mixture was still supplemented at the onset of the reaction with KI or KCl so that the resulting concentration of KI or KCl in the reaction mixtures was always 0.1 mM. At various time intervals, an aliquot of the reaction mixture was withdrawn and assayed by differential pulse polarography (DPP) for platinum not bound to DNA (Kim et al., 1990).

3.18 Statistic analysis

To evaluate statistical differences, the Student *t*-test was applied, unless otherwise indicated. *p*-values lower than 0.05 were considered statistically different.

4. RESULTS

4.1 Characterization of an *in vitro* model for the study of Cisplatin resistance in CRC

4.1.1 Effects of Cisplatin on different CRC cell lines.

We investigated the response of five CRC cell lines, HCT-116, HCT-116 $p53^{-/-}$, HCT-8, HT-29 and H-630 to Cisplatin treatment by measuring their IC_{50} values (Figure 1). HCT-116 cells turned out to be the most resistant, whereas HCT-8 the most sensitive (IC_{50} 22.0 ± 1.1 µM and 5.3 ±0.5 µM, respectively).

(A)

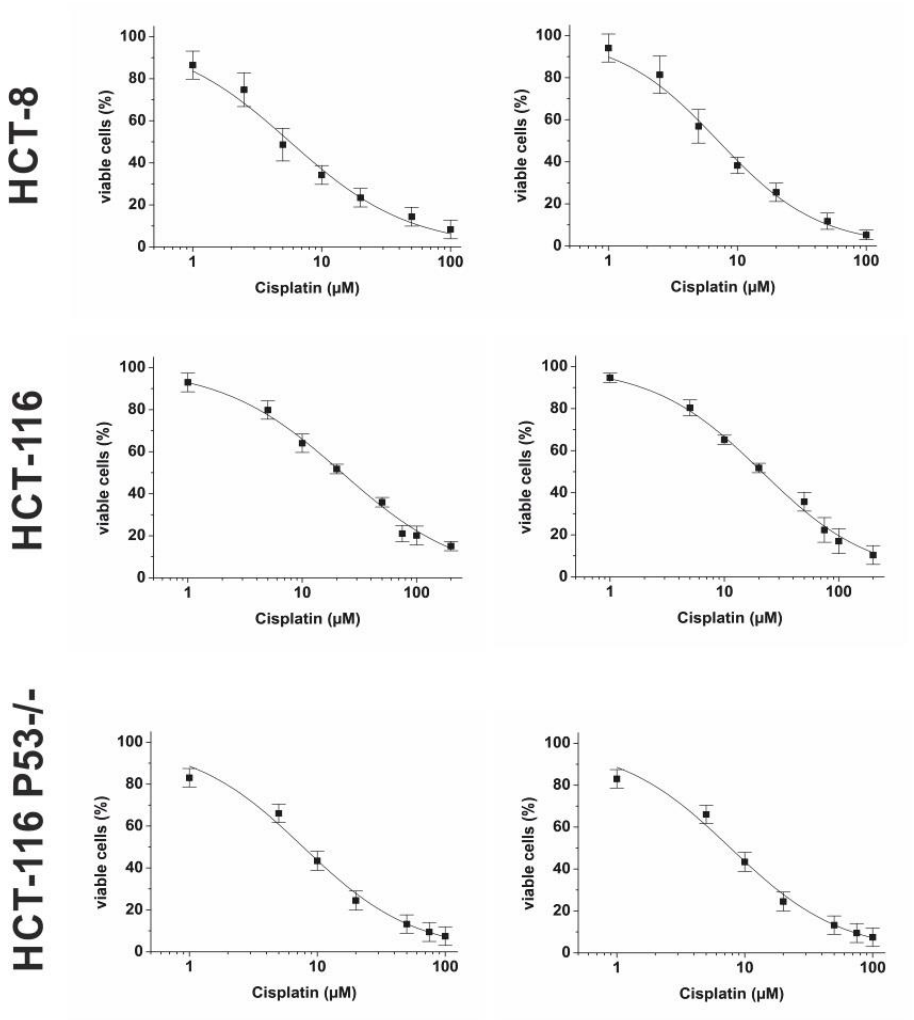

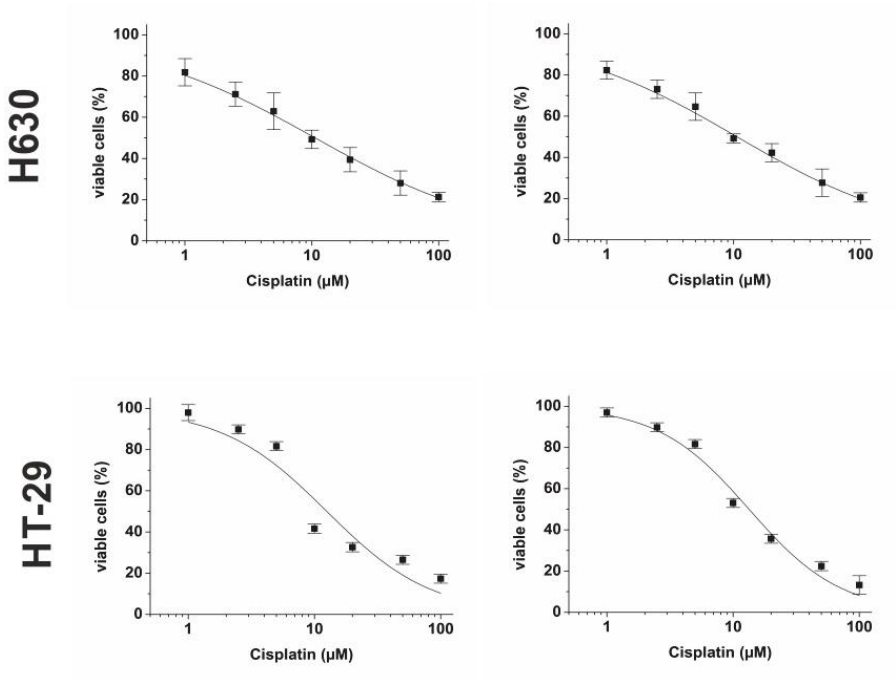

(B)

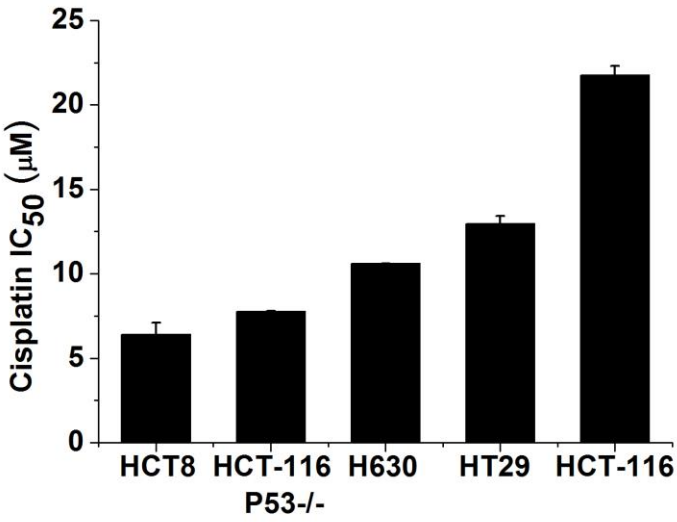

Figure 1. (A) Dose-response curve of Cisplatin effect on cell viability, assessed through the Trypan blue exclusion test after 24 hours of treatment, in different CRC cell lines. **(B)** Histogram of IC_{50} values determined on a panel of CRC cell lines.

The different sensitivity to Cisplatin of HCT-8 compared to HCT-116 was also confirmed when apoptosis (Figure 2), cell cycle distribution (Figure 3) and cell proliferation (Figure 4) were analysed.

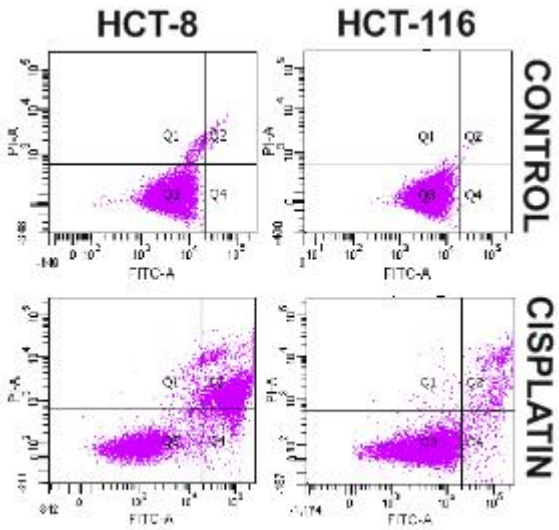

Figure 2 Representative dot plots of HCT-8 and HCT-116 cells treated for 24h at their IC_{50} for Cisplatin. Cells in Q3 (annexin$^-$/PI$^-$) were viable, cells in Q4 (annexin$^+$/PI$^-$) were in early stages of apoptosis, cells in Q2 (annexin$^+$/PI$^+$) were in late stages of apoptosis while cells in Q4 (annexin$^-$/PI$^+$) were dead.

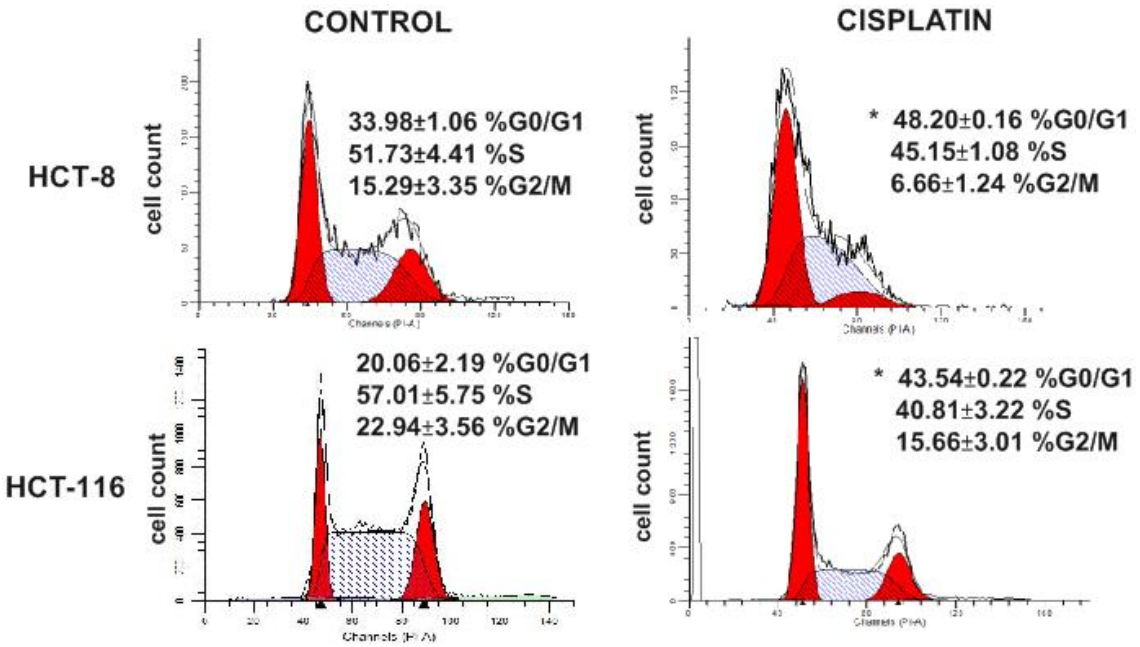

Figure 3 Representative histograms of HCT-8 and HCT-116 cell cycles after 24h of treatment at their Cisplatin IC_{50}.

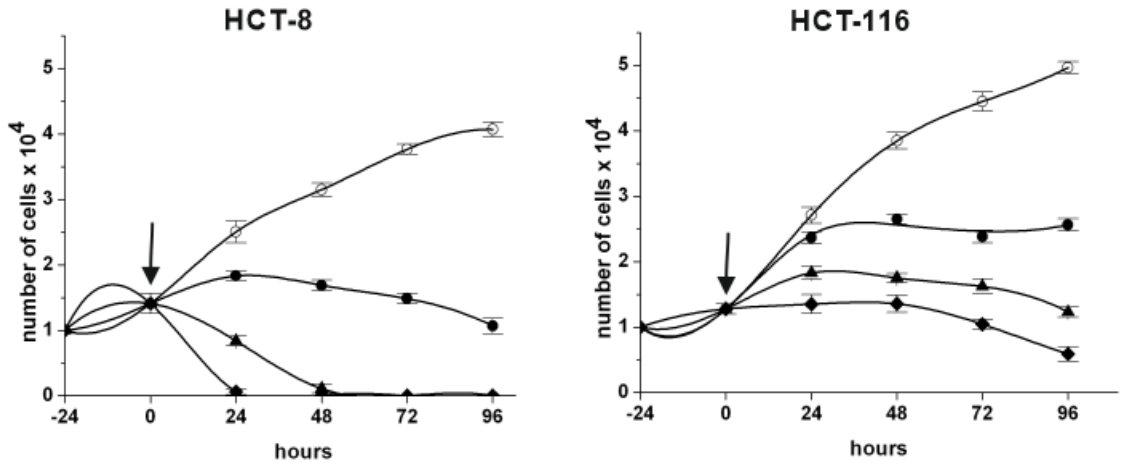

Figure 4 Effects of Cisplatin on proliferation of HCT-8 and HCT-116 cells. Cells were treated with different Cisplatin doses (1, 10 and 20 µM) and the number of live cells was determined in triplicate, and expressed as the number of Trypan Blue negative cells. Data are means ± SEM of six independent experiments. White circle=control, black circle= 1µM Cisplatin, black triangle= 10µM Cisplatin, black rhombus=20 µM Cisplatin. All the data relative to Cisplatin treatment turned out to be significantly different compared to the Control condition.

In all the experiments, Cisplatin was used at the IC_{50} of the two different cell lines; apoptosis and cell cycle phases were analyzed after 24 hours of treatment. Although used at lower concentration (5 µM), Cisplatin induced a greater apoptosis of HCT-8 cells (8.9% of cells in early and 36% of cells in late apoptosis), whereas it was less effective on HCT-116 cells (3.6% of cells in early apoptosis and 5.8 % of cells in late apoptosis (Figure 2 and Table 1) and produced a substantial increase in the percentage of G0/G1 cells in both HCT-8 and HCT-116 cells, accompanied by a decrease of cells in either G2/M (in HCT-8 cells) or S phase (in HCT-116 cells) (Figure 3 and Table 1). Consistent with all the above data, Cisplatin decreased HCT-8 cell proliferation, blocking cell proliferation even at 1 µM and producing a severe cell loss at 10 and 20 µM (Figure 8); on the contrary, it slowed down HCT-116 cell growth at 1 µM, but blocked cell growth only at 20 µM.

	$IC_{50\ (TB)}$ (µM) mean±SEM	$IC_{50\ (W-1)}$ (µM) mean±SEM	Early apoptosis (%)	Late apoptosis (%)
HCT-8				
Control	-		Undetectable	1.6±0.3
Cisplatin	6.4±0.7	7.3±0.9	8.9±0.2	35.5±6.0
	G0/G1 (%)	**S (%)**	**G2/M (%)**	
HCT-8				
Control	32.9±1.1	53.7±4.4	15.3±3.4	
Cisplatin	48.2±0.2	45.1±1.1	6.7±1.2	
	$IC_{50\ (TB)}$ (µM) mean±SEM	$IC_{50\ (W-1)}$ (µM) mean±SEM	Early apoptosis (%)	Late apoptosis (%)
HCT-116				
Control	-	-	Undetectable	Undetectable
Cisplatin	21.8±0.6	20.5±2.8	3.6±0.4	5.8±0.7
	G0/G1 (%)	**S (%)**	**G2/M (%)**	
HCT-116				
Control	20.1±2.2	57.0±5.7	22.9±3.6	
Cisplatin	43.5±0.2	40.8±3.2	15.7±3.0	

Table 1 IC_{50} of Cisplatin was determined after 24 hours of treatment by Trypan Blue and WST-1 assays ($IC50_{(TB)}$ and $IC50_{(W-1)}$ respectively). The IC_{50} values were calculated using Origin Software (Microcal Origin 8.0 software; OriginLab Corporation, Nothampton, MA). All original $IC_{50(TB)}$ are displayed in Figure 1.

4.1.2 Characterization of K^+ channel expression in HCT-116 and HCT-8 CRC cell lines

We then studied the relationships between K^+ channel expression and the effects of Cisplatin, using HCT-8 and HCT-116 cells as a model of Cisplatin-sensitivity and Cisplatin-resistance, respectively. We first analyzed the expression levels of different K^+ channels encoding genes, focusing on those reported to be expressed in CRC (Spitzner. 2007; Arcangeli et al, 2009; Huang et Jan. 2014): the voltage dependent potassium channels Kv10.1 or EAG1 (*KCNH1*), Kv11.1 or hERG1 (*KCNH2*) and Kv1.3 (*KCNA3*), the intermediate-conductance calcium-activated potassium channel KCa3.1 (*KCNN4*), the small-conductance KCa2.3 (*KCNN3*) and the big conductance KCa1.1 channels (*KCNMA1*). RQ-PCR data, expressed as Ct values of the gene under study as well as of the reference gene (*GAPDH*), are shown in Table 2. Only transcript with Ct values higher than 30 were considered to be positively expressed. *KCNH2* was expressed in both cell lines, but at higher level in HCT-116 cells, as previously reported (Lastraioli et al., 2004). *KCNN4* (high expression level) and *KCNN3* (medium expression level) were present almost exclusively in HCT-116 cells. All other transcripts, were negligible in both cell lines.

Table 2 also shows data relative to the expression of the main Cisplatin transporters found to be expressed in cancer cells: the copper transporters CTR1 (*SLC31A1*) and CTR2 (*SLC31A2*) as well as the two P-type ATPases ATP7A (*ATP7A*) and ATP7B (*ATP7B*). Three of them, *SLC31A1*, *ATP7A* and *ATP7B*, were expressed and the expression levels did not differ between the two CRC cell lines.

	HCT-8 Ct value (mean±SEM)	**HCT-116** Ct value (mean±SEM)
KCNH1	**37.19±0.95**	**39.01±0.99**
GAPDH	17.13±0.40	*18.19±0.22*
KCNH2	**28.04±0.53**	**26.51±0.84**
GAPDH	17.17±0.01	17.65±0.77
KCNA3	**30.43±0.14**	**33.81±0.29**
GAPDH	*17.93±0.21*	*18.19±0.22*
KCNMA1	**32.04±0.62**	**31.77±1.91**
GAPDH	*16.99±0.17*	*17.06±0.04*
KCNN3	**37.09±1.63**	**28.34±0.55**
GAPDH	*17.16±0.01*	*17.10±0.02*
KCNN4	**32.22±0.87**	**23.74±0.42**
GAPDH	*17.93±0.21*	*18.19±0.22*
SLC31A1	**22.78±0.15**	**22.37±0.18**
GAPDH	*17.09±0.07*	*16.96±0.14*
SLC31A2	**31.18±0.34**	**32.86±0.22**
GAPDH	*17.09±0.07*	*16.96±0.14*
ATP7A	**23.94±0.18**	**25.06±0.28**
GAPDH	*17.09±0.07*	*16.96±0.14*
ATP7B	**25.21±0.06**	**26.45±0.10**
GAPDH	*17.09±0.07*	*16.96±0.14*

Table 2 Gene expression levels were evaluated by RQ-PCR using the primer pairs reported in Materials and Methods. Table shows the mean ± SEM of Ct values of the different transcripts (in bold italics) as well as of the housekeeping gene GAPDH (in italics) obtained in three different experiments. Name of the ion channel/transporters encoding gene are given using the HGNC nomenclature.

Based on the above transcription data, we evaluated the expression of hERG1 and KCa3.1 and KCa2.3 proteins in HCT-8 and HCT-116 cells, by Western Blot (Figure 5) and immunofluorescence (Figure 6). Both these techniques showed a higher expression of hERG1 in HCT-116 compared to HCT-8 cells. These results fully agree with what was previously shown (Lastraioli et al., 2004). HCT-116 cells also expressed a very

high amount of KCa3.1 and KCa2.3 proteins, whereas HCT-8 showed a smaller KCa3.1 and KCa2.3 bands (Figure 5) and a lower IF signal as well (Figure 6).

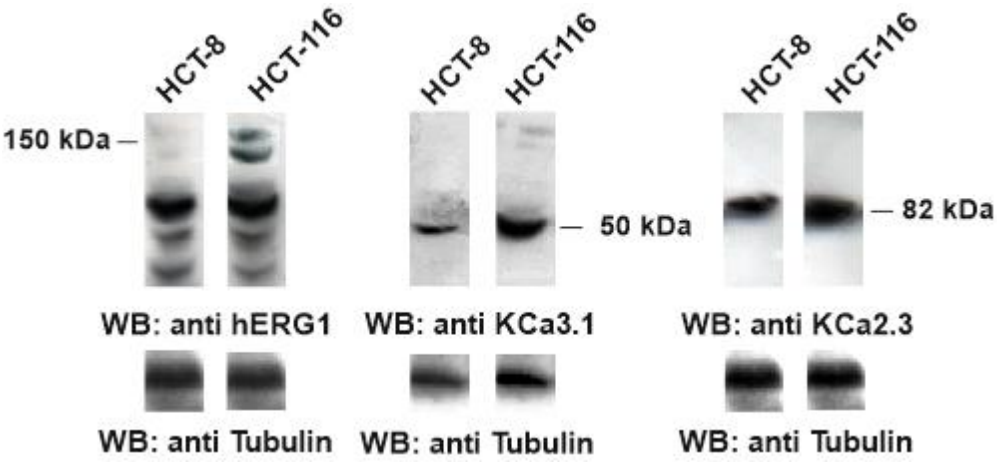

Figure 5 Western blots of hERG1, KCa3.1 and KCa2.3 protein expression in HCT-8 and HCT-116 cells. Cell lysates from HCT-8 and HCT-116 cells were probed with the anti-KCa3.1 and anti-KCa 2.3 antibodies and anti-pan hERG1 antibody. Reprobing of the membranes with anti-tubulin antibody is reported in the bottom panels. The arrows indicate the bands corresponding to hERG1 (panel on the left), KCa3.1 (central panel) and KCa2.3 respectively (panel on the right).

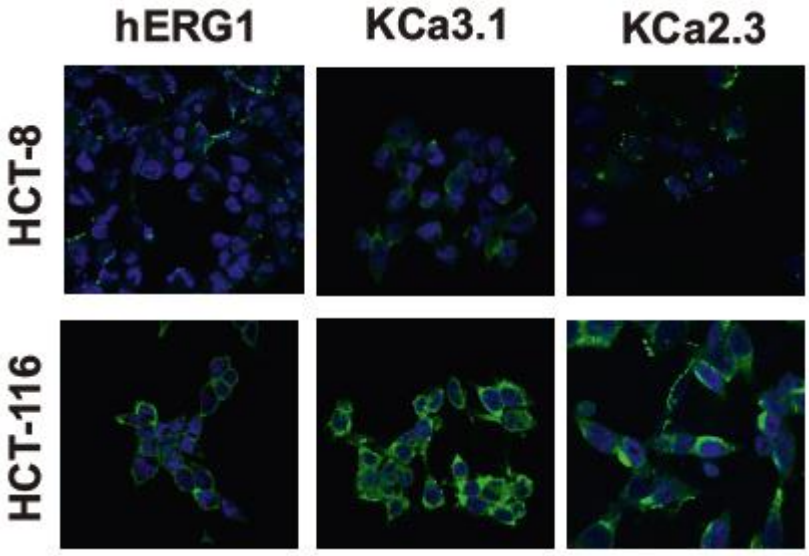

Figure 6 Immunofluorescence of hERG1, KCa3.1 and KCa2.3 proteins in HCT-8 and HCT-116 cells seeded onto glass slides. For HCT-116 cells antigen colocalization was also evaluated. The anti-hERG1mAb antibody (Dival Toscana Srl) (and the Alexa488-conjugated secondary anti mouse antibody) (left panels) , the anti-KCa3.1 polyclonal antibody (Sigma Aldrich - AV35098) (and Alexa488-conjugated secondary anti rabbit antibody) (central panels) and the anti-KCa2.3 polyclonal antibody (Sigma Aldrich - P4747) (and Alexa488-conjugated secondary anti rabbit antibody) (right panels) were used. Magnification was 60X.

Then we evaluated the presence of selective hERG1 and KCa3.1/KCa2.3 currents on both cell lines. Traces for hERG1 channel on HCT-116 and HCT-8 cells obtained after application of a "ramp" protocol at either -70 or 0 mV holding potential are shown in Figure 7. The difference in hERG1 current (i.e. the inward inactivating current elicited at -120 mV starting from a 0 mV holding potential) between the two cell lines is evident.

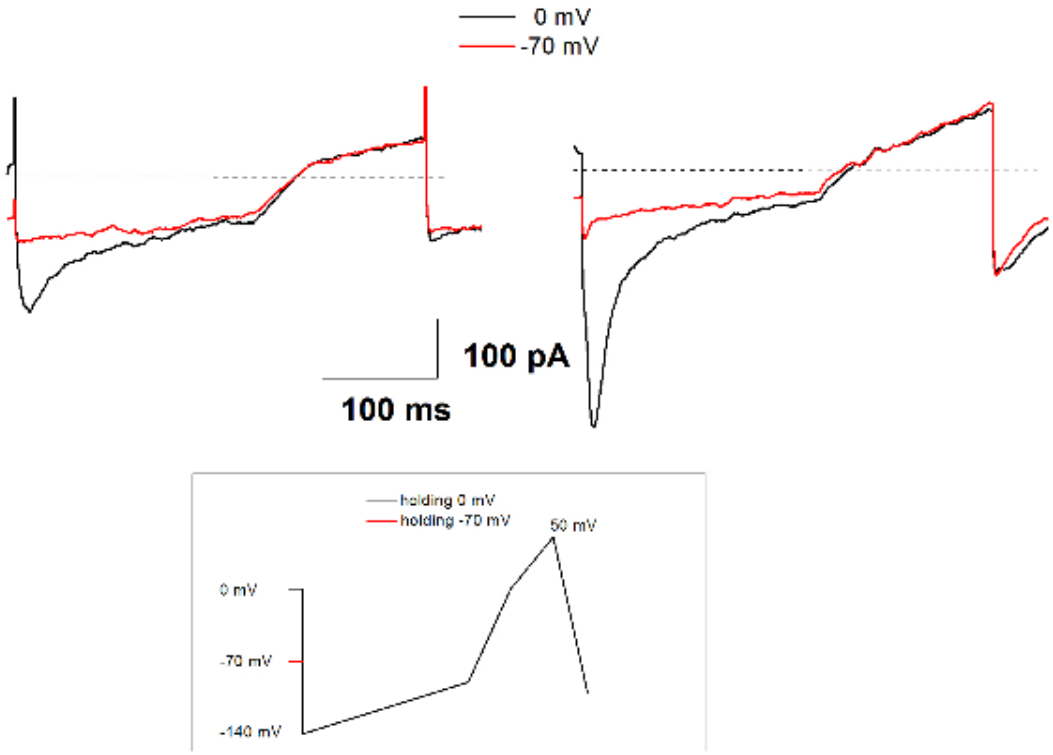

Figure 7 Exemplificative hERG1 current traces elicted with the outlined protocol in HCT-8 (left) and HCT-116 (right) cells.

This protocol does not allow to elicit "pure" KCa3.1 or 2.3 currents and since it was difficult to discriminate between KCa2.3 and KCa3.1 currents elicited after applying the protocol as in Sankaranarayanan et al. 2009 without using additional pharmacological tools, we address the currents recorded in these conditions as KCa2/3 currents.

We finally evaluated the membrane potential (Vrest) of the two cell lines. HCT-116 cells showed a significantly more hyperpolarized Vrest compared to HCT-8 cells, consistent with their higher expression of K^+ currents (Table 3).

	V_{rest}
HCT-8	-13.08±2.55 (n=12)
HCT-116	-33.50±3.19 (n=6)

Table 3 Membrane potential (Vrest) of HCT-8 and HCT-116 cells.

4.2 Effect of Cisplatin and K^+ channel modulators on CRC cells.

We then tested the effects of different K^+ channel modulators targeting the main K^+ channel proteins expressed in CRC cells (i.e. KCa3.1, KCa2.3 and hERG1) on cell vitality (Table 4, Table 5 and Figure 8), apoptosis (Table 4 and Figure 9), cell cycle and proliferation (Table 4, Table 5 and Figure 10) of HCT-8 and HCT-116 cells. For some compounds, the effects on selected currents was tested (Figure 12). Overall, the following compounds were tested: (1) Riluzole, a broad modulator of ion channels

(Sankaranarayanan et al. 2009; Bellingham et al. 2011) capable to activate both KCa2.3 and KCa3.1 channels, as well as to inhibit hERG1 and voltage-gated sodium channels; (2) SKA-31, a more potent and selective activator of KCa3.1 currents; (3) TRAM-34, an inhibitor of KCa3.1 channels, (4) E4031, a specific hERG1 inhibitor. We also evaluated the viability effect of Oxaliplatin, the Cisplatin analogue currently used in CRC therapy; this drug exhibited a less efficacy at 24h in our in vitro model for both the cell lines tested.

	$IC_{50\ (TB)}$ (µM) mean±SEM	**$IC_{50\ (W-1)}$ (µM)** mean±SEM	**Early apoptosis (%)**	**Late apoptosis (%)**
HCT-8				
Control	-		Undetectable	1.6±0.3
Oxaliplatin	24.1±3.0	21.5±0.3	ND	ND
Riluzole	12.9±0.2	11.9±0.7	2.6±0.2	7.9±0.2
SKA-31	49.3±4.0	31.6±1.5	3.8±0.5	25.5±4.2
TRAM-34	20.1±0.7	22.0±0.8	0.8±0.1	1.5±0.5
E4031	11.7±0.5	12.5±0.3	0.8±0.2	5.1±0.7
	G0/G1 (%)	**S (%)**	**G2/M (%)**	
HCT-8				
Control	32.9±1.1	53.7±4.4	15.3±3.4	
Riluzole	1.6±0.3	5.5±0.3	93.0±0.1	
SKA-31	50.9±0.2	48.5±0.6	0.6±0.6	
TRAM-34	66.1±0.7	33.3±1.3	0.6±0.6	
E4031	25.4±0.7	55.5±2.6	19.1±3.3	

Table 4 IC_{50} of Oxaliplatin, Riluzole, SKA-31, TRAM-34 and E4031 were determined after 24 hours of treatment by Trypan Blue and WST-1 assays ($IC50_{(TB)}$) and $IC50_{(W-1)}$ respectively. The IC_{50} values were calculated using Origin Software (Microcal Origin 8.0 software; OriginLab Corporation, Nothampton, MA). Apoptosis and cell cycle distributions were evaluated by treating HCT-8 cells with IC_{50} values of each drug for 24h. Data of means±ESM of two independent experiments. ND = not determined. Percentage of cells in early (Annexin +/PI-

cells) and late apoptosis (Annexin +/PI+ cells) was determined by Annexin/PI assay. Cell cycle distribution (percentage of cells in each phase of the cell cycle) was assessed by flow cytometry after staining cells with propidium iodide (PI).

	$IC_{50\ (TB)}$ (µM) mean±SEM	**$IC_{50\ (W-1)}$ (µM)** mean±SEM	**Early apoptosis (%)**	**Late apoptosis (%)**
HCT-116				
Control	-	-	Undetectable	Undetectable
Oxaliplatin	57.4±9.4	51.8±2.9	ND	ND
Riluzole	8.5±0.1	8.1±1.1	24.5±1.5	22.8±1.7
SKA-31	4.6±0.1	4.7±0.1	5.7±1.7	1.9±0.6
TRAM-34	27.6±0.4	24.8±3.6	8.3±2.1	4.0±1.0
E4031	4.5±0.5	3.6±0.2	1.8±0.3	2.4±0.2
	G0/G1 (%)	**S (%)**	**G2/M (%)**	
HCT-116				
Control	20.1±2.2	57.0±5.7	22.9±3.6	
Riluzole	57.5±0.9	17.4±1.4	25.2±2.2	
SKA-31	57.4±2.0	23.7±0.2	18.9±1.7	
TRAM-34	47.4±1.8	29.7±3.8	23.0±2.0	
E4031	47.6±3.4	24.3±6.1	28.2±2.7	

Table 5 IC_{50} of Oxaliplatin, Riluzole, SKA-31, TRAM-34 and E4031 were determined after 24 hours of treatment by Trypan Blue and WST-1 assays ($IC50_{(TB)}$) and $IC50_{(W-1)}$ respectively. The IC_{50} values were calculated using Origin Software (Microcal Origin 8.0 software; OriginLab Corporation, Nothampton, MA). Apoptosis and cell cycle distributions were evaluated by treating HCT-116 cells with IC_{50} values of each drug for 24h. Data of means±ESM of two independent experiments. ND = not determined. Percentage of cells in early (Annexin +/PI- cells) and late apoptosis (Annexin +/PI+ cells) was determined by Annexin/PI assay. Cell cycle distribution (percentage of cells in each phase of the cell cycle) was assessed by flow cytometry after staining cells with propidium iodide (PI).

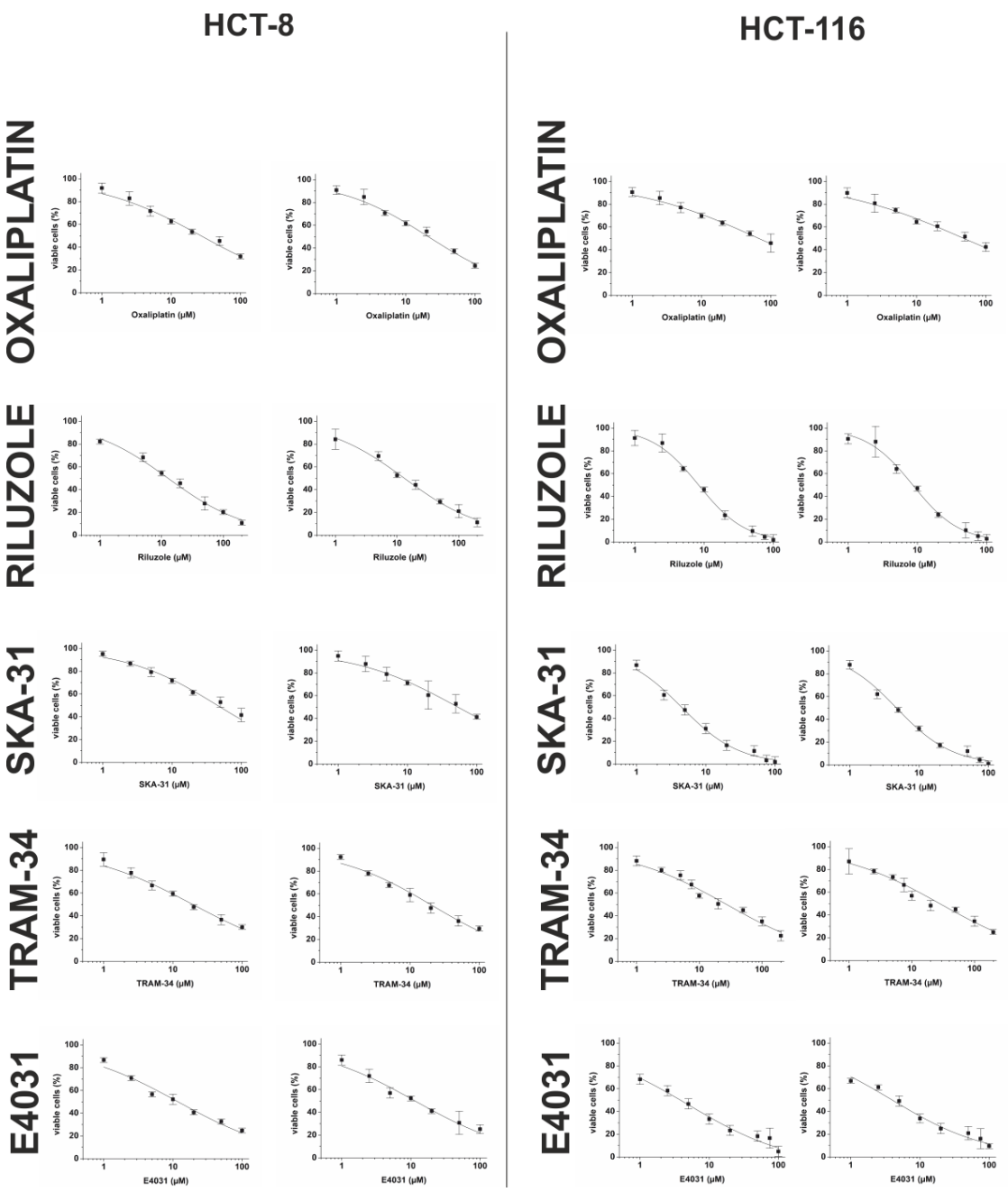

Figure 8 IC_{50} values of Oxaliplatin, Riluzole, SKA-31, TRAM-34 and E4031 on HCT-8 and HCT-116 CRC cell lines. Cell viability was assessed through the Trypan blue exclusion test after 24 hours of treatment.

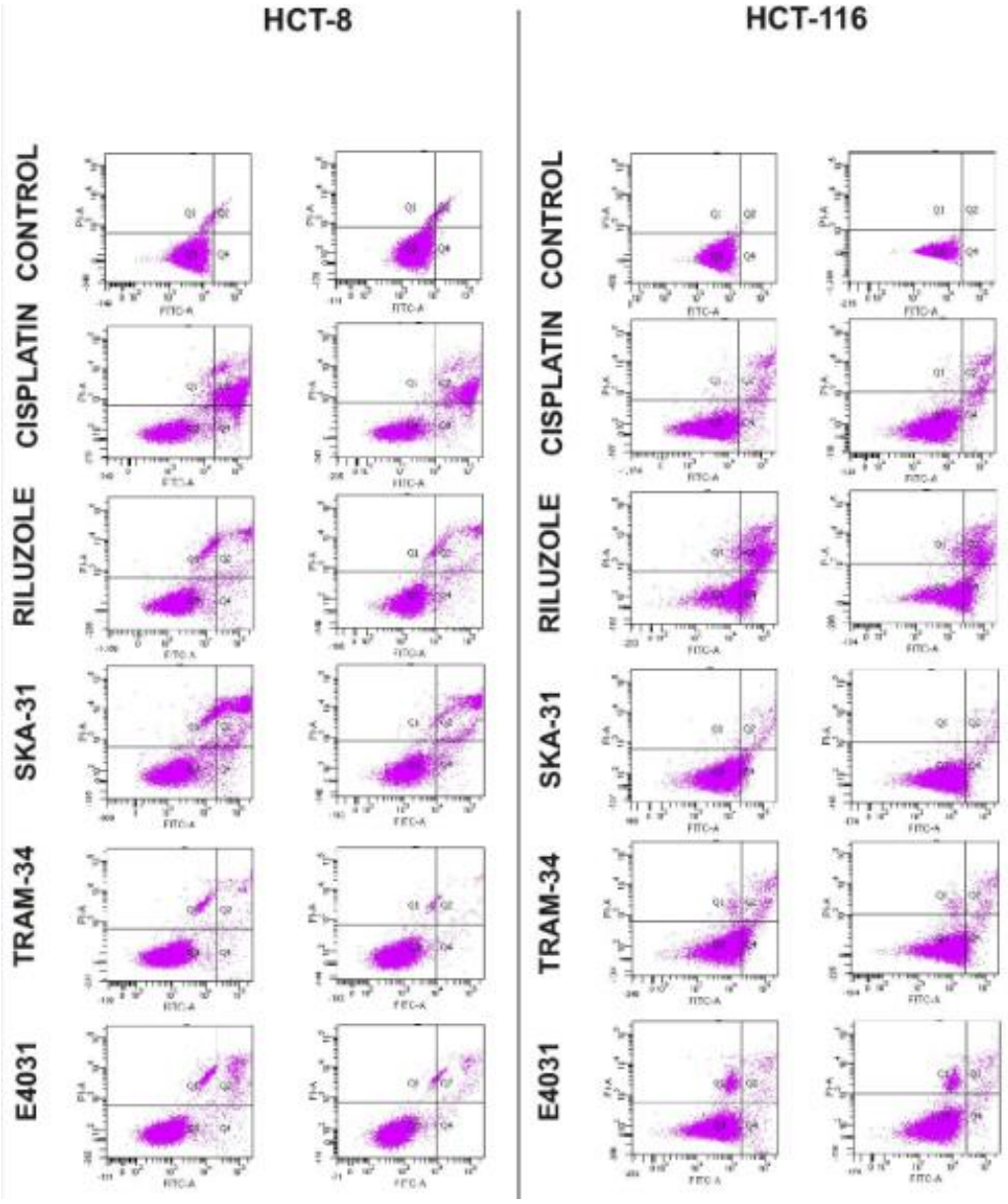

Figure 9 Effects of Cisplatin, Riluzole, SKA-31, TRAM-34 and E4031 on apoptosis distribution of HCT-8 and HCT-116 cells. Apoptosis was evaluated after 24 hours of treatment through the Annexin/PI assay. The figure shows dot plots of control and treated cells at the same experimental time point.

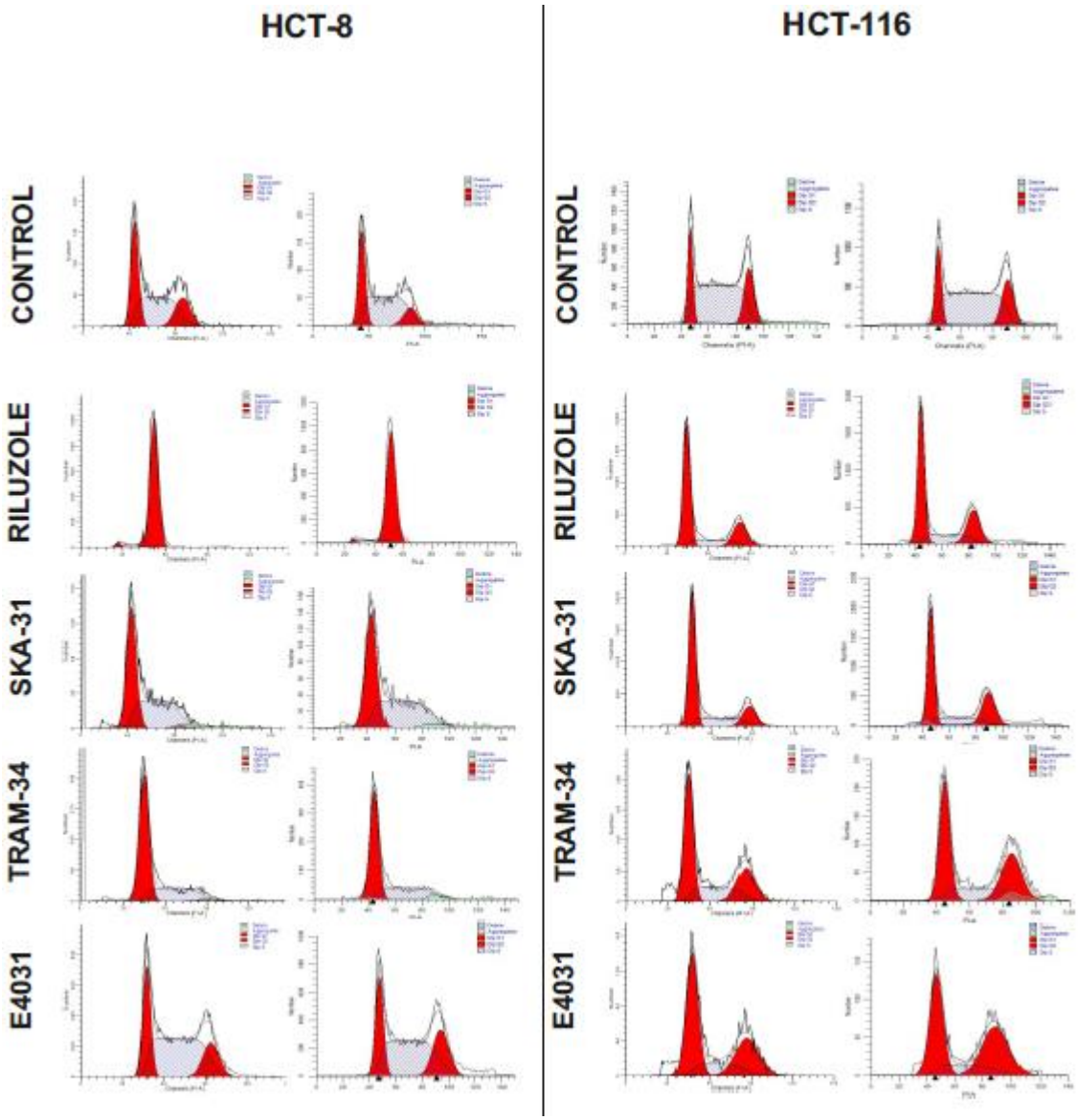

Figure 10 Plot of the number of cells labelled with Propidium Iodide determined by flow cytometry, in Control conditions and after 24 hours of treatment at IC50 concentrations of Riluzole, SKA-31, TRAM-34, E4031 and NS-1643 on cell cycle distribution of HCT-8 and HCT-116 cells .

All the K^+ channel modulators were cytotoxic for CRC cells but, in contrast to Cisplatin, their IC_{50} values were generally lower (and hence the drug more effective) on HCT-116 compared to HCT-8 cells. TRAM-34 displayed high IC_{50} values in both cell lines. Overall, the HCT-116 cells, which are more resistant to Cisplatin turned out to be sensitive to KCa3.1 (and KCa2.3) activation or hERG1 inhibition.

Riluzole induced 23% of HCT 116 cells to undergo apoptotic death, and a lower percentage (8%) of HCT-8 cells, whilst it produced a G0/G1 block only in HCT-116 cells. Also SKA-31 produced a significant G0/G1 block in HCT-116 cells, whilst it induced significant apoptosis in HCT-8 cells, with a minimal effect on HCT-116 cells. It is however worth noting that SKA-31 concentration used in HCT-8 cells was ten times higher than in HCT-116 cells. The inhibition of KCa3.1 currents by TRAM-34 did not induce any apoptotic effect in either cell line. hERG1 inhibition triggered only a low level of apoptosis (only 5 % late apoptotic cells after 24 hours of treatment in HCT-8 cells); but induced a significant G0/G1 block in HCT-116 cells.

A set of experiments was then conducted in which the different K^+ channel modulators were added at time 0, and cell growth was measured at different times of incubation in the absence or in the presence of the drug. No further re-addition of the compounds was performed. The analysis of cell proliferation showed that all the K^+ channel modulators, when tested at the IC_{50} value, inhibited the growth of both HCT-8 and HCT-116 cells. In HCT-116 the inhibitory effect of SKA-31 and E4031, which induced scarce apoptosis, tended to decline at longer incubation times (Figure 11).

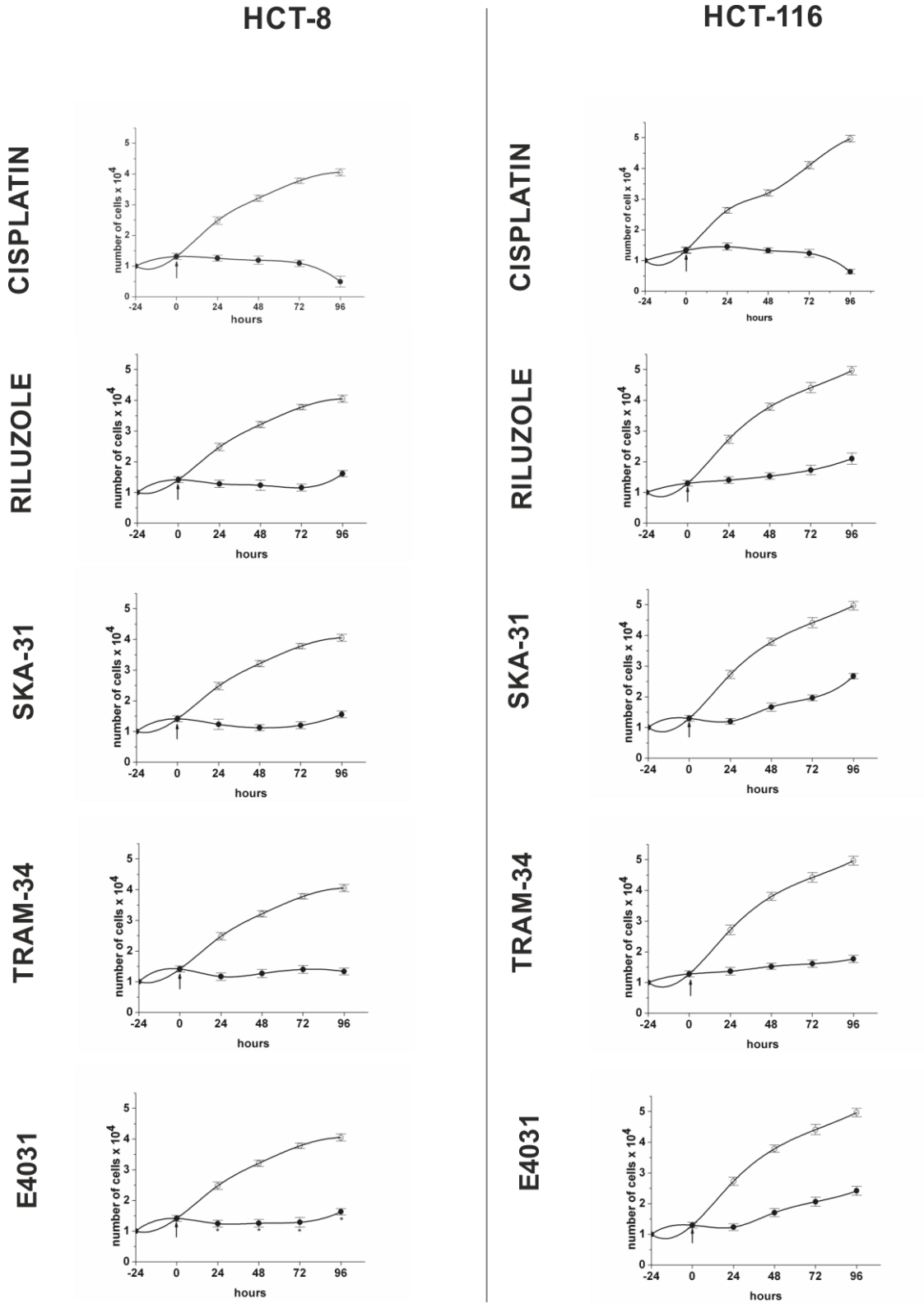

Figure 11 Effects of Cisplatin, Riluzole, SKA-31, E4031 and TRAM-34 (at the IC_{50} value) on the proliferation of HCT-8 and HCT-116 after a single treatment (arrow) given as the number of Trypan Blue negative cells. Data are means ± SEM of two independent experiments. All the data relative to treatment with the different K^+ channel modulators turned out to be significantly different compared to the Control condition.

4.2.1 Effects of Riluzole, SKA-31 and Cisplatin on K^+ currents

We tested the effects of Riluzole and SKA-31 on K^+ currents (calcium-dependent K^+ and hERG1 currents) of HCT-116 cells (Figure 18). Both drugs were tested at the IC_{50} value, unless otherwise indicated. The effects of both E4031 and TRAM-34 on hERG1 and KCa3.1 currents in such cells has been previously reported (Crociani et al., 2013; Wulff et al. 2007, respectively). Since it was difficult to discriminate between KCa2.3 and KCa3.1 currents elicited in HCT-116 cells after applying the protocol as in Sankaranarayanan et al. 2009 without using additional pharmacological tools, we address the currents recorded in these conditions as KCa2/3 currents. Both Riluzole and SKA-31 activated KCa2/3 currents (Figure 12), with a fold increase over control of 2.11 ± 0.46 n=9 and 4.46 ± 1.74 n=10, respectively (Table 6). Riluzole also inhibited hERG1 currents, as expected (Sankaranarayanan et al. 2009), with a 23 % inhibitory effect at 10 µM (close to IC_{50} values) which reached 44% at 45 µM concentration (Table 6). We also tested the effects of Cisplatin on the same K^+ currents: Cisplatin did not significantly affect KCa2/3 currents neither in control conditions or after SKA-31 stimulation (Figure 13), and displayed a small inhibitory effect on hERG1 currents (Figure 13 and Table 6). All the drugs used didn't exhibit a relevant change in HCT-116 resting potential compared to the control (Table 7).

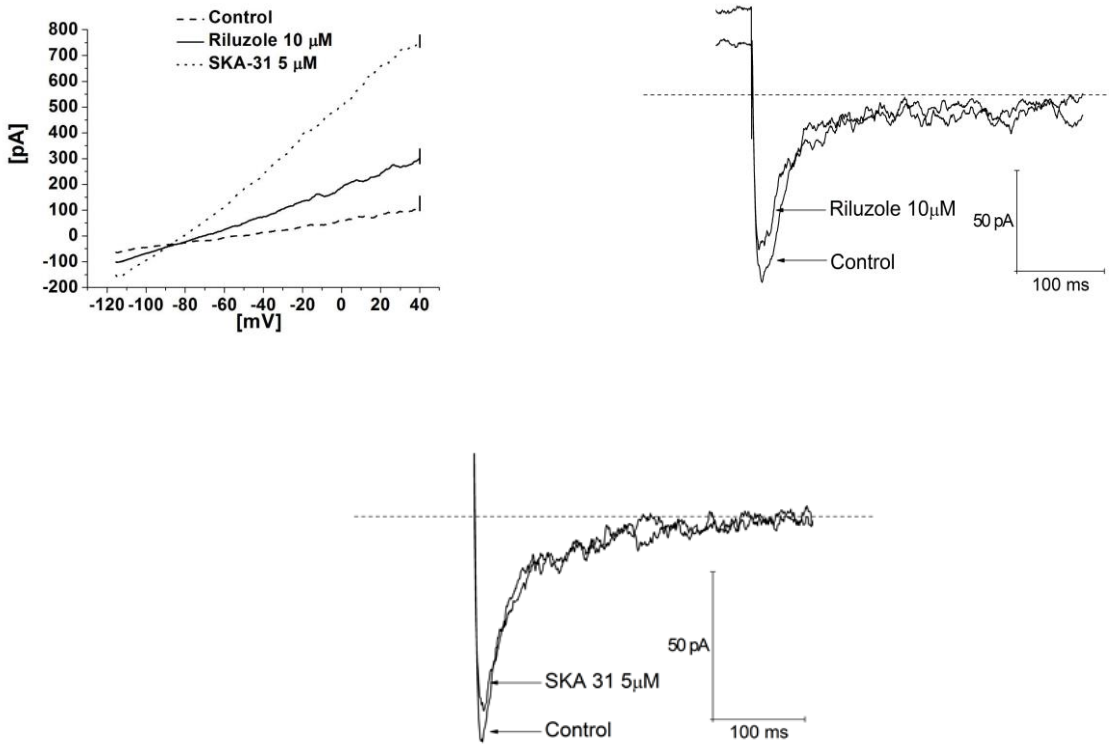

Figure 12: Effect of Riluzole and SKA-31 at IC_{50} values on native KCa3.1 (top) and hERG1 (bottom) currents on HCT-116 cell line. In comparison with controls, Riluzole and SKA-31 significantly increased KCa3.1 currents (paired *t*-test respectively p= 0.00511, n=9 and p=0.0183, n=10), with the latter exerting a higher activity on KCa3.1 channels.

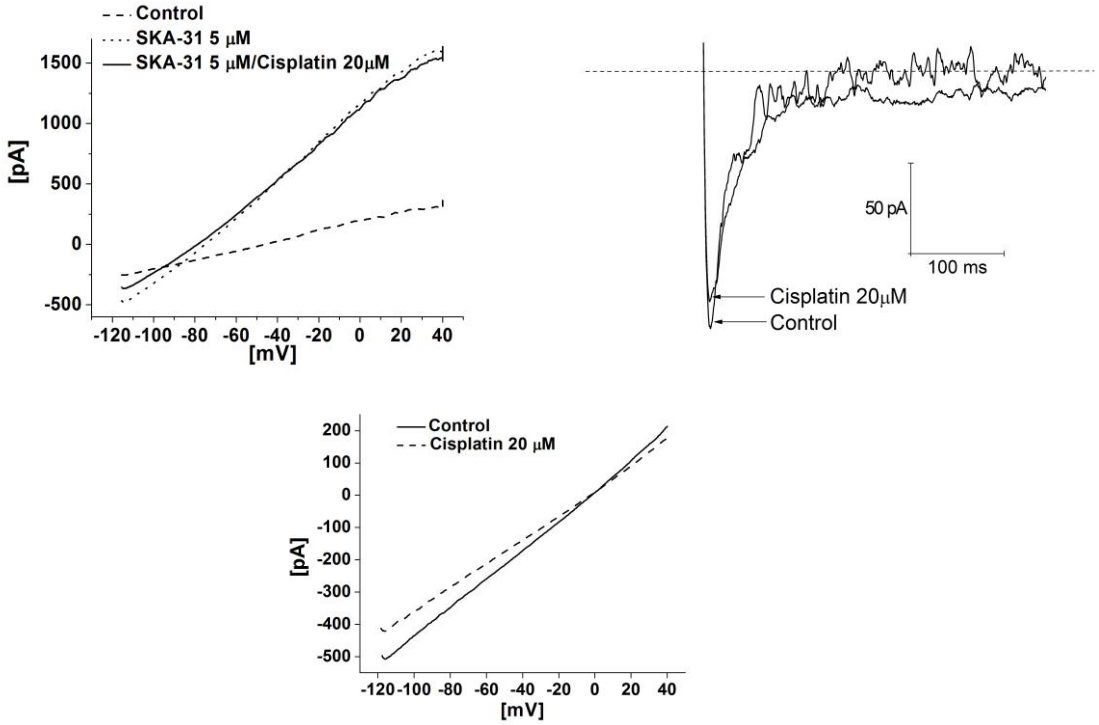

Figure 13: Effect of Cisplatin at near IC_{50} concentrations on KCa2/3 and hERG1 currents.

Drug (μM)	KCa 2/3 slope fold variation (mean ± SEM)	hERG1 current inhibition (%) (mean ± SEM)
Cisplatin (20)	1.04 ± 0.25 (n=9)	5.75 ± 2.16 (n=10)
Cisplatin (20) after SKA-31 (5)	1.10 ± 0.12 (n=10)	ND
Riluzole (10)	2.11 ± 0.46 (n=9) *	23.26 ± 4.49 (n=6) *
Riluzole (45)	6.74 ± 7.74 (n=6)	43.83 ± 7.02 (n=6) *
SKA-31 (5)	4.36± 1.67 (n=10) *****	7.53 ± 1.81 (n=11)

Table 6: Effect of Cisplatin, SKA-31 and Riluzole at different concentrations on KCa2/3 and hERG1 currents. The "*" indicate a statistical significance (paired *t*-test >0.05).

Drug (μM)	$V_{rest24h}$ (mean ± SEM)
Riluzole (8)	-41.40±5.78 (n=5)
SKA-31 (5)	-30.83±3.57 (n=6)
TRAM-34 (28)	-36.50±3.21 (n=6)
E4031 (4)	-35.29±4.67 (n=7)

Table 7: Effect of Riluzole, SKA-31, TRAM-34 and E4031, at IC_{50} values, after 24h of treatment on resting potential of HCT-116 cells.

4.3 Effects of Cisplatin in combination with K^+ channel modulators.

The above reported effects of the different K^+ channels modulators on CRC cells, as well as the ability of Riluzole to increase the cytotoxic effect of Cisplatin in epidermoid cancer cells (Lee et al., 2008) prompted us to test their combination with Cisplatin in both HCT-8 and HCT-116 cells. We followed the procedure already applied in Pillozzi et al., 2011 and calculated the combination index (CI) to assess synergic,

antagonistic or additive effect of the different combinations. Data in Table 8 show the CI values at the IC_{50}, whereas data relative to CI values at IC_{75} and IC_{90} are in Table 9.

	Combination index at IC_{50} mean±SEM (Tripan Blue)	**Combination index at IC_{50}** mean±SEM (WST-1)
HCT-8		
Cisplatin + Riluzole	2.75±0.45	ND
Cisplatin + SKA-31	2.00±0.10	ND
Cisplatin + TRAM-34	1.90±0.06	ND
Cisplatin + E4031	1.84±0.08	ND
HCT-116		
Cisplatin + Riluzole	0.87±0.14	0.88±0.09
Cisplatin + SKA-31	0.50±0.25	0.74±0.07
Cisplatin + TRAM-34	4.39±1.02	2.89±0.24
Cisplatin + E4031	0.60±0.01	0.78±0.10
Oxaliplatin + Riluzole	0.98±0.01	0.97±0.01
Oxaliplatin + SKA-31	0.71±0.05	0.82±0.09
Oxaliplatin + TRAM-34	3.36±0.34	3.13±0.18
Oxaliplatin + E4031	0.83±0.01	0.57±0.04

Table 8: HCT-8 and HCT-116 cells were exposed to concentrations of Cisplatin and Oxaliplatin corresponding to their $IC_{50(TB)}$ value in combination with IC_{50} of Riluzole, SKA-31, TRAM-34 and E4031 with a 2-fold serial dilution (1/1, 1/2, 1/4, 1/8, 1/16, 1/32, 1/64) for 24 hours and then cell viability was evaluated using Trypan blue exclusion assay. For HCT-116, also the WST-1 assay was used. Means±ESM are relative to two independent experiments. CI values were calculated using Calcusyn software Version 2 (Biosoft). CI > 1, antagonisms; CI = 1, additivity; CI < 1, synergy. ND= Not Determined

	Combination index at IC_{75} mean±SEM (Trypan blue)	**Combination index at IC_{75}** mean±SEM (WST-1)	**Combination index at IC_{90}** mean±SEM (Trypan blue)	**Combination index at IC_{90}** mean±SEM (WST-1)
HCT-8				
Cisplatin + Riluzole	3.99±0.11	ND	6.13±0.63	ND
Cisplatin + SKA-31	4.11±0.21	ND	8.73±0.43	ND
Cisplatin + TRAM-34	3.86±0.74	ND	8.37±2.74	ND
Cisplatin + E4031	2.92±0.08	ND	5.01±0.06	ND
HCT-116				
Cisplatin + Riluzole	1.43±0.26	0.98±0.13	2.42±0.49	1.08±0.16
Cisplatin + SKA-31	0.91±0.25	0.68±0.06	1.86±0.12	1.28±0.70
Cisplatin + TRAM-34	4.78±0.21	2.13±0.07	7.24±1.06	1.62±0.23
Cisplatin + E4031	0.92±0.19	0.87±0.08	1.63±0.63	0.98±0.05
Oxaliplatin + Riluzole	1.21±0.29	0.92±0.01	2.07±0.94	0.89±0.01
Oxaliplatin + SKA-31	0.74±0.13	1.03±0.13	1.00±0.28	1.30±0.18
Oxaliplatin + TRAM-34	2.08±0.35	5.12±0.15	1.40±0.58	8.99±0.01
Oxaliplatin + E4031	0.41±0.05	1.23±0.29	0.23±0.08	2.74±1.05

Table 9: HCT-116 cell line was exposed to IC_{50} of Cisplatin and Oxaliplatin (while HCT-8 only to IC_{50} of Cisplatin) in combination with IC_{50} of Riluzole, SKA-31, TRAM-34 and E4031 with a 2-fold serial dilution (1/1, 1/2, 1/4, 1/8, 1/16, 1/32, 1/64) for 24 hours and then cell viability was evaluated using Trypan blue exclusion assay and, for HCT-116, also by WST-1 assay. The means are relative to two independent experiments. CI values were calculated using Calcusyn software Version 2 (Biosoft). CI > 1, antagonisms; CI = 1, additivity; CI < 1, synergy.

Riluzole, SKA-31 and E4031 had a synergic effect with Cisplatin. On the contrary, TRAM-34 was antagonistic. The synergy of Cisplatin with Riluzole, SKA-31 or E4031 occurred only in Cisplatin-resistant HCT-116 cells, and was also observed when cells were treated with Oxaliplatin.

Riluzole, SKA-31 and E4031 significantly increased the pro-apoptotic effect of Cisplatin in HCT-116 cells (Table 10 and Figure 14). The strongest effect was obtained with Riluzole. Both Riluzole and SKA-31 also induced an increase in the percentage of

cells in G2/M phase, while E4031 induced a G0/G1 block in HCT-116 cells (Table 10 and Figure 15). TRAM-34 only significantly increased in HCT-116 the percentage of G2/M cells. On the contrary, the antagonistic effect of K^+ channel modulators with Cisplatin in HCT-8 cells could be explained by an overall decrease of apoptosis (Table 10).

HCT-116	**Late apoptosis (%)**	**G0/G1 (%)**	**S (%)**	**G2/M (%)**
Cisplatin	5.75±0.65	43.54±0.22	40.81±3.22	15.63±3.01
Cisplatin + Riluzole	22.00±5.10	38.34±3.40	23.00±12.89	38.67±9.49
Cisplatin + SKA-31	12.15±2.25	43.14±3.38	26.15±14.06	30.72±10.67
Cisplatin + E4031	17.85±3.85	49.12±0.41	30.39±1.21	20.50±0.81
Cisplatin + TRAM-34	8.65±1.85	47.98±2.28	8.35±5.15	43.66±2.87
HCT-8	**Late apoptosis (%)**	**G0/G1 (%)**	**S (%)**	**G2/M (%)**
Cisplatin	35.45±5.95	48.20±0.16	45.15±1.08	6.66±1.24
Cisplatin + Riluzole	55.95±3.45	7.27±3.95	45.01±4.86	47.73±0.91
Cisplatin + SKA-31	11.30±3.80	31.38±0.83	56.29±2.43	12.34±1.31
Cisplatin + E4031	28.45±9.15	38.96±2.62	57.11±0.39	3.93±3.01
Cisplatin + TRAM-34	21.00±7.20	45.58±0.77	50.29±3.47	4.13±2.69

Table 10: HCT-116 and HCT-8 cells were exposed to IC_{50} concentrations of either Cisplatin alone or in combination with IC_{50} concentrations of Riluzole, SKA-31, TRAM-34 and E4031. Data are means ± SEM relative to two independent experiments, each carried out in triplicate. The percentage of cells in early late apoptosis (Annexin +/PI+ cells) was determined by Annexin/PI assay. Cell cycle distribution (expressed as percentage of cells in each phase of the cell cycle) was assessed by flow cytometry after staining cells with propidium iodide.

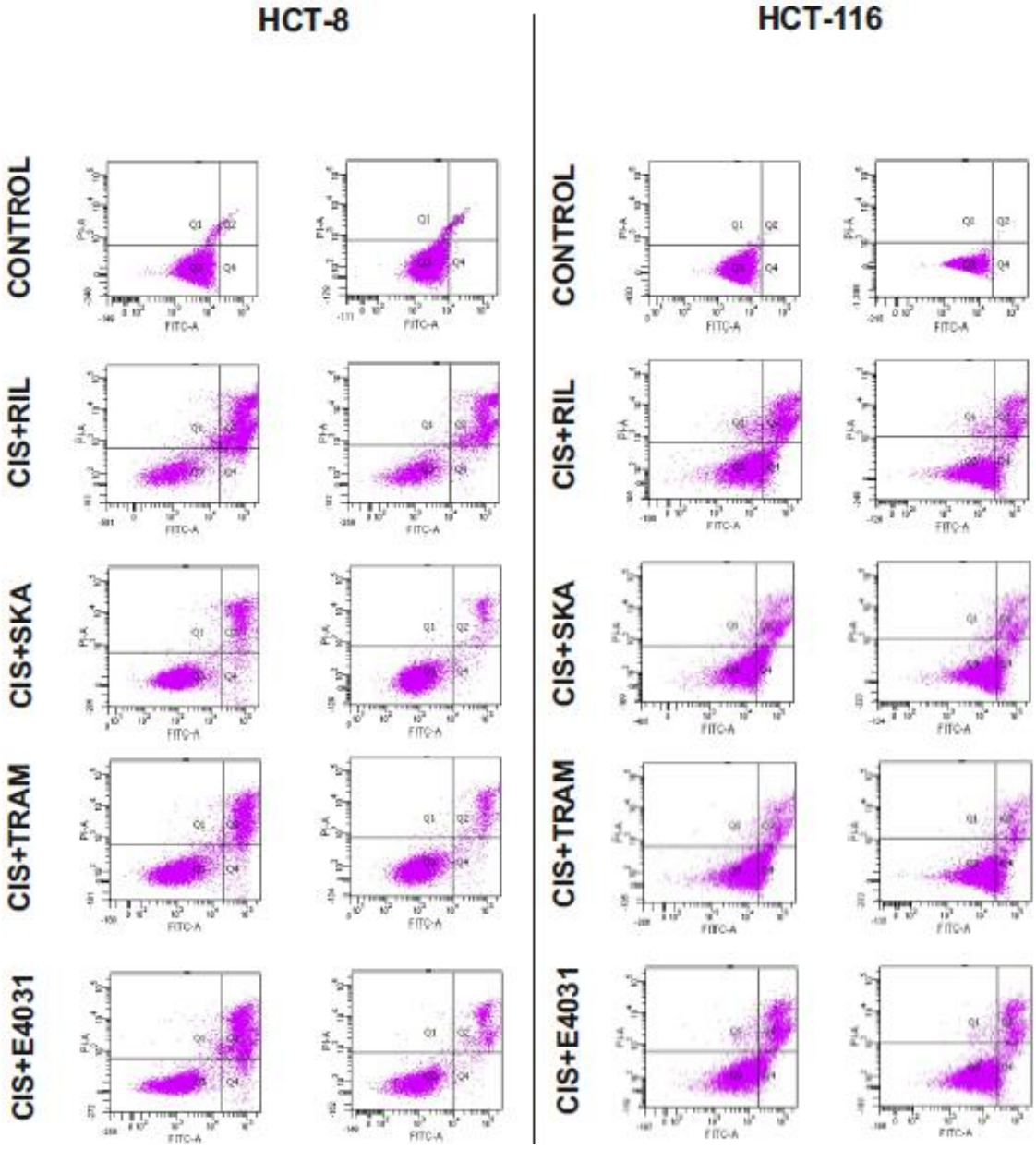

Figure 14 Effects of Cisplatin in combination with Riluzole, SKA-31, TRAM-34 and E4031 on apoptosis distribution of HCT-8 and HCT-116 cells. Apoptosis was evaluated after 24 hours of treatment through the Annexin/PI assay. The figure shows dot plots of control and treated cells at the same experimental time point.

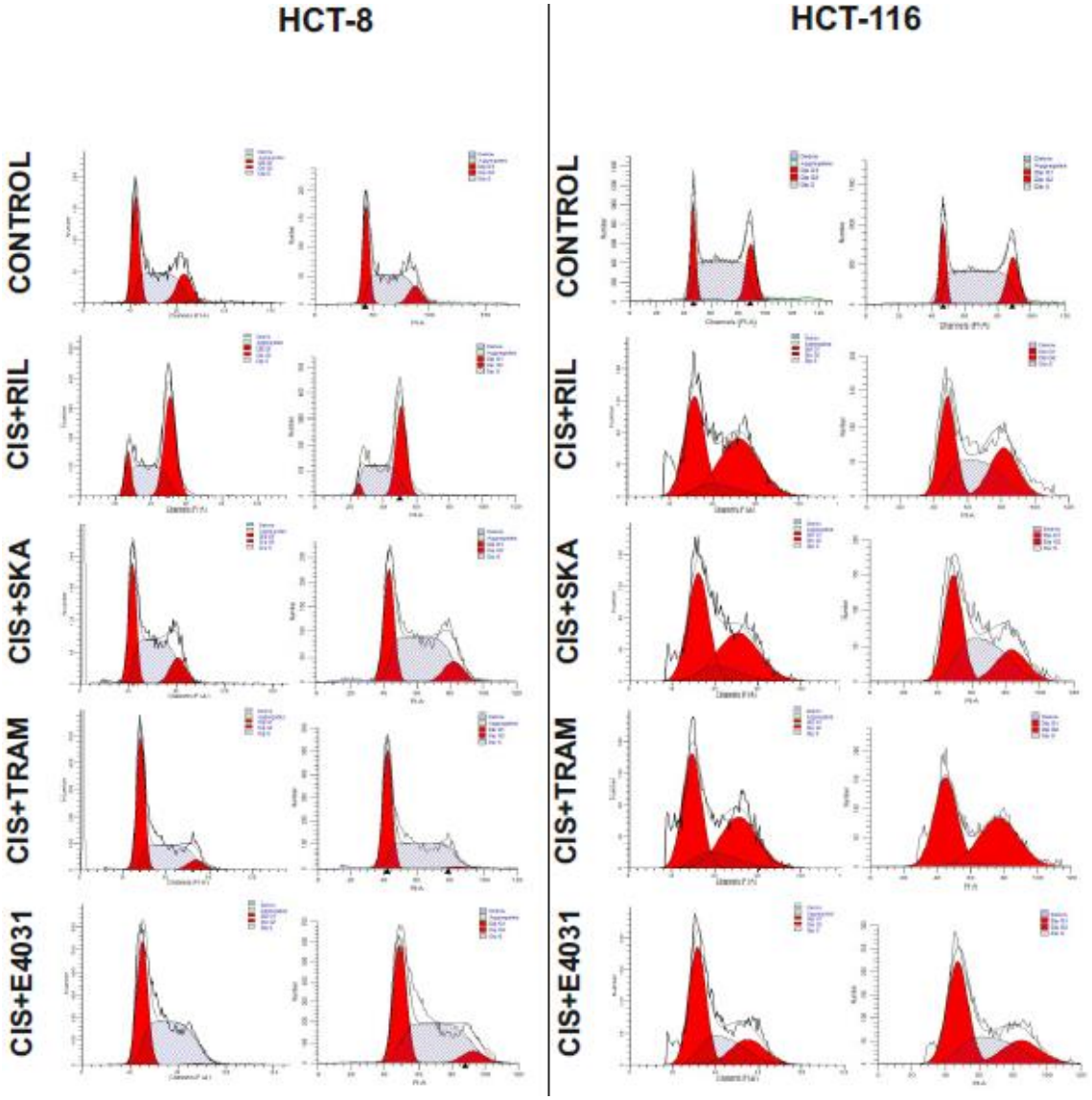

Figure 15: Plot of the number of cells labelled with Propidium Iodide determined by flow cytometry, in Control conditions and after 24 hours of treatment at IC_{50} concentrations of Cisplatin in combination with Riluzole, SKA-31, TRAM-34 and E4031 on cell cycle distribution of HCT-8 and HCT-116 cells.

4.3.1 Effects of Riluzole, SKA-31 and E4031 in combination with Cisplatin on HCT-116 cell proliferation

Finally Riluzole, SKA-31 and E4031 were added to HCT-116 cells in combination with different Cisplatin concentrations (1, 10 and 20 µM) and the effects on cell proliferation analysed. Figure 16 shows that the three K^+ channel modulators indeed cooperate with Cisplatin in inhibiting HCT-116 cell proliferation. In particular, in the presence of either Riluzole, SKA-31 or E4031, even low concentrations of Cisplatin (1 and 10 µM), which had only a slight effect on these cells, slowed down or even completely blocked cell proliferation when added in conjunction with the K^+ channel modulators. The strongest effect was obtained with E4031. Raw data of the single experiments are in Figure 17.

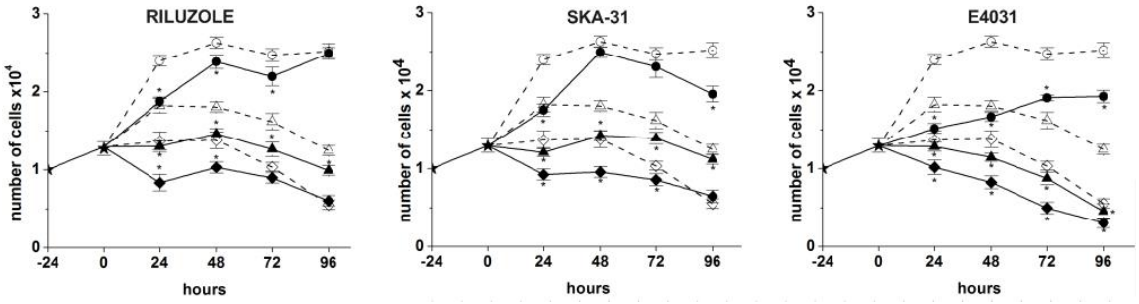

Figure 16: Effects of the combination of Cisplatin (at 1, 10 and 20 µM) with the following drugs: Riluzole, SKA-31 and E4031 (at the respective IC_{50} values) on HCT-116 proliferation after a single treatment (see arrow) given as the number of Trypan Blue negative cells. Data are means ± SEM of three independent experiments Statistically significant data are indicated with an asterisk. White circle = 1 µM of Cisplatin, white triangle = 10 µM of Cisplatin, white diamond=20 µM of Cisplatin; black circle 1 µM of Cisplatin + IC_{50} of relative combined drug, black 10 µM Cisplatin + IC_{50} of relative combined drug, black diamond= 20 µM of Cisplatin+ IC_{50} of relative combined drug).

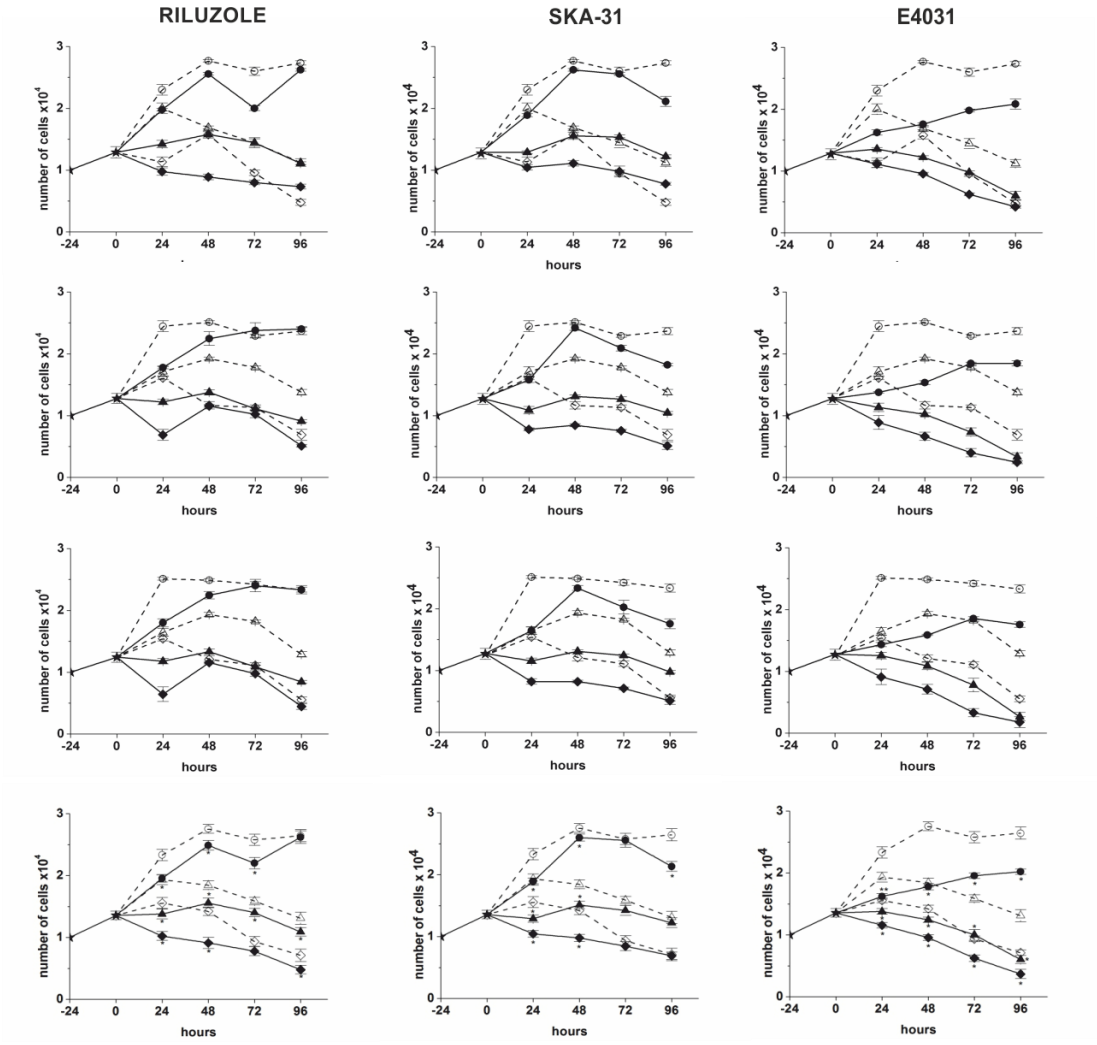

Figure 17: Effects of the combination of Cisplatin (at 1, 10 and 20 μM) with the following drugs: Riluzole, SKA-31 and E4031 (at the respective IC_{50} values) on HCT-116 proliferation after a single treatment (see arrow) given as the number of Trypan Blue negative cells. Data are means ± SEM of three independent experiments Statistically significant data are indicated with an asterisk. White circle = 1 μM of Cisplatin, white triangle = 10 μM of Cisplatin, white diamond=20 μM of Cisplatin; black circle 1 μM of Cisplatin + IC_{50} of relative combined drug, black 10 μM Cisplatin + IC_{50} of relative combined drug, black diamond= 20 μM of Cisplatin+ IC_{50} of relative combined drug).

4.3.2 Effects of Riluzole, SKA-31 and E4031 in combination with low doses of Cisplatin on HCT-116WT, HCT-116 hERG1-Sh and HCT-116 KCa3.1-Sh.

We then tested whether the various K^+ channel modulators could be interchanged. We thus performed a set of experiments in which 1 µM Cisplatin was added either alone, or with Riluzole, SKA-31 or E4031 at their IC_{50} or IC_{25} values, or with a combination of two K^+ channel modulators (Riluzole+E4031, Riluzole+SKA-31 or SKA-31 + E4031) at their IC_{50} or IC_{25} values. Figure 18 shows that the combination of two K^+ channel modulators at the IC_{25} values had additive effects on cell viability giving rise to an inhibition even greater than that obtained with the single K^+ channel modulators at the IC_{50} value. This effect was even stronger when two K^+ channel modulators were added at the IC_{50} value. In any case, the most effective combination was Riluzole+E4031.

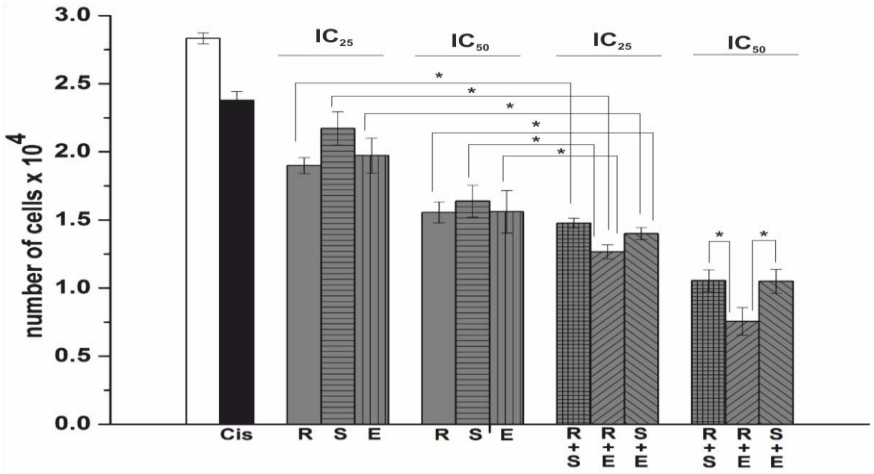

Figure 18: HCT-116 cells were treated with Cisplatin (at 1µM), alone (black bar) or in combination with Riluzole (R), SKA-31 (S) or E4031 (E) at either the IC_{50} or IC_{25} values, as well as with combinations of two of the three drugs (R+E; R+S; S+E) at either the IC_{50} or IC_{25}. Cells were counted after 24 hours of treatment and are reported as the number of Trypan Blue negative cells. Data are means ± SEM of two independent experiments. Statistically significant comparisons are indicated with an asterisk. Besides those graphically indicated in the figure, the following comparisons turned out to be statistically significant: all single drugs (at IC_{25}) vs all single drugs (at IC_{50}), all drugs in combinations (at IC_{25}) vs all drugs in combinations at (IC_{50}), all single drugs (at IC_{25}) vs all drugs in combinations (at IC_{25}), all single drugs (at IC_{50}) vs all drugs in combinations (at IC_{50}), all single drugs (at IC_{25}) vs all drugs in combinations (at IC_{50}), Ril-IC_{25} vs Ska-IC_{25}, all drugs in combinations (at IC_{25}) vs all drugs in combinations (at IC_{25}), R+S (at IC_{50}) & R+E (at IC_{50}), S+E (at IC_{50}) & R+E (at IC_{50}), all single drugs (at IC_{25}) vs 1µM of Cisplatin.

We then, after having conducted a WB analysis to ensure a proper gene silencing (Figure 19), proceeded to test the same type of experiment on HCT-116 cells silenced with specific siRNAs for hERG1 (Figure 20) and KCa3.1 (Figure 21).

hERG1 silenced HCT-116 cells showed a marked decreasing effect of E4031 on cell proliferation, in particular when given at IC_{25} both alone and in combination with Riluzole and SKA-31, E4031 didn't exerted a significant reduction in cell number compared to cells treated only with lipofectamine; when given at IC_{50} the number of cells didn't show a significant reduction either and in two conditions (E4031 alone and Riluzole+E4031) a little increase in cell number was observed although not statistical significant (Figure 20). KCa3.1 silenced HCT-116 cells treated with IC_{25} of Riluzole, SKA-31 and E4031 showed no appreciable decrease of proliferation, IC_{50} doses on the other exerted a slight increase in cell number compared to cells treated only with lipofectamine while no variation was found on cells treated with E4031. The same augment in cell proliferation compared to lipofectamine treated cells was observed when Riluzole, SKA-31 and E4031 were used in combination both at IC_{25} and IC_{50} (Figure 21).

From this experiments we outlined how hERG1 silencing abolished E4031 effect on HCT-116 cells proliferation, confirming its specific role as a modulator on cell viability. The same was found if we silenced KCa3.1, abolishing Riluzole and SKA-31 effect on cell proliferation but not E4031.

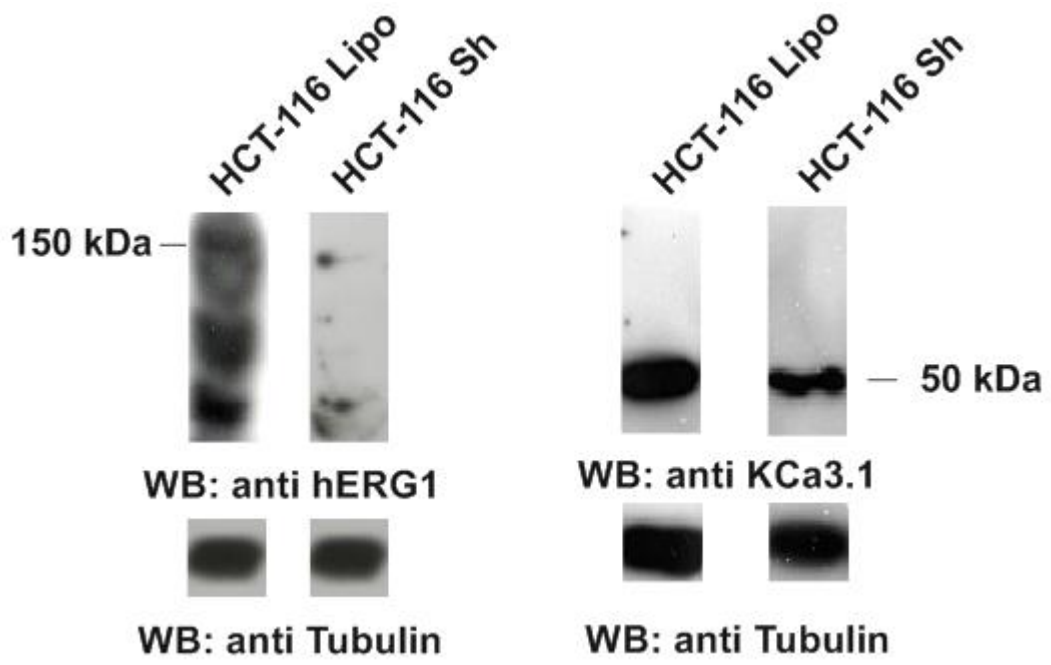

Figure 19: Western blots of hERG1(left) and KCa3.1(right) protein expression in HCT-116 cells treated only with lipofectamine (HCT-116 Lipo), silenced for hERG1(left) or KCa3.1 (right) (HCT-116 Sh). Cell lysates from HCT-116 cells were probed with the anti-KCa3.1 and and anti-pan hERG1 antibody. Reprobing of the membranes with anti-tubulin antibody is reported in the bottom panels. The arrows indicate the bands corresponding to hERG1 and KCa3.1.

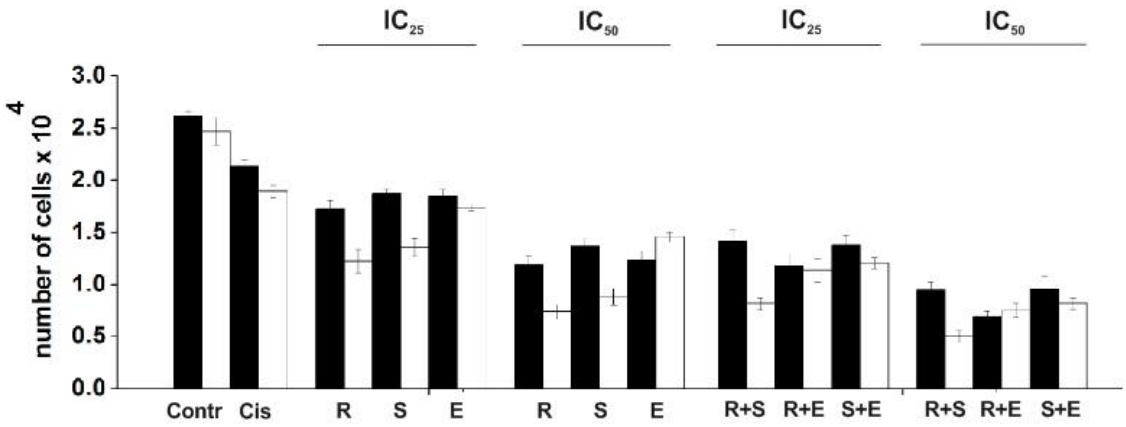

Figure 20: HCT-116 cells treated only with lipofectamine (black) or silenced for hERG1 (white) were treated with Cisplatin (at 1μM) alone or in combination with the following drugs: Riluzole (R), SKA-31 (S) or E4031 (E) at either the IC_{50} or IC_{25} values, as well as with combinations of two of the three drugs (R+E; R+S; S+E) at either the IC_{50} or IC_{25}. Cells were counted after 24 hours of treatment and are reported as the number of Trypan Blue negative cells. Data are means ± SEM of two independent experiments.

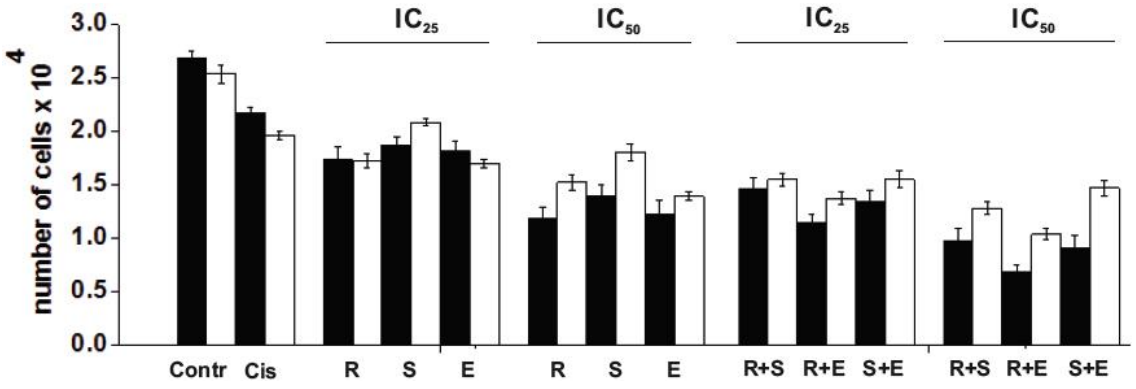

Figure 21: HCT-116 cells treated only with lipofectamine (black) or silenced for KCa3.1 (white) were treated with Cisplatin (at 1µM) alone or in combination with the following drugs: Riluzole (R), SKA-31 (S) or E4031 (E) at either the IC_{50} or IC_{25} values, as well as with combinations of two of the three drugs (R+E; R+S; S+E) at either the IC_{50} or IC_{25}. Cells were counted after 24 hours of treatment and are reported as the number of Trypan Blue negative cells. Data are means ± SEM of two independent experiments.

We found that KCa3.1 activation, exerted with Riluzole and SKA-31, and hERG1 block, exerted with E4031, in modulating with low doses of Cisplatin cell proliferation in HCT-116 cells produced comparable effects. Having confirmed the specific role of the two ion channels, we investigated if their activity on cell proliferation could be explained by a modulation of Cisplatin cellular uptake.

4.3.3 Cisplatin uptake in HCT 116 cells: modulation by Cu transporters inhibitor and K^+ channels modulators.

First, we investigated Platinum (Pt) uptake in HCT-116 cells treated with either 22μM or 200 μM Cisplatin and after either 6 or 24h of treatment (Figure 23). For all the conditions tested cells were collected by either tripsinization or gentle scraping. The number of cells, determined by Trypan Blue exclusion test, and the corresponding protein concentration are reported in Figure 22A. When plotted, a clear linear relationship is evident (Figure 22B). Therefore we determined a conversion factor which allowed us to report our data on Pt intracellular concentration as either nanomoles (or nanog) per 10^6 cells or per mg of proteins.

(A)

Condition	no. of cells	mg of protein
Contr - 6h tripsin	840000	0,24
Cisplatin 22μM 6h tripsin	780000	0,23
Cisplatin 200μM 6h tripsin	700000	0,21
Contr - 24h tripsin	2200000	0,65
Cisplatin 22μM 24h tripsin	1100000	0,34
Cis 200μM 24h tripsin	300000	0,11
Contr - 6h scraper	880000	0,26
Cisplatin 22μM 6h scraper	820000	0,25
Cisplatin 200μM 6h scraper	740000	0,22
Contr - 24h scraper	2600000	0,69
Cisplatin 22μM 24h scraper	1100000	0,33
Cis 200 μM 24h scraper	380000	0,12

(B)

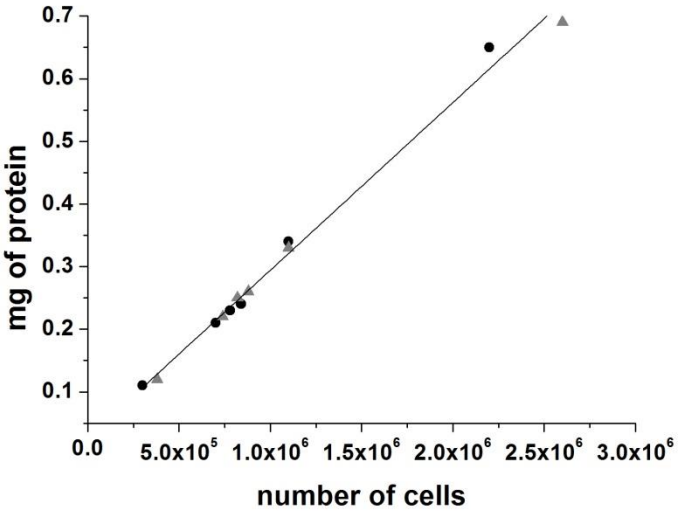

Figure 22: (A) Number of Trypan blue cells counted and relative amount of extracted proteins after exposure for 6 or 24 hours of HCT-116 cells to Cisplatin. Cells were seeded at time 0 at $4*10^5$ in each well of a 6-well cluster. At the end of 6h or 24h treatment supernatant was recovered, cells were washed five times in cold PBS and collected by either tripsinization or gentle scraping. Cells was centrifuged at 1200g for 5 minutes. Pellets were resuspended in 1ml of PBS and 1/10 of the solution was centrifuged at 1200g and pellet was used for protein extraction, the others 9/10 were centrifuged at 1200g and pellet was used for ICP-AES.
(B) Linear correlation between number of cells counted and mg of protein extracted after exposure for 6 or 24 hours of HCT-116 cells to Cisplatin. Data were linearly fitted with Origin Software (Microcal Origin 8.0 software; OriginLab Corporation, Nothampton, MA).
We then determined the amount of Cisplatin in all the experimental conditions described above. Raw data, expressed as either nmol Pt or ng Pt, are reported in Figure 28A.

From a paper recently published by Planells-Cases and colleagues, it was found that, under isotonic condition, half of Pt uptake in HCT-116 cells is modulated by VRAC anion channel while the other half is mediated by passive diffusion through cell membrane (Planells-Cases et al., 2015).

Our experiment outlined that, for short Cisplatin exposition, our data of Pt uptake are in line, among tripsin and scraper method of cells collection, to what reported by them (dashed light gray bars in Figure 23B, relative to HCT-116 and HEK-293 cells exposed to 40μM and 200 μM of Cisplatin either for 6 or 24h.) while for longer incubation times we observed a higher Cisplatin uptake compared to their data.

(A)

Condition	nmol Pt	ng Pt
Contr - 6h tripsin	0,009844166	1,9204
Cisplatin 22μM 6h tripsin	0,115555926	22,54265
Cisplatin 200μM 6h tripsin	0,615926287	120,1549
Contr - 24h tripsin	0	0
Cisplatin 22μM 24h tripsin	0,093706684	18,2803
Cis 200μM 24h tripsin	1,052429772	205,308
Contr - 6h scraper	0	0
Cisplatin 22μM 6h scraper	0,19852804	38,72885
Cisplatin 200μM 6h scraper	3,51640609	685,9805
Contr - 24h scraper	0	0
Cisplatin 22μM 24h scraper	0,114542239	22,3449
Cis 200μM 24h scraper	0,626373795	122,193

(B)

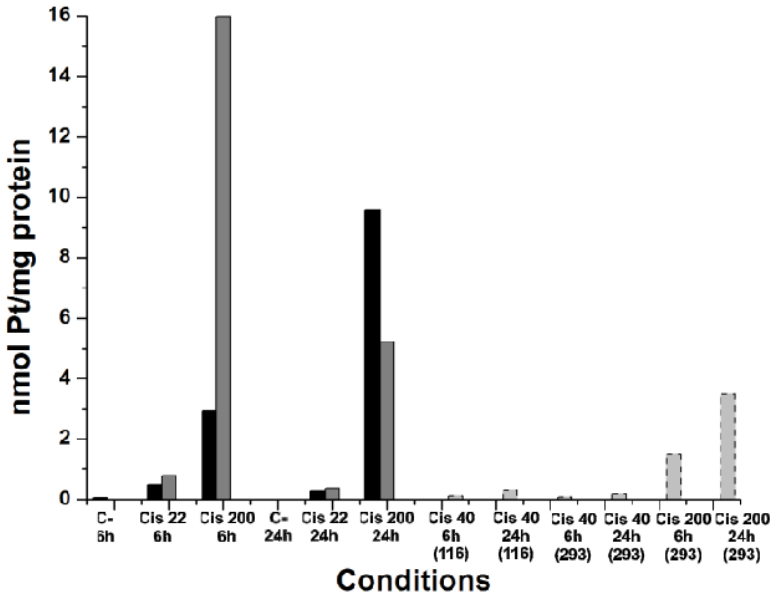

Figure 23: (A) nmol Pt and ng of platin after exposure for 6 or 24 hours of HCT-116 cells to Cisplatin. Cells were seeded at time 0 at $4*10^5$ in each well of a 6-well cluster. At the end of 6h or 24h treatment supernatant were recovered and cells were washed five times in cold PBS and cells collected by either the addition of Tripsin-EDTA solution or by gentle scraping. Cells was centrifuged at 1200g for 5 minutes and the supernatant discarded. Pellet were resuspended in 1ml of PBS and 1/10 of the solution was centrifuged at 1200g and the supernatant discarded and pellet was used for protein extraction, the others 9/10 were centrifuged at 1200g, the supernatant discarded and pellet was used for ICP-AES. **(B)** Data from table in A: (black bars) cell collected with tripsin, (grey bars) cell collected with scraper, (light grey bars) data of Cisplatin uptake reported in Planells-Cases et al., 2015. HCT-116 cells (116), HEK-293 cells (293).

Then we tested the contribution of CTRs transporters, known in literature to be the main proteins involved in Cisplatin uptake (Harrach et Ciarimboli. 2015) and expressed in HCT-116 as well (Table 2), in modulating Pt uptake after 3h of exposition; $CuSO_4$, a known CTRs inhibitor (More et al., 2010), was added with 6µM, 22µM and 67µM of Cisplatin on HCT-116 cells. As reported in Figure 24, the addition of $CuSO_4$ decreased the amount of Pt uptake compared to cells treated only with Cisplatin;. We concluded that the uptake of Pt, in HCT-116 treated with 22µM of Ciplatin, is independent from CTRs expression while only for higher concentrations CTRs contribution becomes relevant.

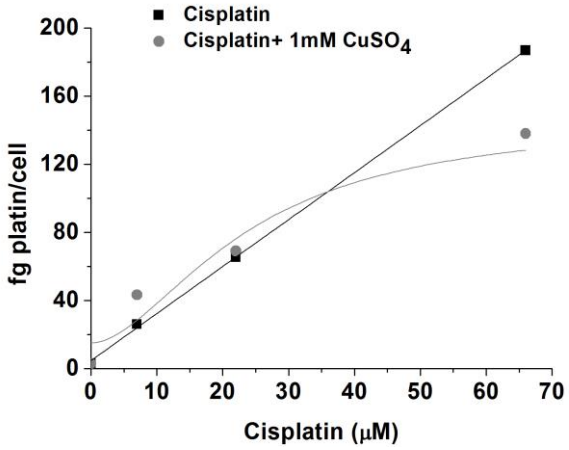

Figure 24: Effect on platinum uptake and extracellular platium concentration on HCT-116 cells after 3h of treatment with Cisplatin at IC_{25}, IC_{50} and IC_{75} doses (black squares) and of Cisplatin at 6µM, 22µM and 67µM in combination with 1mM of $CuSO_4$ (gray dots).

We then proceeded to evaluate the role of TRAM-34, a known KCa3.1 inhibitor (Sankaranarayanan et al., 2009), in modulating Cisplatin uptake at 3h. When given at 100µM with 6µM, 22µM and 67µM of Cisplatin we registered a marked decrease on intracellular platinum compared to Cisplatin-treated cells (Figure 25). This data suggested that a KCa3.1 block is related to a decrease in Cisplatin uptake in HCT-116.

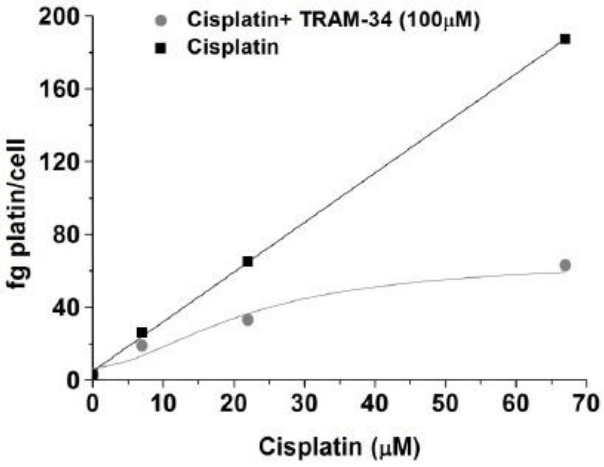

Figure 25: Effect on platinum uptake and extracellular platinum concentration on HCT-116 cells after 3h of treatment with Cisplatin at 6μM, 22μM and 67μM in combination with 100μM of TRAM-34.

Finally we treated HCT-116 with IC_{50} of Cisplatin (22μM) in combination with IC_{50} of the Riluzole, SKA-31, TRAM-34 and E4031 to assess the effect of K^+ channel modulators on Cisplatin uptake. We found that in HCT-116 cells Riluzole, when given in combination with Cisplatin, increases Pt cellular uptake, although this augment is very variable, as SKA-31 and E4031 do with less variability among the three experiments performed, while combination between Cisplatin and TRAM-34 decreases Cisplatin uptake (Figure 26), confirming even for longer times of exposition our data previously obtained (Figure 25) .

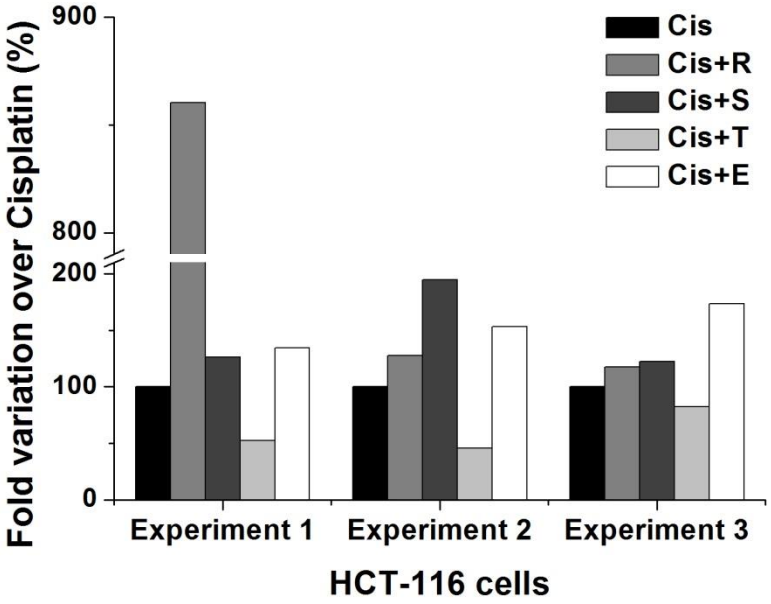

Figure 26: Fold variation in platinum levels over Cisplatin measured after exposure for 24 hours of HCT-116 cells to Cisplatin alone, or in combination with Riluzole, SKA-31, TRAM-34 and E4031. All the drugs were added at their IC_{50} doses.

4.4 Expression of KCa3.1 in precancerous and cancerous lesions of colon and rectum.

Given the importance outlined of KCa3.1 in regulating tumour cell proliferation and in modulating Cisplatin resistance in HCT-116 cells we decided to evaluate its expression on primary CRC tumour specimen and to assess if this could be correlated to other colorectal tumour markers as well.. We studied its expression levels on colorectal precancerous and cancerous lesions: 21 paraffin-embedded colorectal adenomas, 223 adenocarcinomas and 30 normal mucosa samples.

Examples of IHC for $K_{Ca}3.1$ on colorectal adenomas are reported in Figure 27, summary of analysis is reported in Figure 28 and the complete cohort of samples examined is listed in Table 11.

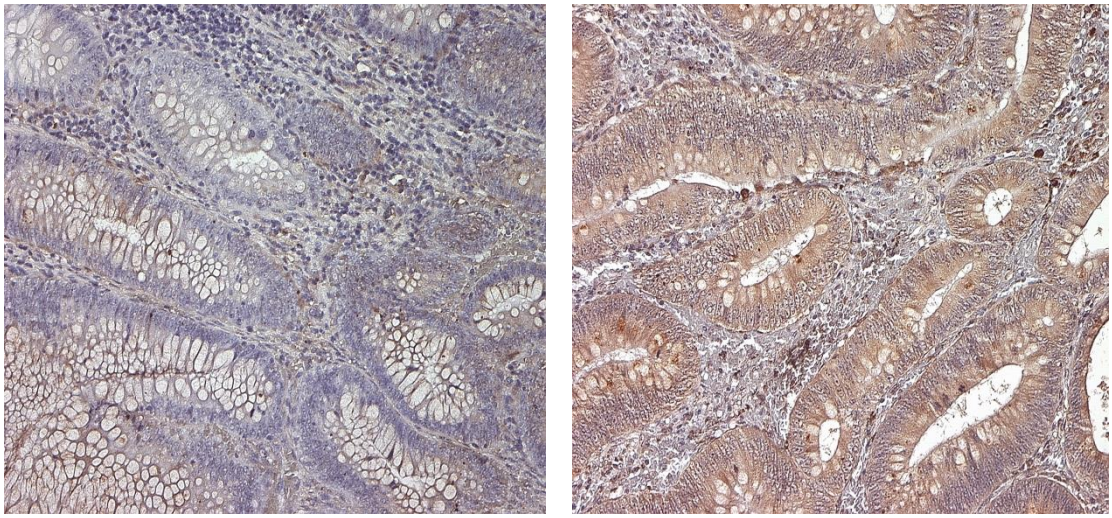

Figure 27. IHC analysis for KCa3.1 on colorectal adenoma samples. Explicative negative sample (Left), Positive sample (right). Magnification 20x.

SAMPLE	SEX	AGE	HISTOLOGY GRADING	hERG1	KCa3.1
CR 13	F	81	ADENOMA	0	0
CR71P	M	81	ADENOMA	0	0
CR87	M	55	HIGH GRADE DISPLASIA	0	1
CR142	M	68	HIGH GRADE DISPLASIA	1	0
CR164P	M	73	ADENOMA	0	0
CR196 P	F	54	ADENOMA	0	0
CR219	F	59	HIGH GRADE DISPLASIA	0	1
CR 256	F	62	HIGH GRADE DISPLASIA	0	0
1322638 A1	M	66	HIGH GRADE DISPLASIA	0	1
1322638 B2	M	66	LOW GRADE DISPLASIA	1	1
1322671 B1	F	72	LOW GRADE DISPLASIA	0	0

SAMPLE	SEX	AGE	HISTOLOGY GRADING	hERG1	KCa3.1
1322576 A1	M	58	LOW GRADE DISPLASIA	0	1
1322492 A1	M	54	LOW GRADE DISPLASIA	0	0
1322492 B1	M	54	LOW GRADE DISPLASIA	.	0
1322666 A1	M	79	HIGH GRADE DISPLASIA	0	1
1322666 A2	M	79	HIGH GRADE DISPLASIA	0	0
1322582 A1	F	67	LOW GRADE DISPLASIA	1	1
1322582 A2	F	67	LOW GRADE DISPLASIA	1	1
1322659 1	M	54	LOW GRADE DISPLASIA	1	1
1322659 2	M	54	LOW GRADE DISPLASIA	.	1
1322659 3	M	54	LOW GRADE DISPLASIA	1	1

Table 11. Markers and clinical-pathological data of colorectal adenoma samples examined via IHC for KCa3.1 staining.

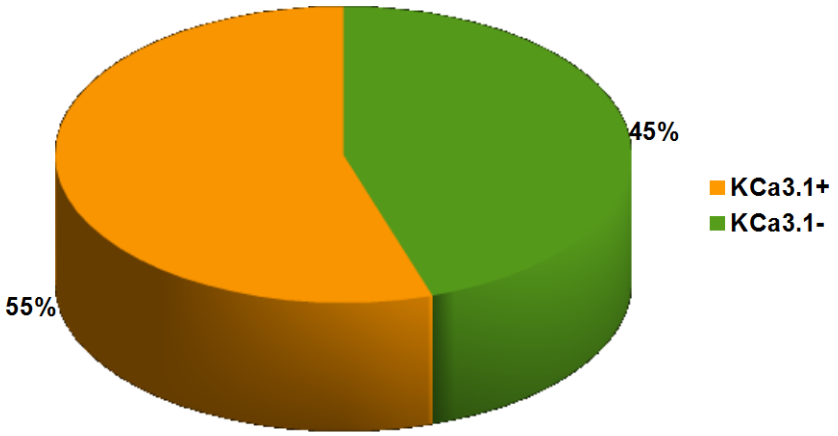

Figure 28. Pie chart of IHC analysis on colorectal adenoma sample. Green slice: negative samples (9/21); Yellow slice: positive samples (11/21).

K_{Ca}3.1 was found expressed on the plasma membrane and in the cytoplasm of neoplastic cells (Figure 27), with a diffuse pattern of labelling and a particular staining pattern in the tumour stroma on red white blood cells according to what reported in literature (Wulff et al. 2007).

An univariate statistical analysis was conducted with software Stata (v.9.2 StataCorp USA) with the application of Fisher Exact Test to evaluate correlations between K_{Ca}3.1 expression and other clinical-pathological parameter and the expression of hERG1 channel, following what published in Translational Oncology for the research of prognostic indicators in CRC (Lastraioli et al. 2012).

The analysis didn't outlined significant correlations between K_{Ca}3.1 and any of the other parameters examined but from our analysis we point out that, in the majority of adenoma samples examined in our small cohort of patients, K_{Ca}3.1 was found over-expressed compared to normal tissue.

As an enrichment of what already reported in Lastraioli et al., 2012 we investigated K_{Ca}3.1 expression and its correlation with other markers as well as clinical-pathological data on our cohort of patients.

An example of IHC staining of K_{Ca}3.1 is reported in Figure 29 while the summary of the analysis is reported in Figure 30. The complete clinical-pathological data and the statistical significant correlation form Fisher Exact Test with other markers are outlined in Table 12 and Table 13.

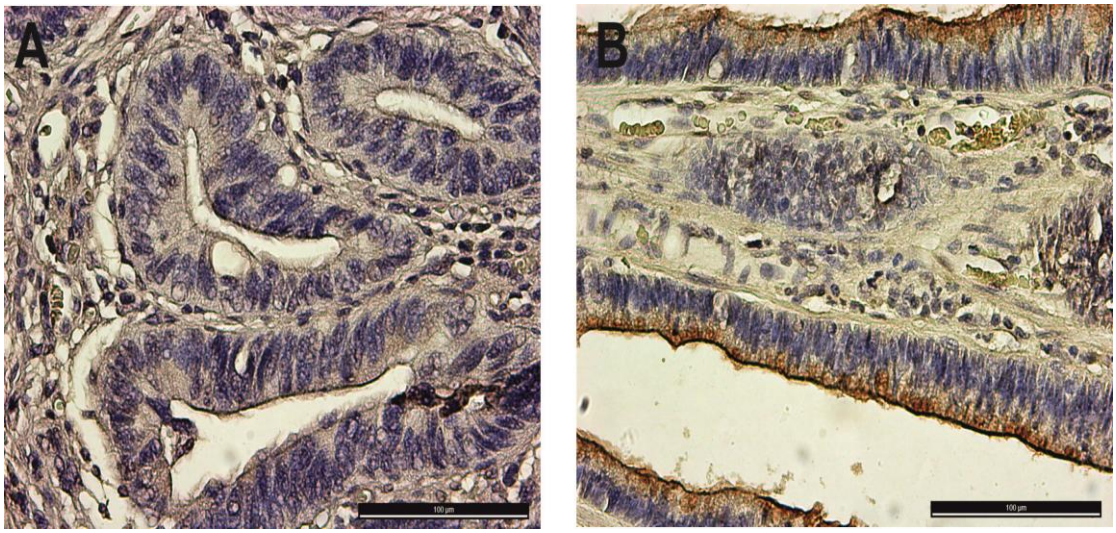

Figure 29. IHC analysis for KCa3.1 on colorectal adenocarcinoma samples. Explicative negative sample (Left), Positive sample (right). Magnification 20x.

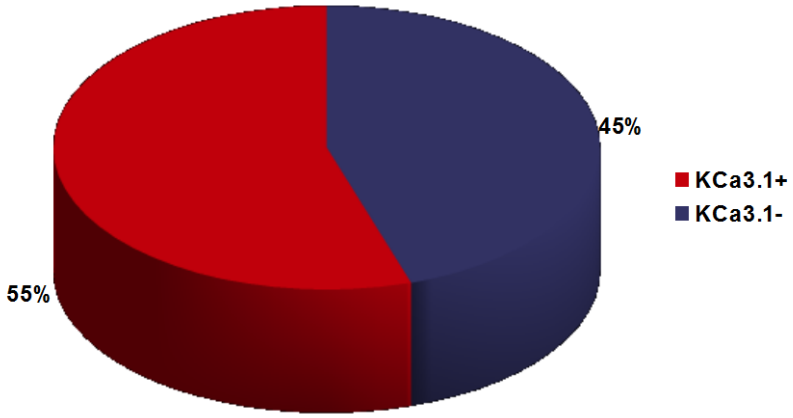

Figure 30. Pie chart of IHC analysis on colorectal adenocarcinoma samples. Blue slice: negative samples (82/184); Red slice: positive samples (102/184).

Parameters	No. of samples	Clinical-pathological data	No. of samples
hERG1 mono	Negative 98 (43.95%)	**Location**	Right colon 99 (42.86%)
	Positive 125 (56.05%)		Tr. colon 15 (6.49%)
			Left colon 62 (26.84%)
hERG1 mono (Score)	0 98 (43.95%)		Rectum 55 (23.81%)
	1 62 (27.80%)		
	2 63 (28.25%)	**Dukes**	A 33 (16.10%)
			B 73 (35.61%)
hERG1 poli	Negative 64 (30.62%)		C 77 (37.56%)
	Positive 145 (69.38%)		D 22 (10.73%)
hERG1 poli (Score)	0 64 (30.62%)	**Jass**	I 13 (7.34%)
	1 59 (28.23%)		II 38 (21.47%)
	2 86 (41.15%)		III 62 (35.03%)
			IV 64 (36.16%)
CA IX	Negative 147 (62.22%)		
	Positive 75 (33.78%)	**TNM**	I 39 (16.88%)
			IIA 80 (34.63%)
VEGF-A	Negative 50 (22.83%)		IIB 9 (3.90%)
	Positive 169 (77.17%)		IIIA 43 (18.61%)
			IIIB 35 (15.15%)
GLUT1	Negative 144 (65.45%)		IV 25 (10.82%)
	Positive 76 (34.55%)		
p53	Negative 112 (62.22%)	**COLL**	NO 169 (73.16%)
	Positive 68 (37.78%)		YES 62 (26.84%)
EGFR	Negative 52 (24.88%)	**MTX**	NO 202 (87.83%)
	Positive 157 (75.12%)		YES 28 (12.17%)
HIF1α	Negative 147 (87.50%)	**GRAD**	G1 11 (5.21%)
	Positive 21 (12.50%)		G2 198 (93.84%)
			G3 2 (0.95%)
KCa3.1	Negative 82 (44.57%)		
	Positive 102 (55.43%)	**Gender**	F 122 (52.81%)
			M 109 (47.19%)
KCa3.1 poli (Score)	0 77 (43.75%)		
	1 20 (11.36%)	**Age**	<70 years 123 (52.79%)
	2 34 (19.32%)		>70 years 110 (48.21%)
	3 45 (25.57%)		

Table 15. Markers and clinical-pathological data of colorectal adenocarcinoma samples examined via IHC for KCa3.1 expression. (COLL: Colloid presence, GRAD: tumour grading, MTX: metastasis status)

Correlations		p-value	No. of samples
hERG1mono	CA IX	0,004	216
hERG1mono	VEGF	0,000	214
hERG1mono	GLUT1	0,000	216
hERG1mono	EGFR	0,000	207
hERG1mono	KCa3.1	0,024	181
hERG1mono	GRAD	0,005	206
hERG1poli	VEGF	0,000	204
hERG1poli	GLUT1	0,000	206
hERG1poli	p53	0,022	180
hERG1poli	EGFR	0,003	197
hERG1poli	GRAD	0,001	189
CA IX	VEGF	0,003	216
CA IX	KCa3.1	0,038	179
VEGF	GLUT1	0,000	214
VEGF	p53	0,001	180
VEGF	EGFR	0,000	205
VEGF	KCa3.1	0,004	177
GLUT1	SEDE	0,026	219
GLUT1	GRAD	0,031	201
EGFR	HIF1α	0,030	168
EGFR	COLL	0,003	209
EGFR	KCa3.1	0,021	176
KCa3.1	hERG1mono	0,024	181
KCa3.1	CAIX	0,048	170
KCa3.1	VEGF	0,009	168
KCa3.1	EGFR	0,021	176

Table 16. Statistical significant correlations between markers and clinical-pathological data of colorectal adenocarcinoma samples examined via IHC for KCa3.1.

From the univariate statistical analysis conducted to evaluate the correlations between KCa3.1 expression the clinical-pathological parameter, the expression of hERG1 channel as well as angiogenic markers (EGFR and VEGF), hypoxia factors (HIF1α and CAIX), transporters (GLUT-1) and classical tumour markers (p53), significant correlations emerged for KCa3.1. Not only KCa3.1 was found over-expressed in the majority of the samples examined while its expression was not found in normal mucosa,

but its expression was correlated with hERG1 expression as well as with several important angiogenic factors (VEGF, EGFR and CAIX).

4.5 Effects of new Cisplatin analogues in tumour cells.

We evaluate another possible strategy to overcome Cisplatin resistance, in creating and testing, in collaboration with Prof. Luigi Messori and Dr. Tiziano Marzo – Department of Chemistry "Ugo Schiff" – University of Florence, the cytotoxic effect of two new Cisplatin-analogue compounds, cis-Pt-I_2 and cis-Pt-Br_2 (Figure 31).

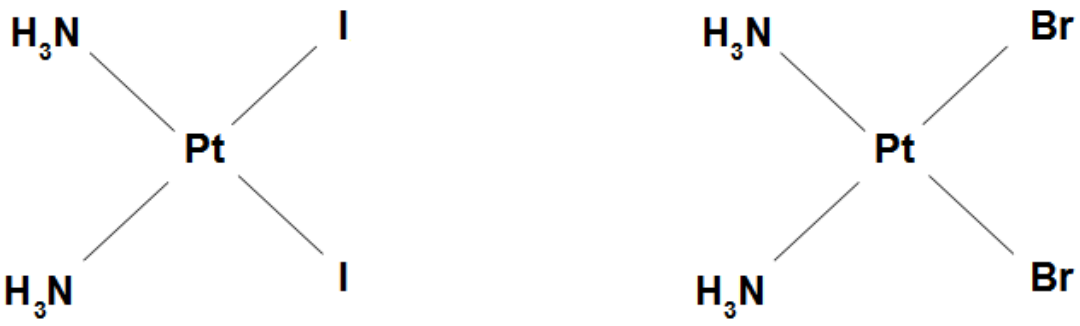

Figure 31: Structure model of cis-Pt-I_2 and cis-Pt-Br_2.

4.5.1 Solution chemistry of cis-Pt $I_2(NH_3)_2$ and cis-Pt$Br_2(NH_3)_2$: activation profiles and their logP determination.

Firstly Dr. Tiziano Marzo determined the UV-Vis analysis of both the complexes (Figure 34); cis-Pt$Br_2(NH_3)_2$ manifest typical absorption bands in the UV-visible, with a

main band at 330 nm and a pronounced shoulder at 300 nm (Figure 32). These bands are tentatively assignable to a d-d and LMCT transitions respectively in analogy with other Cisplatin derivatives (Marzo et al., 2015). After dissolution of the study compound in the reference buffer, progressive spectral changes are observed that are assigned to the progressive release of the two bromide ligands. The process is similar to what observed in the case of Cisplatin with a comparable kinetics (Marzo et al., 2015). By comparison of the spectral profiles of cis-$PtBr_2(NH_3)_2$ and Cisplatin recorded after 24 h of analysis, a good agreement was found, indicating that final species are the same for both the drugs.

For cis-$PtI_2(NH_3)_2$ some important spectral changes are slowly detected consisting of the progressive and regular decrease of the two main bands and in the appearance of a new band, of lower intensity, around 280 nm. The observed spectral changes are tentatively traceable to the progressive release of the two iodido ligands and to their replacement by water molecules according to a moderately biphasic kinetics. This would mean that the aquation process of cisPtI_2 is quite close to that of Cisplatin, involving the progressive detachment of the two halide ligands while both ammonia ligands are retained as confirmed by some further experiments. In particular, addition of KI at increasing concentrations completely eliminated and even reverted the above described spectral changes strongly supporting the proposed interpretation. In any case, the rate of the aquation process for cisPtI_2 is appreciably slower than that for Cisplatin (by at least a factor 2) possibly because of the greater strength of the Pt–I bond and/or greater inertness related to the increased “soft” character of iodide over chloride.

Furthermore, log P determination was carried out on cis$PtBr_2$ and cisPtI_2. Values of -1.04 and -0.13 were found. Remarkably these indicates a higher lipophilicity than Cisplatin itself (logP: -2.04). It is conceivable that these differences may have some effect in term of pharmacological activity of these new compounds.

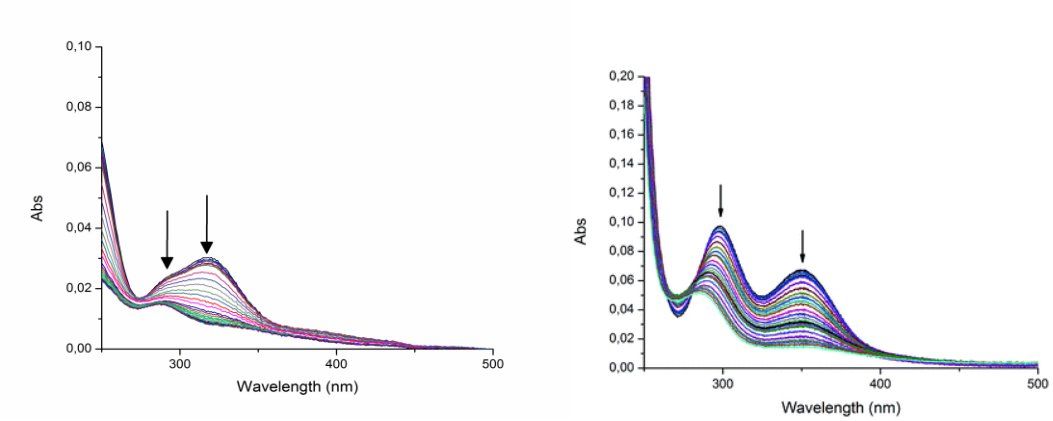

Figure 32: Time course spectra of cisPtBr$_2$ (left) and cisPtI$_2$ (right) 10^{-4} M in 50mM phosphate buffer over 24 h at RT.

4.5.2 CD experiments and interaction with ctDNA

Since nuclear DNA is believed to be the primary target for the pharmacological effect of Cisplatin, (Siddik. 2003) Dr Tiziano Marzo characterized the interaction of cis-PtBr$_2$(NH$_3$)$_2$ with calf thymus DNA through CD experiments, and compared the results with Cisplatin. The CD spectrum of ctDNA, before addition of the drugs is in line with literature (Tamburro et al. ,1977; Srivastava et al., 1978) (Fig. 33).

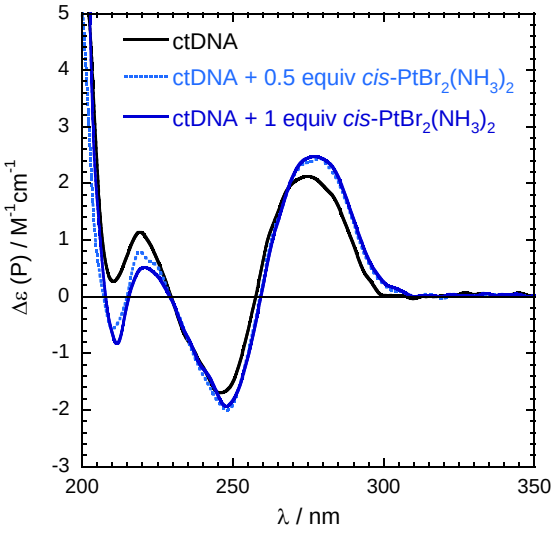

Figure 33. CD spectra of ctDNA without and with cis-PtBr$_2$(NH$_3$)$_2$, 0.5 and 1 equiv, after 72h incubation.

Addition of 0.5 equiv of cis-$PtBr_2(NH3)_2$ did not lead to any immediate change in the CD spectrum (data not shown). However, after incubation at 22°C for 72 h, the spectrum changed showing clear differences on the whole wavelength range (Fig. 33). In particular, both CD bands at 280 and 250 nm increased in intensity, the first by about 15%. From inspection of CD spectra it is apparent that the CD profiles measured after addition of 0.5 or 1 equivalents of cis-$PtBr_2(NH_3)_2$ were consistent and no significant changes in the spectral profiles were detected. Evidence that cis-$PtBr_2(NH_3)_2$ interacts with ctDNA very similarly to Cisplatin derive from the comparative analysis of the CD spectra of ctDNA after incubation with 1 equivalent of cis-$PtBr_2(NH_3)_2$ or Cisplatin (Fig. 34).

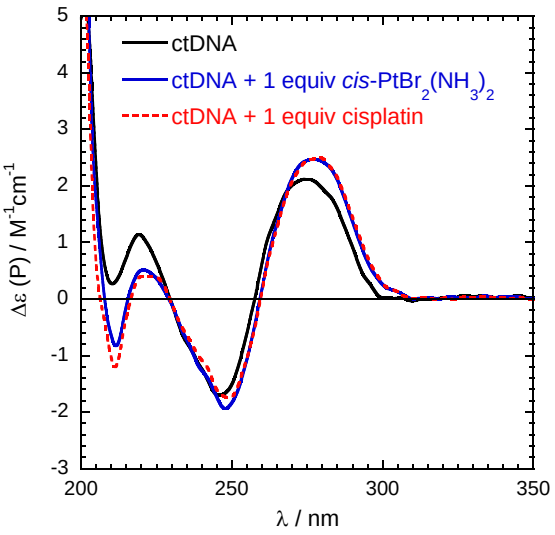

Figure 34. CD spectra of ctDNA with cis-$PtBr_2(NH_3)_2$ and Cisplatin, 1 equivalent, after 72h incubation.

Modification in the CD spectral profiles are well detectable, consistent and superimposable for the two complexes. A direct comparison with previous CD investigations on the ctDNA/Cisplatin system (Cleare et Hoeschele. 1973; Srivastava et al., 1978) is complicated by different experimental conditions and ctDNA samples (non-sonicated vs. sonicated). Qualitatively speaking, the differences observed upon binding occur in the same spectral regions and at a similar extent. However, our fragmented ctDNA (800 bp) shows a full enhancement of the main CD bands and already with 0.5 equivalent of ligand per base.

To determine the nature of the DNA interactions of cisPtI_2, the DNA binding properties of this complex were examined through a variety of methods and compared with those of Cisplatin. First, we aimed at quantifying the binding of cisPtI_2 to mammalian (CT) double-helical DNA in a cell free medium. The amount of platinum bound to DNA increased with time and the times at which the binding reached 50% (t50%) are summarized in Table 17.

Compound	**$t_{50\%}$ (min) ***
cis-PtI 2(NH3)2 aged in H2O	105 ± 11
Cisplatin aged in H2O	64 ± 5
cis-PtI 2(NH3)2 aged in 10 mM KI	390 ± 24
Cisplatin aged in 10 mM KCl	136 ± 19

Table 17 Binding of cis-$PtI_2(NH_3)_2$ and Cisplatin to calf thymus DNA. * The time at which the binding reached 50%. Values shown in the table are the means ± SEM of three separate experiments.

Importantly, after 24h, cisPtI_2 and Cisplatin aged in water or in 10 mM KI/KCl were quantitatively bound. As expected, the PtII complexes preincubated in water reacted with DNA significantly more rapidly than those preincubated in KI/KCl (10 mM), but the rate of the reaction of Cisplatin was considerably higher than that of cisPtI_2.

The lower rate of the reaction of cisPtI_2 with double-helical DNA in comparison with that of Cisplatin can be interpreted as the rate of the aquation of the leaving ligands in cisPtI_2 is significantly lower than that in Cisplatin. Since interstrand and intrastrand cross-links formation are believed to be responsible for anticancer activity of bifunctional platinum compounds, we have quantitated the interstrand cross-linking efficiency of cisPtI_2 in the linear pUC19 DNA (linearized with EcoRI restriction enzyme). Results point out that interstrand cross-linking efficiency of cisPtI2 (5 ± 2%) was similar to that of Cisplatin (6%).

4.5.3 Cellular studies

We examined the cytotoxic effect of cis-Pt-I_2 and cis-Pt-Br_2 on a panel of tumour cell lines in order to evaluate their IC_{50} (Table 18) and, on the most effective cell line, HCT-116 for cis-Pt-I_2 and FLG 29.1 for cis-Pt-Br_2, we evaluated cell cycle distribution (Figure 35) in comparison with Cisplatin.

We then proceeded to measure the amount of platin uptake exerted on HCT-116 in comparison with HCT116 p53-/- cells both for Cisplatin and for the di-iodioanalogue (Table 19) and for cis-Pt-Br_2 to assess apoptosis induction compared to Cisplatin (Figure 36).

Cell Line	**Cisplatin IC_{50} (μM)**	**cis-Pt-I_2 IC_{50} (μM)**
HCT-116	21.96±1.11	4.15±0.23
HCT-116 p53-/-	7.65±0.63	13.42±0.49
HT-29	13.39±1.10	11.69±1.45
A549	5.77±0.60	3.54±0.49
IGROV-1	25.30±0.40	7.36±0.31
PANC-1	2.48±0.11	0.91±0.10
Cell Line	**Cisplatin IC_{50} (μM)**	**cis-Pt-Br_2 IC_{50} (μM)**
A549	8.61±0.73	10.08±0.73
FLG 29.1	24.33±0.75	14.66±0.63
HCT-116	20.04±0.95	28.28±3.11
IGROV-1	24.12±0.49	25.63±0.25

Table 18: A549,FLG 29.1,HCT-116 and IGROV-1 cell lines were exposed to IC_{50} concentrations of Cisplatin and cis-Pt-Br_2, while HCT-116, KCT-116 p53-/-, HT-29, A549 and IGROV-1 to IC_{50} concentrations of Cisplatin and cis-Pt-Br_2 for 24 hours. Cell viability was evaluated via Trypan Blue exclusion assay. Means and SEMs are relative to one experiment mounted in triplicate.

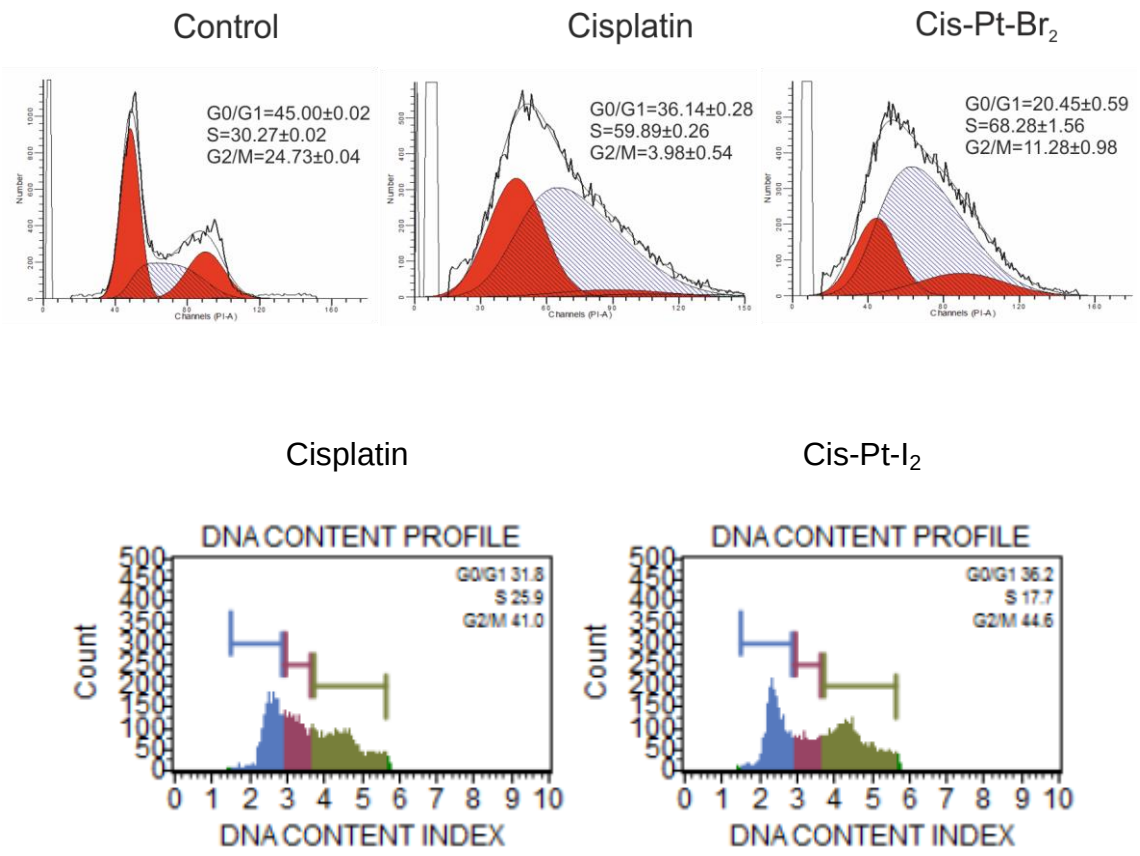

Figure 35: Plot of the number of cells labelled with Propidium Iodide determined by flow cytometry, after 24 hours of treatment at IC_{50} concentrations of Cisplatin and cis-Pt-I_2/cis-Pt-Br_2 on cell cycle distribution of HCT-116/FLG 29.1 cells.

Cell line	Drug	Platinum level (fg)	Internalized Pt (%)
HCT-116 p53-/-	Cisplatin	25.3	0.98
HCT-116 p53-/-	Cis-Pt-I_2	53.7	1.91
HCT-116	Cisplatin	14.6	0.50
HCT-116	Cis-Pt-I_2	66.6	2.41

Table 19: Platinum level (per cell) measured after exposure (3 hours) of HCT-116 and HCT-116 p53-/- to 20 µM of Cisplatin and cis-Pt-I_2.

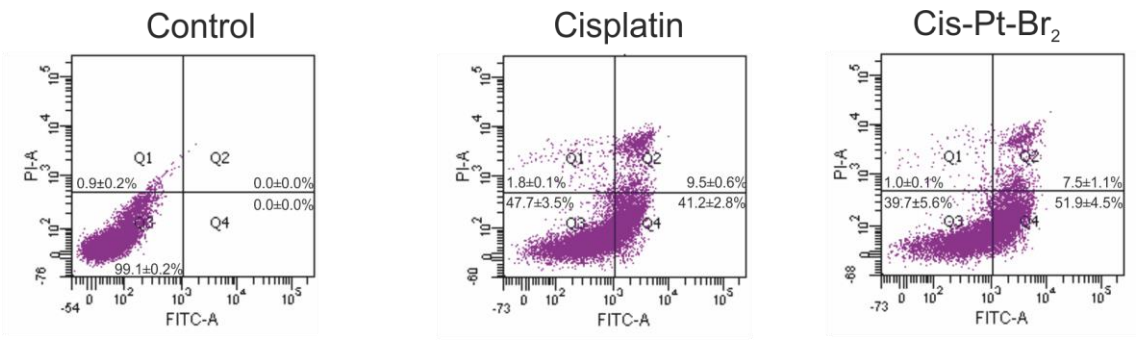

Figure 36: Effects of Cisplatin and cis-Pt-Br_2 on apoptosis distribution of FLG 29.1 cells. Apoptosis was evaluated after 24 hours of treatment through the Annexin/PI assay. The figure shows dot plots of control and treated cells at the same experimental time point. The results are the Means±ESM of two independent experiments.

Finally we mounted an experiment to assess the different cytotoxic effect of Cisplatin and cis-$PtBr_2(NH_3)_2$ during the passage of time; FLG 29.1 were exposed to 19µM of both the drugs, given singularly for 72h. As reported in Figure 37 treatment of cells with the dibromido analogue significantly diminished the percentage of living cells during the passage of time, both at 48h and at 72h, compared to Cisplatin.

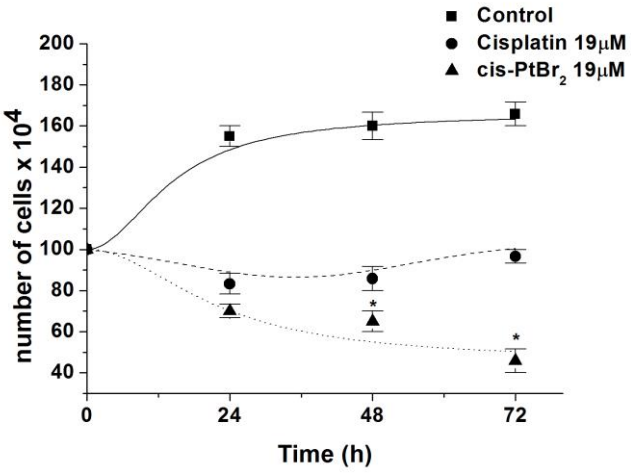

Figure 37: Effects of Cisplatin (black dots) and cis-$PtBr_2$ (black triangles) on FLG 29.1 cell line proliferation during the passage of time given as the number of Trypan Blue negative cells. Drugs were added once a t=0. Data are means ± SEM of two independent experiments. Statistically significant data compared to Cisplatin treatment, accordingly to paired t-student test, are indicated with an asterisk.

Taken together these results confirmed the potential value of cis-Pt-Br_2 on FLG29.1 cell line as, in comparison with Cisplatin, it exerted a higher induction of apoptosis (% of cell in early apoptosis 41.2±2.8% vs 51.9±4.5%) and a stronger accumulation of cells in S phase while cis-Pt-I_2 exhibited for all the cell lines of the panel, except for HCT-116 p53-/- a stronger effect compared to Cisplatin, a higher platin internalization and a higher block on HCT-116 cells on the transition between G0/G1 and S phase, resulting in a decrease of cell proliferation.

Finally we decided then to test cis-Pt-I_2 in our model of Cisplatin resistance colorectal cell line, the HCT-116 cells, in combination with K^+ channel modulators, to see if its higher efficacy could be improved by the specific modulation of selective ion channels. We performed a series of CI experiments which revealed an additive effect at IC_{50} values of this new Cisplatin analogue with Riluzole, but not with the other modulators (Table 20).

HCT-116	**Combination index at IC_{50}** mean±SEM	**Combination index at IC_{75}** mean±SEM	**Combination index at IC_{90}** mean±SEM
Cis-Pt-I_2+Riluzole	1.00±0.01	1.44±0.16	2.33±0.49
Cis-Pt-I_2+SKA-31	1.64±0.24	1.59±0.20	1.67±0.17
Cis-Pt-I_2+TRAM-34	2.27±0.39	1.95±0.64	2.16±1.49
Cis-Pt-I_2+E4031	1.43±0.04	1.29±0.01	1.17±0.04

Table 20: HCT-116 cell line was exposed to IC_{50} Cis-Pt-I_2 in combination with IC_{50} of Riluzole, SKA-31, TRAM-34 and E4031 with a 2-fold serial dilution (1/1, 1/2, 1/4, 1/8, 1/16, 1/32, 1/64) for 24 hours and then cell viability was evaluated using Trypan blue exclusion assay. The means are relative to two independent experiments. CI values were calculated using Calcusyn software Version 2 (Biosoft). CI > 1, antagonisms; CI = 1, additivity; CI < 1, synergy.

5. DISCUSSION

Chemoresistance is a major problem in clinical oncology. Cisplatin, one of the drugs most widely used in the therapy of solid cancers, often triggers the development of resistance to its pro-apoptotic effects (Kartalou et Essigmann., 2001; Siddik et al., 2003; Wang et al., 2005). Hence, the development of new protocols capable of overcoming Cisplatin chemoresistance could have a great clinical significance.

We studied two possible ways of overcoming this problem: (1) using ion channels as targets in an *in vitro* model of Cisplatin resistance in colorectal cancer (CRC) with the aim to test the possible use of K^+ channel modulating agents and (2) test two new Cisplatin-analogues with the intent of characterizing their activation properties in aqueous solutions, their reactivity with DNA and their cytotoxic effect on a small panel of tumor cell lines in comparison with Cisplatin.

(1) Starting from analyzing a panel of CRC cell lines we found that Cisplatin resistant CRC cells (HCT-116) have a higher expression of K^+ channels compared to the most sensitive cell line (HCT-8) while there was no appreciable difference in the expression levels of the main transporters known in literature to mediate Cisplatin uptake and efflux.

We analyzed the expression levels of different K^+ channels encoding genes, focusing on those reported to be expressed in CRC (Spitzner, 2007; Arcangeli et al, 2009; Huang. et al 2014; Planells-Cases et al., 2015): the voltage dependent potassium channels Kv10.1 or EAG1 (*KCNH1*), Kv11.1 or hERG1 (*KCNH2*) and Kv1.3 (*KCNA3*), the intermediate-conductance calcium-activated potassium channel KCa3.1 (*KCNN4*), the

small-conductance KCa2.3 (*KCNN3*) and the big conductance KCa1.1 channels (*KCNMA1*).

From our analysis *KCNH2* was found expressed in both cell lines, but at higher level in HCT-116 cells, as previously reported (Lastraioli et al., 2004). *KCNN4* (high expression level) and *KCNN3* (medium expression level) were present almost exclusively in HCT-116 cells. All other ion channels transcripts were negligible in both cell lines.

Our data are consistent to what found by Spitzner et al., 2007 in T84 colon carcinoma cells for the RT-PCR expression levels of hERG1 and KCa3.1 while we didn't detect in both our cell lines studied considerable expression levels of KCa1.1, Kv1.3 and EAG channels. Lee and colleagues also found high expression KCa3.1 in KB colon cell line (Lee et al., 2008) which was also reported to be expressed in HCT-116 mitochondria (De Marchi et al., 2009). As for the main Cisplatin transporters found to be expressed in cancer cells (Harrach et Ciarimboli 2015; Spreckelmeyer et al.,2014), the copper transporters CTR1 (*SLC31A1*) and CTR2 (*SLC31A2*) as well as the two P-type ATPases ATP7A (*ATP7A*) and ATP7B (*ATP7B*), three of them, *SLC31A1*, *ATP7A* and *ATP7B*, were found expressed in both HCT-116 and HCT-8 but their expression levels did not differ between the two CRC cell lines. The high expression levels of CTR1 are known in literature to be associated with several tumour cancer lines and, given its almost ubiquitously expression, it may not be the decisive transporter for specific Cisplatin toxicities (Harrach et Ciarimboli. 2015) while, given ATP7A and ATP7B role in mediating Cisplatin efflux from the cell or its distribution to specific sub-cellular compartments, our data suggests that in our *in vitro* model other mechanisms of efflux could be implicated in a different cytoxicity, like organic cation transporters and multidrug and toxin extrusion proteins (Spreckelmeyer et al., 2014).

Consistently with the abundance of K^+ channels we found that HCT-116 have a more hyperpolarized membrane potential (Vrest) value compared to sensitive HCT-8.

Liang et colleagues, using the same KB-3-1 cell line (Cisplatin sensitive) and a similar derived clone KB-CP1 (Cisplatin-resistant) used by Lee and his collaborators, found that Cisplatin-resistant clones displayed a more hyperpolarized cell membrane potential compared to the sensitive one, in accordance to what we found in our model (Liang et al., 2005).

These results indicated to us that the ion homeostasis of Cisplatin-resistant cells is different than that of the sensitive one. In addition, several other data in literature indicated that altered K^+ fluxes and the expression of K^+ channels on plasma membranes are associated with Cisplatin resistance (Liang et al., 2004; Mahaswari et al., 2000) and that hERG1 upregulation is often present in the acquisition of this characteristic (Liang et al., 2005). All this considered, we focused our interest on the ion channels found differently expressed between our Cisplatin-sensitive (HCT-8) and Cisplatin-resistant colorectal cell line (HCT-116).

From our work different K^+ channel modulators (Riluzole, SKA-31 and E4031) displayed a relevant inhibition of HCT-116 cell growth; this is consistent to what reported in literature. Riluzole, an activator of KCa3.1 and an hERG1 inhibitor (Sankaranarayanan et al. 2009), known for being already approved for human use for ALS treatment, recently demonstrated to reduce human prostate cancer cells viability, inducing apoptotic cell death following endoplasmic reticulum stress (Akamatsu. 2009) as well as migration, invasion, and proliferation of melanoma cells (Le et al., 2010).

Although there are no evidence in literature for SKA-31, a known selective KCa3.1 activator, effect of cancer cells proliferation we speculate a similar mechanism compared to Riluzole, given its selectivity of action for KCa3.1 channel. E4031, an experimental class III antiarrhythmic drug able to selectively block hERG1 channel, is

known to inhibit cell proliferation and invasion in neuroblastoma cell lines (Crociani et al., 2003), gastric cancer cells (Lastraioli et al., 2005) and Acute B Lymphoblastic Leukemia cell lines (Pillozzi et al., 2007). All these data confirmed to us the strong effect we reported on reduction of cell proliferation both on HCT-8 and HCT-116 cell lines. When given in combination with Cisplatin, Riluzole, SKA-31 and E4031 exhibited a synergic effect. This could be traced back to an increase in the percentage of apoptotic cells (Table 10).

The K^+ channel modulators we tested could at least exert part of their efficacy by affecting cell volume homeostasis and could have a prominent role in the induction of apoptotic volume decrease (AVD). In cancer a hallmark of apoptosis is a marked cell shrinkage (Kerr et al., 1972), which is AVD (Maeno et al., 2000). AVD is an early event required for triggering of full apoptosis (Poulsen et al., 2010), and there is strong evidence that preventing cell volume regulation after shrinkage is associated with induction of apoptosis (Lang et Hoffmann, 2012). AVD results from a loss of KCl via K^+ and Cl^- channels and concomitant loss of water; this is linked with both hERG1 and KCa3.1 channels as well as VRAC anion channel (Pedersen et al., 2011).

During AVD, cells lose the capacity for counteracting cell shrinkage by triggering a regulatory volume increase (RVI) response (Maeno et al., 2006), which would be normally operating in a healthy cell. It important to note that in MCF-7 cells hERG1 was found to be related to RVD; in particular its inhibition with E4031 has been linked to the complete abolition of RVD (Roy et al., 2008).

Although there is no evidence in literature that Cisplatin can alter KCa3.1 mRNA levels, it is involved in altered calcium homeostasis and extracellular Ca^{2+} has been observed to be necessary for Cisplatin-induced activation, in human carcinoma HeLa-S3 cells, of a Ca^{2+}-dependent K^+ conductance inhabitable by charybdotoxin (Splettstoesser et al., 2007).

Calcium signaling is involved in various tumorigenic pathways, and the inhibition or activation of specific Ca^{2+}channels or pumps can reduce cellular proliferation and/or induce apoptosis (Monteith et al., 2007; Lipskaia et Lompré, 2004; Florea et Büsselberg, 2013). Al-Taweel and colleagues correlated an increased cytosolic calcium levels to treatment with Cisplatin in MFC-7 cells, while in a Cisplatin-resistant MCF-7 clone, this response, following Cisplatin treatment, was far less evident (Al-Taweel et al., 2014).

Riluzole activity has been also related to a disruption in calcium homeostasis, in particular it was found to reduce prostate carcinoma cells viability by a reduction in DNA synthesis, induction of apoptosis following endoplasmic reticulum stress, abnormal release of calcium in the cytoplasm and caspase-4 induction (Akamatsu et al., 2009).

Additionally, reactive oxygen species (ROS), which are produced upon Cisplatin treatment (Casares et al., 2012) may have also a role in KCa3.1 activation. One report provides evidence that ROS stimulate the KCa3.1 conductance in the Calu-3 airway epithelial cell line (Cowley et Linsdell. 2002) and also VRAC channel was activated by ROS in apoptosis of HeLa epithelial cancer cells (Shimizu et al. 2004) suggesting a common role of both the channels in apoptosis modulation.

We also reported that treatment of HCT-116 cells for 24h with Riluzole, SKA-31 and E4031 was accompanied by an augment of intracellular Cisplatin concentration (Figure 26) but not with a significant modulation of cell membrane potential (Table 7) and that the combination of Riluzole, SKA-31 or E4031 with low Cisplatin doses strongly reduced HCT-116 cell growth.

Concerning Cisplatin uptake measurements our investigation outlined that data could be either expressed by number of cells or by mg of proteins, given the linearity of their correlation (Figure 22). Compared to what reported by Planells-Cases and colleagues on

both HEK-293 and HCT-116 cells our analysis outlined consistency for short exposure times treatment while differed for prolonged times (Figure 23). At 3h we clearly demonstrated that CTRs are not relevant on Cisplatin uptake in HCT-116 (Figure 24) and that TRAM-34, given in combination with Cisplatin, is able to decrease its uptake. These data suggest that other transporters are involved in Cisplatin uptake in HCT-116 as anion channel VRAC which, was recently found to be responsible for half of its uptake under isotonic condition (Planells-Cases et al., 2015). TRAM-34 effect could be related to the block of KCa3.1 in regulating VRAC activity, following K^+ and Cl^- ion lost during AVD induction and consequently Cisplatin uptake through VRAC channel.

The high variability affecting our data at 24h could be explained by the relative small number of cells seeded compared to the high effect of Cisplatin and K^+ channels modulators on cell viability at longer incubation times, which could also have affected manual and instrumental difficulties in sample preparation.

Despite this technical bias, we were able to assess at 24h, in three independent experiments, the effect of K^+ channel modulators in affecting Cisplatin uptake levels in HCT-116 cells. We found that Riluzole, SKA-31 and E4031, given in combination with Cisplatin, were able to increase its intracellular levels while TRAM-34 induced a decrease in its concentration (Figure 26).

To explain how potassium channels modulators can exert all their effects on cell viability through a modulation of Cisplatin uptake, we propose a mechanism consistent to what reported by Planells-Cases and colleagues concerning VRAC ability to modulate platinum uptake in HCT-116 cells (Planells-Cases et al., 2015).

In their article the authors pointed out how VRAC is the main Cisplatin transporter and that a downregulation of two specific VRAC subunits, LRRC8A and LRRC8D, is directly linked to a significant decrease of Cisplatin uptake at 24h, both in HEK-293 and HCT-116 cell lines (Planells-Cases et al., 2015).

We speculate that Riluzole and SKA-31 activation of KCa3.1 in HCT-116 cells could result in a volume decrease by potassium and consequent chloride ions lost, not affecting cellular Vrest. This reduction in cell volume could lead not only to AVD, but also to induce an increase in Cisplatin uptake through VRAC channel (Planells-Cases et al. 2015). This could lead to a more severe AVD as Cisplatin is known to induce apoptotic volume decrease as a first step during the induction of apoptosis (Cai et al., 2015).

We speculate that hERG1 block by E4031 could operate on the other hand by a decrease in cell proliferation by modulation of AKT signaling pathway as already reported in HCT-116 (Crociani et al. 2013). Although this hypothesis will need further confirmation we suggest the possibility that this could cooperate with Riluzole and SKA-31 in affecting cell viability, resulting in a global decrease of cell proliferation, enhancing Cisplatin cytotoxic cellular concentration and apoptosis induction. This model is summarized in Figure 38.

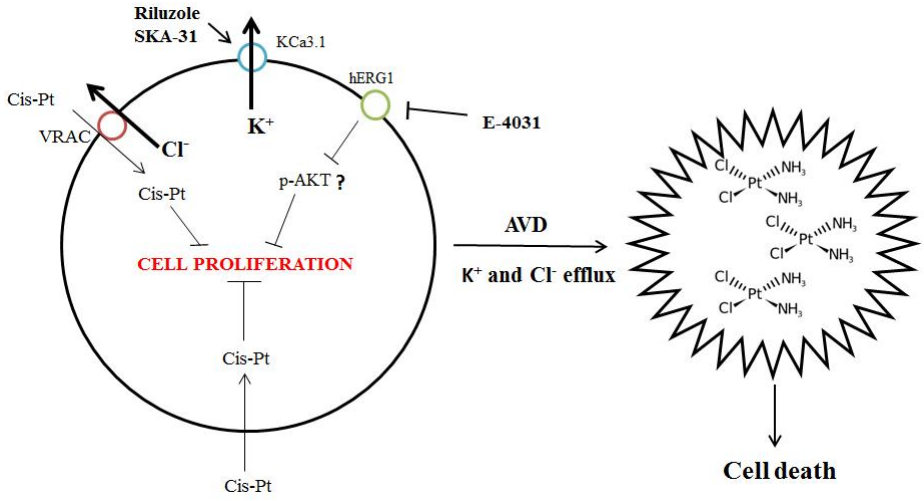

Figure 38: Schematic model of interaction of synergic potassium channel modulators with their targets and effect on cell proliferation in HCT-116 cell line. Cis-Pt: Cisplatin

(2) The test of cis-Pt-I_2 and cis-Pt-Br_2 properties in aqueous solution outlined how the diiodio analogue display a higher binding time compared with Cisplatin (Table 17) while the dibromo analogue displayed no significant difference (Figure 34). Despite these initial results cis-Pt-I_2 and cis-Pt-Br_2 were found to be more lypophilic compared to Cisplatin.

From our cytotoxicity studies cis-Pt-I_2 and cis-Pt-Br_2 resulted in a higher efficacy compared to Cisplatin, particularly in HCT-116 and FLG29.1 cell lines respectively. To explain the higher effect of cis-Pt-I_2 compared to Cisplatin in our panel of cell lines tested, we point out that, in spite of its lower reactivity with DNA, an unconventional off-target reactivity toward the model protein cytochrome c has been highlighted, unexpectedly characterized by the loss of the amino ligands and retention of iodido ligands (Messori et al., 2012; Messori et al., 2010). Furthermore, Messori and his colleagues structurally described the reaction of cis-Pt-I_2 with lysozyme, confirming the peculiar and different interaction mode toward this model protein in comparison to Cisplatin (Messori et al., 2013). Another aspect which can evidence cis-Pt-I_2 as well as cis-Pt-Br_2 effectiveness is their higher lipophilicity compared to Cisplatin which can assess an increase in their cellular uptake and advocate for a higher cell cycle block (in G0/G1 phase for cis-Pt-I_2 and in S phase in cis-Pt-Br_2) compared to Cisplatin (Figure 36). In particular the higher efficacy of cis-Pt-Br_2 was more evident during the passage of time, suggesting a more effective role in inhibiting cellular growth compared to Cisplatin, possibly linked to its higher lipophilicity (Figure 37).

The lesser efficacy we found on HCT-116 $p53^{-/-}$ is quite puzzling but data from literature on p53 role in Cisplatin resistance are mixed; several authors indicates how a mutation of p53 results in an increase of Cisplatin resistance (Boulikas et Vougiouka. 2003) while others points out how an augment of cytoplasmic p53 expression levels is

correlated with an increase Cisplatin resistance, for its role in negatively modulating caspase 9 (Chee et al., 2013).

Finally we report that when cis-Pt-I_2 was tested with the same K^+ channels modulators instead of Cisplatin, its effect were quite different; only Riluzole remained synergic with the diiodio-analogue (Table 20), confirming not only different potential off-target effects but, we speculate, different effects on VRAC modulation as well.

Taken together both the approaches followed in this thesis demonstrated capability in overcoming Cisplatin resistance, either with the exploit of K^+ channels modulators drugs in combination with Cisplatin or through the increase selectivity of new platinum based compounds, as cis-Pt-I_2 and cis-Pt-Br_2.

6. REFERENCES

Ahmed-Ouameur A, Diamantoglou S, Sedaghat-Herati MR, Nafisi Sh, Carpentier R, Tajmir-Riahi HA. The effects of drug complexation on the stability and conformation of human serum albumin: protein unfolding. *Cell Biochem Biophys*. 2006;45(2):203-13.

Akamatsu K, Shibata MA, Ito Y, Sohma Y, Azuma H, Otsuki Y. Riluzole induces apoptotic cell death in human prostate cancer cells via endoplasmic reticulum stress. *Anticancer Res.* 2009 Jun;29(6):2195-204.

Airtum et Aoim. Il numeri del cancro in Italia. 2014

Alderden, R.A.; Hall, M.D.; Hambley, T.W. The discovery and development of Cisplatin. J. *Chem. Educ*., 2006, 83 (5), 728-734.

Alkam Y, Mitomi H, Nakai K, Himuro T, Saito T, Takahashi M, Arakawa A, Yao T, Saito M. Protein expression and methylation of DNA repair genes hMLH1, hMSH2, MGMT and BRCA1 and their correlation with clinicopathological parameters and prognosis in basal-like breast cancer. *Histopathology.* 2013 Nov;63(5):713-25.

Al-Taweel N, Varghese E, Florea AM, Büsselberg D. Cisplatin (CDDP) triggers cell death of MCF-7 cells following disruption of intracellular calcium ([Ca(2+)]i) homeostasis. *J Toxicol Sci*. 2014;39(5):765-74.

American Cancer Society *Cancer Facts and Figures 2015*. Atlanta, Ga, 2015.

André T, Boni C, Mounedji-Boudiaf L, Navarro M, Tabernero J, Hickish T, Topham C, Zaninelli M, Clingan P, Bridgewater J, Tabah-Fisch I, de Gramont A, Multicenter International Study of Oxaliplatin/5-Fluorouracil/Leucovorin in the Adjuvant Treatment

of Colon Cancer (MOSAIC) Investigators Oxaliplatin, fluorouracil, and leucovorin as adjuvant treatment for colon cancer. *N Engl J Med*. 2004 Jun 3; 350(23):2343-51.

Appelqvist H, Nilsson C, Garner B, Brown AJ, Kågedal K, Ollinger K. Attenuation of the lysosomal death pathway by lysosomal cholesterol accumulation. *Am J Pathol*. 2011 Feb;178(2):629-39. doi: 10.1016/j.ajpath.2010.10.030.

Arcangeli A, Crociani O, Lastraioli E, Masi A, Pillozzi S, Becchetti A. Targeting ion channels in cancer: a novel frontier in antineoplastic therapy. *Curr Med Chem*. 2009;16(1):66-93.

Arumuggam N, Bhowmick NA, Rupasinghe HP A Review: Phytochemicals Targeting JAK/STAT Signaling and IDO Expression in Cancer. *Phytother Res*. 2015 Jun;29(6):805-17.

Asher V, Warren A, Shaw R, Sowter H, Bali A, Khan R. The role of Eag and HERG channels in cell proliferation and apoptotic cell death in SKOV-3 ovarian cancer cell line. *Cancer Cell Int.* 2011 Mar 10;11:6. doi: 10.1186/1475-2867-11-6.

Barzi A, Lenz AM, Labonte MJ, Lenz HJ. Molecular pathways: Estrogen pathway in colorectal cancer. *Clin Cancer Res*. 2013 Nov 1;19(21):5842-8.

Bellingham MC. A review of the neural mechanisms of action and clinical efficiency of Riluzole in treating amyotrophic lateral sclerosis: what have we learned in the last decade? *CNS Neurosci Ther*. 2011 Feb;17(1):4-31.

Berridge MJ, Bootman MD, Roderick HL. Calcium signalling: dynamics, homeostasis and remodelling. *Nat Rev Mol Cell Biol.* 2003 Jul;4(7):517-29.

Binefa G, Rodríguez-Moranta F, Teule A, Medina-Hayas M. Colorectal cancer: from prevention to personalized medicine. *World J Gastroenterol*. 2014 Jun 14;20(22):6786-808. doi: 0.3748/wjg.v20.i22.6786.

Bortner CD, Cidlowski JA. Ion channels and apoptosis in cancer. *Philos Trans R Soc Lond B Biol Sci*. 2014 Feb 3;369(1638):20130104.

Bouhy D, Ghasemlou N, Lively S, Redensek A, Rathore KI, Schlichter LC, David S. Inhibition of the Ca^{2+}-dependent K^+ channel, KCNN4/KCa3.1, improves tissue protection and locomotor recovery after spinal cord injury. *J Neurosci*. 2011 Nov 9;31(45):16298-308.

Boulikas T, Vougiouka M. Cisplatin and platinum drugs at the molecular level. (Review). *Oncol Rep*. 2003 Nov-Dec;10(6):1663-82.

Bouron A, Kiselyov K, Oberwinkler J. Permeation, regulation and control of expression of TRP channels by trace metal ions. *Pflugers Arch*. 2015 Jun;467(6):1143-64.

Bozic I, Reiter JG, Allen B, Antal T, Chatterjee K, Shah P, Moon YS, Yaqubie A, Kelly N, Le DT, Lipson EJ, Chapman PB, Diaz LA Jr, Vogelstein B, Nowak MA Evolutionary dynamics of cancer in response to targeted combination therapy. *Elife.* 2013 Jun 25; 2():e00747.

Bradding P, Wulff H. The K^+ channels K(Ca)3.1 and K(v)1.3 as novel targets for asthma therapy. *Br J Pharmacol.* 2009 Aug;157(8):1330-9.

Brisson L, Driffort V, Benoist L, Poet M, Counillon L, Antelmi E, Rubino R, Besson P, Labbal F, Chevalier S, Reshkin SJ, Gore J, Roger S. NaV1.5 Na^+ channels allosterically regulate the NHE-1 exchanger and promote the activity of breast cancer cell invadopodia. *J Cell Sci.* 2013 Nov 1;126(Pt 21):4835-42.

Brozovic A, Fritz G, Christmann M, Zisowsky J, Jaehde U, Osmak M, Kaina B Long-term activation of SAPK/JNK, p38 kinase and fas-L expression by Cisplatin is attenuated in human carcinoma cells that acquired drug resistance. *Int J Cancer*. 2004 Dec 20; 112(6):974-85.

Burn J, Gerdes AM, Macrae F, Mecklin JP, Moeslein G, Olschwang S, Eccles D, Evans DG, Maher ER, Bertario L, Bisgaard ML, Dunlop MG, Ho JW, Hodgson SV, Lindblom A, Lubinski J, Morrison PJ, Murday V, Ramesar R, Side L, Scott RJ, Thomas HJ, Vasen HF, Barker G, Crawford G, Elliott F, Movahedi M, Pylvanainen K, Wijnen JT, Fodde R, Lynch HT, Mathers JC, Bishop DT; CAPP2 Investigators. Long-term effect of aspirin on cancer risk in carriers of hereditary colorectal cancer: an analysis from the CAPP2 randomised controlled trial. *Lancet.* 2011 Dec 17;378(9809):2081-7. doi: 10.1016/S0140-6736(11)61049-0.

Cai S, Zhang T, Zhang D, Qiu G, Liu Y. Volume-sensitive chloride channels are involved in Cisplatin treatment of osteosarcoma. *Mol Med Rep*. 2015 Apr;11(4):2465-70.

Casares C, Ramírez-Camacho R, Trinidad A, Roldán A, Jorge E, García-Berrocal JR. Reactive oxygen species in apoptosis induced by Cisplatin: review of physiopathological mechanisms in animal models. *Eur Arch Otorhinolaryngol*. 2012 Dec;269(12):2455-9..

Catacuzzeno L, Fioretti B, Franciolini F. Expression and Role of the Intermediate-Conductance Calcium-Activated Potassium Channel KCa3.1 in Glioblastoma. *J Signal Transduct.* 2012;2012:421564.

Chae YJ, Lee KJ, Lee HJ, Sung KW, Choi JS, Lee EH, Hahn SJ. Endoxifen, the active metabolite of tamoxifen, inhibits cloned hERG potassium channels. *Eur J Pharmacol*. 2015 Apr 5;752:1-7.

Chee JL, Saidin S, Lane DP, Leong SM, Noll JE, Neilsen PM, Phua YT, Gabra H, Lim TM. Wild-type and mutant p53 mediate Cisplatin resistance through interaction and inhibition of active caspase-9. *Cell Cycle*. 2013 Jan 15;12(2):278-88.

Chen L, Zhao Y, Halliday GC, Berry P, Rousseau RF, Middleton SA, Nichols GL, Del Bello F, Piergentili A, Newell DR, Lunec J, Tweddle DA. Structurally diverse MDM2-p53 antagonists act as modulators of MDR-1 function in neuroblastoma. *Br J Cancer*. 2014 Aug 12;111(4):716-25.

Cherubini A1, Hofmann G, Pillozzi S, Guasti L, Crociani O, Cilia E, Di Stefano P, Degani S, Balzi M, Olivotto M, Wanke E, Becchetti A, Defilippi P, Wymore R, Arcangeli A. Human ether-a-go-go-related gene 1 channels are physically linked to beta1 integrins and modulate adhesion-dependent signaling. *Mol Biol Cell*. 2005 Jun;16(6):2972-83. Epub 2005 Mar 30.

Chioni AM, Shao D, Grose R, Djamgoz MB. Protein kinase A and regulation of neonatal Nav1.5 expression in human breast cancer cells: activity-dependent positive feedback and cellular migration. *Int J Biochem Cell Biol.* 2010 Feb;42(2):346-58.

Chou TC, Talalay P. Quantitative analysis of dose-effect relationships: the combined effects of multiple drugs or enzyme inhibitors. *Adv Enzyme Regul*. 1984;22:27-55.

Choura M, Rebaï A. Receptor tyrosine kinases: from biology to pathology. *J Recept Signal Transduct Res.* 2011 Dec;31(6):387-94.

Cleare, M. J.; Hoeschele, J. D. "Studies on the Antitumor Activity of Group VIII Transition Metal Complexes, Part I. Platinum(II) Complexes" *Bioinorganic Chemistry* 1973, 2, 187-210.

Comes N, Bielanska J, Vallejo-Gracia A, Serrano-Albarrás A, Marruecos L, Gómez D, Soler C, Condom E, Ramón Y Cajal S, Hernández-Losa J, Ferreres JC, Felipe A. The

voltage-dependent K(+) channels Kv1.3 and Kv1.5 in human cancer. *Front Physiol.* 2013 Oct 10;4:283.

Cowley EA, Linsdell P. Characterization of basolateral K+ channels underlying anion secretion in the human airway cell line Calu-3. *J Physiol*. 2002 Feb 1;538(Pt 3):747-57.

Crociani, O.; Guasti, L.; Balzi, M.; Becchetti, A.; Wanke, E.; Olivotto, M.; Wymore, R. S.; Arcangeli, A. Cell cycle-dependent expression of HERG1 and HERG1B isoforms in tumor cells. *J.Biol. Chem.*, 2003, 278, 2947-2955.

Crociani O, Zanieri F, Pillozzi S, Lastraioli E, Stefanini M, Fiore A, Fortunato A, D'Amico M, Masselli M, De Lorenzo E, Gasparoli L, Chiu M, Bussolati O, Becchetti A, Arcangeli A. hERG1 channels modulate integrin signaling to trigger angiogenesis and tumor progression in colorectal cancer. *Sci Rep.* 2013 Nov 25;3:3308.

Cui Y, König J, Buchholz JK, Spring H, Leier I, Keppler D. Drug resistance and ATP-dependent conjugate transport mediated by the apical multidrug resistance protein, MRP2, permanently expressed in human and canine cells. *Mol Pharmacol*. 1999 May;55(5):929-37.

Cuzick J, Otto F, Baron JA, Brown PH, Burn J, Greenwald P, Jankowski J, La Vecchia C, Meyskens F, Senn HJ, Thun M. Aspirin and non-steroidal anti-inflammatory drugs for cancer prevention: an international consensus statement. *Lancet Oncol*. 2009 May;10(5):501-7.

Dasari S, Tchounwou PB. Cisplatin in cancer therapy: molecular mechanisms of action. *Eur J Pharmacol*. 2014 Oct 5;740:364-78.

De Marchi U, Sassi N, Fioretti B, Catacuzzeno L, Cereghetti GM, Szabò I, Zoratti M. Intermediate conductance Ca2+-activated potassium channel (KCa3.1) in the inner

mitochondrial membrane of human colon cancer cells. *Cell Calcium*. 2009 May;45(5):509-16.

De Mattia E, Cecchin E, Toffoli G. Pharmacogenomics of intrinsic and acquired pharmacoresistance in colorectal cancer: Toward targeted personalized therapy. *Drug Resist Updat*. 2015 May;20:39-70.

Dhara SC. A rapid method for the synthesis of cis-[Pt(NH3)2Cl2] *Indian J Chem*. 1970;8:193–194.

Ding XW, Luo HS, Luo B, Xu DQ, Gao S. Overexpression of hERG1 in resected esophageal squamous cell carcinomas: a marker for poor prognosis. *J Surg Oncol* 2008; 97: 57–62.

Driffort V, Gillet L, Bon E, Marionneau-Lambot S, Oullier T, Joulin V, Collin C, Pagès JC, Jourdan ML, Chevalier S, Bougnoux P, Le Guennec JY, Besson P, Roger S. Ranolazine inhibits NaV1.5-mediated breast cancer cell invasiveness and lung colonization. *Mol Cancer.* 2014 Dec 11;13:264.

Durdagi S, Subbotina J, Lees-Miller J, Guo J, Duff HJ, Noskov SY. Insights into the molecular mechanism of hERG1 channel activation and blockade by drugs. *Curr Med Chem*. 2010;17(30):3514-32.

Emert-Sedlak L, Shangary S, Rabinovitz A, Miranda MB, Delach SM, Johnson DE. Involvement of cathepsin D in chemotherapy-induced cytochrome c release, caspase activation, and cell death. *Mol Cancer Ther*. 2005 May;4(5):733-42.

Farmer H, McCabe N, Lord CJ, Tutt AN, Johnson DA, Richardson TB, Santarosa M, Dillon KJ, Hickson I, Knights C, Martin NM, Jackson SP, Smith GC, Ashworth A Targeting the DNA repair defect in BRCA mutant cells as a therapeutic strategy. *Nature*. 2005 Apr 14; 434(7035):917-21.

Félétou M Calcium-activated potassium channels and endothelial dysfunction: therapeutic options? *Br J Pharmacol.* 2009 Feb;156(4):545-62.

Ferlay J, Soerjomataram I, Ervik M, Dikshit R, Eser S, Mathers C, Rebelo M, Parkin DM, Forman D, Bray, F. GLOBOCAN 2012 v1.0, Cancer Incidence and Mortality Worldwide: IARC CancerBase No. 11 [Internet]. Lyon, France: *International Agency for Research on Cancer;* 2013.

Fijołek J, Wiatr E, Rowińska-Zakrzewska E, Giedronowicz D, Langfort R, Chabowski M, Orłowski T, Roszkowski K p53 and HER2/neu expression in relation to chemotherapy response in patients with non-small cell lung cancer. *Int J Biol Markers*. 2006 Apr-Jun; 21(2):81-7.

Florea, A.M. and Büsselberg, D. (2013): Breast cancer and possible mechanisms of therapy resistance. *Journal of Global and Local Health Science* Vol. 2013, 2.

Flossmann E and Rothwell PM Effect of aspirin on long-term risk of colorectal cancer: consistent evidence from randomised and observational studies. *Lancet.* 2007 May 12;369(9573):1603-13.

Fraser SP, Ozerlat-Gunduz I, Brackenbury WJ, Fitzgerald EM, Campbell TM, Coombes RC, Djamgoz MB. Regulation of voltage-gated sodium channel expression in cancer: hormones, growth factors and auto-regulation. *Philos Trans R Soc Lond B Biol Sci.* 2014 Feb 3;369(1638):20130105.

Freeman HJ Colorectal cancer risk in Crohn's disease. World J Gastroenterol. 2008 Mar 28;14(12):1810-1.

Fulda S, Vucic D. Targeting IAP proteins for therapeutic intervention in cancer. *Nat Rev Drug Discov*. 2012 Feb 1;11(2):109-24.

Furuta T, Ueda T, Aune G, Sarasin A, Kraemer KH, Pommier Y Transcription-coupled nucleotide excision repair as a determinant of Cisplatin sensitivity of human cells. *Cancer Res*. 2002 Sep 1; 62(17):4899-902.

Gasparoli L, D'Amico M, Masselli M, Pillozzi S, Caves R, Khuwaileh R, Tiedke W, Mugridge K, Pratesi A, Mitcheson JS, Basso G, Becchetti A, Arcangeli A. New pyrimido-indole compound CD-160130 preferentially inhibits the KV11.1B isoform and produces antileukemic effects without cardiotoxicity. *Mol Pharmacol.* 2015 Feb;87(2):183-96.

Gavrilova-Ruch O, Schönherr K, Gessner G, Schönherr R, Klapperstück T, Wohlrab W, Heinemann SH. Effects of imipramine on ion channels and proliferation of IGR1 melanoma cells. *J Membr Biol.* 2002 Jul 15;188(2):137-49.

Gerlach AC, Gangopadhyay NN, Devor DC Kinase-dependent regulation of the intermediate conductance, calcium-dependent potassium channel, hIK1. *J Biol Chem*. 2000 Jan 7; 275(1):585-98.

Gerlinger M, Swanton C How Darwinian models inform therapeutic failure initiated by clonal heterogeneity in cancer medicine. *Br J Cancer*. 2010 Oct 12;103(8):1139-43. doi: 10.1038/sj.bjc.6605912.

Gustavsson B, Carlsson G, Machover D, Petrelli N, Roth A, Schmoll HJ, Tveit KM, Gibson F A review of the evolution of systemic chemotherapy in the management of colorectal cancer. *Clin Colorectal Cancer*. 2015 Mar;14(1):1-10. doi: 10.1016/j.clcc.2014.11.002. Epub 2014 Nov 15.

Hamilton SR, Bosman FT, Boffetta P, et al. Carcinoma of the colon and rectum. In: WHO Classification of Tumours of the Digestive System. Bosman FT, Carneiro F, Hruban RH, Theise ND, eds. Lyon: *IARC Press*, 2010:134-46

Han X, Chesney RW. Mechanism of TauT in protecting against Cisplatin-induced kidney injury (AKI). *Adv Exp Med Biol*. 2009;643:105-12.

Harrach S, Ciarimboli G. Role of transporters in the distribution of platinum-based drugs. *Front Pharmacol*. 2015 Apr 24;6:85.

Hartzell HC, Yu K, Xiao Q, Chien LT, Qu Z. Anoctamin/TMEM16 family members are $Ca2^{+}$-activated Cl- channels. *J Physiol.* 2009 May 15;587(Pt 10):2127-39.

He C, Tang Z, Tian H, Chen X. Co-delivery of chemotherapeutics and proteins for synergistic therapy. *Adv Drug Deliv Rev*. 2015 Nov 6. pii: S0169-409X(15)00246-X

Heminger, K.A.; Hartson, S.D.; Rogers, J.; Matts, R.L. Cisplatin inhibits protein synthesis in rabbit reticulocyte lysate by causing an arrest in elongation. *Arch. Biochem.* Biophys., 1997, 344 (1), 200-207.

Hodges LM, Markova SM, Chinn LW, Gow JM, Kroetz DL, Klein TE, Altman RB. Very important pharmacogene summary: ABCB1 (MDR1, P-glycoprotein). *Pharmacogenet Genomics.* 2011 Mar;21(3):152-61.

Hoeffel C., Mulé S, Laurent V., Bouché O., Volet J., Soyer P. Primary rectal cancer local staging *Diagn. Interv. Imaging*, 95 (2014), pp. 485–494

Hoffman JF, Joiner W, Nehrke K, Potapova O, Foye K, Wickrema A The hSK4 (KCNN4) isoform is the Ca2+-activated K+ channel (Gardos channel) in human red blood cells. *Proc Natl Acad Sci* U S A. 2003 Jun 10; 100(12):7366-71.

Hoffmann EK, Lambert IH. Ion channels and transporters in the development of drug resistance in cancer cells. *Philos Trans R Soc Lond B Biol Sci.* 2014 Feb 3;369(1638):20130109.

http://www.airc.it/tumori/tumore-al-colon-retto.asp

Huang CP, Fofana M, Chan J, Chang CJ, Howell SB. Copper transporter 2 regulates intracellular copper and sensitivity to Cisplatin. *Metallomics.* 2014 Mar;6(3):654-61. doi: 10.1039/c3mt00331k. Epub 2014 Feb 13.

Huang X, Jan LY. Targeting potassium channels in cancer. *J Cell Biol.* 2014 Jul 21;206(2):151-62.

Hwang JJ Irinotecan and 5-FU/ leucovorin in metastatic colorectal cancer: balancing efficacy, toxicity, and logistics. *Oncology (Williston Park*). 2004 Dec;18(14 Suppl 14):26-34.

Infrared and Raman Spectra of Inorganic and Coordination Compounds, Part B. Application in Coordination, Organometallic and Bioinorganic Chemistry, Nakamoto, K, Wiley Interscience, John Wiley and Sons, Inc., New York, 5th edn, 1997, ISBN 0-471-16392-9.

Jahchan NS, Dudley JT, Mazur PK, Flores N, Yang D, Palmerton A, Zmoos AF, Vaka D, Tran KQ, Zhou M, Krasinska K, Riess JW, Neal JW, Khatri P, Park KS, Butte AJ, Sage J. A drug repositioning approach identifies tricyclic antidepressants as inhibitors of small cell lung cancer and other neuroendocrine tumors. *Cancer Discov.* 2013 Dec;3(12):1364-77.

Jain RK. Normalization of tumor vasculature: an emerging concept in antiangiogenic therapy. Science. 2005;307:58–62

Jamali B, Nakhjavani M, Hosseinzadeh L, Amidi S, Nikounezhad N, H Shirazi F. Intracellular GSH Alterations and Its Relationship to Level of Resistance following Exposure to Cisplatin in Cancer Cells. *Iran J Pharm Res*. 2015 Spring;14(2):513-9.

Jamieson, E. R. & Lippard, S. J. Structure, recognition, and processing of Cisplatin–DNA adducts. *Chem. Rev*. 99, 2467–2498 (1999).

Jasperson K, Burt RW. The Genetics of Colorectal Cancer. *Surg Oncol Clin N Am*. 2015 Oct;24(4):683-703.

Jehle J, Schweizer PA, Katus HA, Thomas D. Novel roles for hERG K(+) channels in cell proliferation and apoptosis. *Cell Death Dis*. 2011 Aug 18;2:e193.

Jensen BS, Strøbæk D, Christophersen P, Jorgensen TD, Hansen C, Silahtaroglu A, Olesen SP, Ahring PK. Characterization of the cloned human intermediate-conductance Ca2+-activated K+ channel. *Am J Physiol Cell Physiol.* 1998;275:C848–856.

Jentsch TJ, Stein V, Weinreich F, Zdebik AA. Molecular structure and physiological function of chloride channels. *Physiol Rev.* 2002 Apr;82(2):503-68.

Jiang Q, Zheng S, Wang G. Development of new estrogen receptor-targeting therapeutic agents for tamoxifen-resistant breast cancer. *Future Med Chem*. 2013 Jun;5(9):1023-35.

Kadikoylu G, Bolaman Z, Demir S, Balkaya M, Akalin N, Enli Y. The effects of desferrioxamine on Cisplatin-induced lipid peroxidation and the activities of antioxidant enzymes in rat kidneys. *Hum Exp Toxicol*. 2004 Jan;23(1):29-34.

Kalayda GV, Wagner CH, Buss I, Reedijk J, Jaehde U. Altered localisation of the copper efflux transporters ATP7A and ATP7B associated with Cisplatin resistance in human ovarian carcinoma cells. *BMC Cancer*. 2008 Jun 19;8:175.

Kartalou M, Essigmann JM. Mechanisms of resistance to Cisplatin. *Mutat Res*. 2001 Jul 1;478(1-2):23-43.

Katano K, Kondo A, Safaei R, Holzer A, Samimi G, Mishima M, Kuo YM, Rochdi M, Howell SB. Acquisition of resistance to Cisplatin is accompanied by changes in the cellular pharmacology of copper. *Cancer Res*. 2002 Nov 15;62(22):6559-65.

Kelland L. The resurgence of platinum-based cancer chemotherapy. *Nat Rev Cancer*. 2007 Aug;7(8):573-84.

Kerr JF, Wyllie AH, Currie AR Apoptosis: a basic biological phenomenon with wide-ranging implications in tissue kinetics. *Br J Cancer*. 1972 Aug; 26(4):239-57.

Kim H.Y., Kim G.D., Kim H.J. The effect of Cisplatin on endoplasmic reticulum stress of human cervical cancer cells. *Korean J Obstet Gynecol*, 54 (2011), pp. 175–183

Kim L, Kimmel AR GSK3, a master switch regulating cell-fate specification and tumorigenesis. *Curr Opin Genet Dev*. 2000 Oct; 10(5):508-14.

Kim, S. D., Vrana, O., Kleinwachter, V., Niki, K. & Brabec, V. (1990) Polarographic determination of subnanogram quantities of free platinum in reaction mixture with DNA, Anal. Lett. 23, 1505-1518.

Koepsell H, Endou H. The SLC22 drug transporter family. *Pflugers Arch*. 2004 Feb;447(5):666-76. Epub 2003 Jul 19.

Korita P.V, T. Wakai, Y. Shirai, Y. Matsuda, J. Sakata, M. Takamura, M. Yano, A. Sanpei, Y. Aoyagi, K. Hatakeyama, Y. Ajioka Multidrug resistance-associated protein 2 determines the efficacy of Cisplatin in patients with hepatocellular carcinoma *Oncol. Rep*., 23 (2010), pp. 965–972

Kunkel TA, Erie DA DNA mismatch repair. *Annu Rev Biochem*. 2005; 74():681-710.

Kunzelmann K Ion channels and cancer. *J Membr Biol.* 2005 Jun;205(3):159-73.

Kunzmann AT, Coleman HG, Huang WY, Kitahara CM, Cantwell MM, Berndt SI. Dietary fiber intake and risk of colorectal cancer and incident and recurrent adenoma in the Prostate, Lung, Colorectal, and Ovarian Cancer Screening Trial. *Am J Clin Nutr.* 2015 Oct;102(4):881-90.

Kuroda T, Tsuchiya T. Multidrug efflux transporters in the MATE family. *Biochim Biophys Acta*. 2009 May;1794(5):763-8. doi: 10.1016/j.bbapap.2008.11.012.

Kuznetsova AY, Seget K, Moeller GK, de Pagter MS, de Roos JA, Dürrbaum M, Kuffer C, Müller S, Zaman GJ, Kloosterman WP, Storchová Z. Chromosomal instability, tolerance of mitotic errors and multidrug resistance are promoted by tetraploidization in human cells. *Cell Cycle*. 2015 Sep 2;14(17):2810-20.

Lang F Mechanisms and significance of cell volume regulation. *J Am Coll Nutr*. 2007 Oct;26(5 Suppl):613S-623S.

Lang F, Hoffmann EK. Role of ion transport in control of apoptotic cell death. *Compr Physio*l. 2012 Jul;2(3):2037-61.

Lang F, Föller M, Lang KS, Lang PA, Ritter M, Gulbins E, Vereninov A, Huber SM. Ion channels in cell proliferation and apoptotic cell death. *J Membr Biol*. 2005 Jun;205(3):147-57.

Largent JA, Bernstein L, Horn-Ross PL, Marshall SF, Neuhausen S, Reynolds P, Ursin G, Zell JA, Ziogas A, Anton-Culver H. Hypertension, antihypertensive medication use, and breast cancer risk in the California Teachers Study cohort. *Cancer Causes Control.* 2010 Oct;21(10):1615-24.

Larsen AP, Olesen SP, Grunnet M, Jespersen T. Characterization of hERG1a and hERG1b potassium channels-a possible role for hERG1b in the I (Kr) current. *Pflugers Arch.* 2008 Sep;456(6):1137-48.

Larsen AP, Olesen SP. Differential expression of hERG1 channel isoforms reproduces properties of native I(Kr) and modulates cardiac action potential characteristics. *PLoS One*. 2010 Feb 2;5(2):e9021.

Lastraioli E, Guasti L, Crociani O, Polvani S, Hofmann G, Witchel H *et al*. herg1 gene and HERG1 protein are overexpressed in colorectal cancers and regulate cell invasion of tumor cells. *Cancer Res* 2004; 64: 606–611.

Lastraioli, E.; Gasperi Campani, F.; Taddei, A.; Giani, I.; Messerini,L.; Comin, C.E.; Tomezzoli, A.; Saragoni, L.; Zoli, W.; Morgagni, P.; De Manzoni, G.; Bechi, P.; Arcangeli, A. hERG1 channels are overexpresed in human gastric cancer and their activity regulates cell proliferation: a novel prognostic and therapeutic target? In: Proc. 6th International Gastric Cancer Congress *IGCC*, 2005, 151.

Lastraioli E, Bencini L, Bianchini E, Romoli MR, Crociani O, Giommoni E, Messerini L, Gasperoni S, Moretti R, Di Costanzo F, Boni L, Arcangeli A. hERG1 Channels and Glut-1 as Independent Prognostic Indicators of Worse Outcome in Stage I and II Colorectal Cancer: A Pilot Study. *Transl Oncol*. 2012 Apr;5(2):105-12. Epub 2012 Apr 1.

Lawrence TS, Ten Haken RK, Giaccia A. Principles of Radiation Oncology. In: DeVita VT Jr., Lawrence TS, Rosenberg SA, editors. *Cancer: Principles and Practice of Oncology*. 8th ed. Philadelphia: Lippincott Williams and Wilkins, 2008.

Le MN, Chan JL, Rosenberg SA, Nabatian AS, Merrigan KT, Cohen-Solal KA, Goydos JS. The glutamate release inhibitor Riluzole decreases migration, invasion, and proliferation of melanoma cells. *J Invest Dermatol*. 2010 Sep;130(9):2240-9.

Lee EL, Hasegawa Y, Shimizu T, Okada Y. IK1 channel activity contributes to Cisplatin sensitivity of human epidermoid cancer cells. *Am J Physiol Cell Physiol*. 2008 Jun;294(6):C1398-406.

Lee JK, Delaney CP, Lipman JM. Current state of the art in laparoscopic colorectal surgery for cancer: Update on the multi-centric international trials. *Ann Surg Innov Res*. 2012;6:5

Lee SH, Hahn SJ, Min G, Kim J, Jo SH, Choe H, Choi BH. Inhibitory actions of HERG currents by the immunosuppressant drug cyclosporin a. *Korean J Physiol Pharmacol*. 2011 Oct;15(5):291-7.

Lee SH, Sung MJ, Lee HM, Chu D, Hahn SJ, Jo SH, Choe H, Choi BH. Blockade of HERG human K+ channels by the antidepressant drug paroxetine. *Biol Pharm Bull*. 2014;37(9):1495-504.

Liang XJ, Taylor B, Cardarelli C, Yin JJ, Annereau JP, Garfield S, Wincovitch S, Szakács G, Gottesman MM, Aszalos A. Different roles for K+ channels in Cisplatin-resistant cell lines argue against a critical role for these channels in Cisplatin resistance. *Anticancer Res*. 2005 Nov-Dec;25(6B):4113-22.

Lieberman DA, Rex DK, Winawer SJ, Giardiello FM, Johnson DA, Levin TR; United States Multi-Society Task Force on Colorectal Cancer. Guidelines for colonoscopy surveillance after screening and polypectomy: a consensus update by the US Multi-Society Task Force on Colorectal Cancer. *Gastroenterology*. 2012 Sep;143(3):844-57.

Lindström L, Lapidus A, Ost A, Bergquist A. Increased risk of colorectal cancer and dysplasia in patients with Crohn's colitis and primary sclerosing cholangitis. *Dis Colon Rectum.* 2011 Nov;54(11):1392-7.

Lipskaia, L. and Lompré, A. M. (2004): Alteration in temporal kinetics of Ca2+ signaling and control of growth and proliferation. *Biol. Cell,* 96, 55-68

Liu JJ, Lu J, McKeage MJ. Membrane transporters as determinants of the pharmacology of platinum anticancer drugs. *Curr Cancer Drug Targets*. 2012 Oct;12(8):962-86.

Longley DB, Harkin DP, Johnston PG. 5-fluorouracil: mechanisms of action and clinical strategies. *Nat Rev Cancer*. 2003 May;3(5):330-8.

Madoff RD. Defining quality in colon cancer surgery. *J Clin Oncol*. 2012;30:1738–1740

Maeno E, Ishizaki Y, Kanaseki T, Hazama A, Okada Y Normotonic cell shrinkage because of disordered volume regulation is an early prerequisite to apoptosis. *Proc Natl Acad Sci* U S A. 2000 Aug 15; 97(17):9487-92.

Mandic A, Viktorsson K, Varsanyi M, Hansson J, Linder S, Shoshan M. BAK, BAX and p53 proteins in the apoptotic response to Cisplatin. *Nat Genet*. 2001;27:86.

Manolopoulos VG, Liekens S, Koolwijk P, Voets T, Peters E, Droogmans G, Lelkes PI, De Clercq E, Nilius B. Inhibition of angiogenesis by blockers of volume-regulated anion channels. *Gen Pharmacol*. 2000 Feb;34(2):107-16.

Marcucci F, Bellone M, Rumio C, Corti A. Approaches to improve tumor accumulation and interactions between monoclonal antibodies and immune cells. *MAbs*. 2013 Jan-Feb;5(1):34-46

Marzo T, Pillozzi S, Hrabina O, Kasparkova J, Brabec V, Arcangeli A, Bartoli G, Severi M, Lunghi A, Totti F, Gabbiani C, Quiroga AG, Messori L. cis-Pt $I_2(NH_3)_2$: a reappraisal. *Dalton Trans*. 2015 Sep 7;44(33):14896-905.

Martinez-Ares D, Aguirre PA, López JY, Barrenechea IM, Cadilla JM, Martinez DR, Peral AP. Sensitivity of ultrasonography for gastric cancer diagnosis in symptomatic patients. *Dig Dis Sci*. 2009 Jun;54(6):1257-64.

Maheswari KU, Ramachandran T, Rajaji D. Interaction of Cisplatin with planar model membranes - dose dependent change in electrical characteristics. *Biochim Biophys Acta.* 2000 Feb 15;1463(2):230-40.

Masgras I., Carrera S., Verdier P.J. de, Brennan P., Majid A., Makhtar W., Reactive oxygen species and mitochondrial sensitivity to oxidative stress determine induction of cancer cell death by p21 *J Biol Chem*, 287 (2012), pp. 9845–9854

McNeil EM, Astell KR, Ritchie AM, Shave S, Houston DR, Bakrania P, Jones HM, Khurana P, Wallace C, Chapman T, Wear MA, Walkinshaw MD, Saxty B, Melton DW. Inhibition of the ERCC1-XPF structure-specific endonuclease to overcome cancer chemoresistance. *DNA Repair (Amst).* 2015 Jul;31:19-28.

Messori L, Casini A, Gabbiani C, Michelucci E, Cubo L, Ríos-Luci C, Padrón JM, Navarro-Ranninger C, Quiroga AG. Cytotoxic Profile and Peculiar Reactivity with Biomolecules of a Novel "Rule-Breaker" Iodidoplatinum(II) Complex. *ACS Med Chem Lett.* 2010 Jul 21;1(8):381-5.

Messori L, Cubo L, Gabbiani C, Álvarez-Valdés A, Michelucci E, Pieraccini G, Ríos-Luci C, León LG, Padrón JM, Navarro-Ranninger C, Casini A, Quiroga AG. Reactivity and biological properties of a series of cytotoxic PtI2(amine)2 complexes, either cis or trans configured. *Inorg Chem*. 2012 Feb 6;51(3):1717-26.

Messori L, Marzo T, Gabbiani C, Valdes AA, Quiroga AG, Merlino A. Peculiar features in the crystal structure of the adduct formed between cis-PtI2(NH3)2 and hen egg white lysozyme. *Inorg Chem*. 2013 Dec 16;52(24):13827-9.

Mezencev R. Interactions of Cisplatin with non-DNA targets and their influence on anticancer activity and drug toxicity: the complex world of the platinum complex. *Curr Cancer Drug Targets.* 2015;14(9):794-816.

Miquel C, Borrini F, Grandjouan S, Aupérin A, Viguier J, Velasco V, Duvillard P, Praz F, Sabourin JC: Role of bax mutations in apoptosis in colorectal cancers with microsatellite instability. *Am J Clin Pathol* 2005,23(4):562–570.

Mitri Z, Constantine T, O'Regan R. The HER2 Receptor in Breast Cancer: Pathophysiology, Clinical Use, and New Advances in Therapy. *Chemother Res Pract*. 2012;2012:743193.

Miyazaki T, Kato H, Faried A, Sohda M, Nakajima M, Fukai Y, Masuda N, Manda R, Fukuchi M, Ojima H, Tsukada K, Kuwano H Predictors of response to chemo-radiotherapy and radiotherapy for esophageal squamous cell carcinoma. *Anticancer Res*. 2005 Jul-Aug; 25(4):2749-55.

MM Center, A Jemal, RA Smith, E Ward Worldwide variations in colorectal cancer CA *Cancer J Clin*, 59 (2009), pp. 366–378

Monteith, G.R., McAndrew, D., Faddy, H.M. and Roberts-Thomson, S.J. (2007): Calcium and cancer: targeting Ca2+ transport. *Nat. Rev. Cancer*,7, 519-530.

Morais Cabral JH, Lee A, Cohen SL, Chait BT, Li M, Mackinnon R. Crystal structure and functional analysis of the HERG potassium channel N terminus: a eukaryotic PAS domain. *Cell.* 1998 Nov 25;95(5):649-55.

More SS, Akil O, Ianculescu AG, Geier EG, Lustig LR, Giacomini KM. Role of the copper transporter, CTR1, in platinum-induced ototoxicity. *J Neurosci*. 2010 Jul 14;30(28):9500-9.

Moriyama Y, Hiasa M, Matsumoto T, Omote H. Multidrug and toxic compound extrusion (MATE)-type proteins as anchor transporters for the excretion of metabolic waste products and xenobiotics. *Xenobiotica.* 2008 Jul;38(7-8):1107-18

Nafisi, S.; Norouzi, Z. A comparative study on the interaction of cis- and trans-platin with DNA and RNA. *DNA Cell Biol*., 2009, 28 (9), 469-477.

National Cancer Institute*:* PDQ® Genetics of Colorectal Cancer. Bethesda, MD: National Cancer Institute. Date last modified <07/06/2015>. Available at: http://www.cancer.gov/types/colorectal/hp/colorectal-genetics-pdq. Accessed <09/28/2015>.

Niemeyer B.A., Mery L., Zawar C., Suckow A., Monje F., Pardo L.A., Stuhmer W., Flockerzi V., Hoth M. Ion channels in health and disease. 83rd Boehringer Ingelheim Fonds International Titisee Conference. *EMBO Rep*., 2 (2001), pp. 568–573

Northcott PA, Dubuc AM, Pfister S, Taylor MD. Molecular subgroups of medulloblastoma. *Expert Rev Neurother*. 2012 Jul;12(7):871-84.

Ohishi Y, Oda Y, Uchiumi T, Kobayashi H, Hirakawa T, Miyamoto S, Kinukawa N, Nakano H, Kuwano M, Tsuneyoshi M. ATP-binding cassette superfamily transporter gene expression in human primary ovarian carcinoma. *Clin Cancer Res*. 2002 Dec;8(12):3767-75.

Oostindjer M, Alexander J, Amdam GV, Andersen G, Bryan NS, Chen D, Corpet DE, De Smet S, Dragsted LO, Haug A1, Karlsson AH, Kleter G, de Kok TM, Kulseng B, Milkowski AL, Martin RJ, Pajari AM, Paulsen JE, Pickova J, Rudi K, Sødring M, Weed DL, Egelandsdal B. The role of red and processed meat in colorectal cancer development: a perspective. *Meat Sci*. 2014 Aug;97(4):583-96.

Soyer P., Hamzi L., Sirol M., Duchat F., Dray X., Hristova L. Colon cancer: comprehensive evaluation with 64-section CT colonography using water enema as intraluminal contrast agent-a pictorial review *Clin. Imaging*, 36 (2012), pp. 113–125

Panayiotidis MI, Bortner CD, Cidlowski JA On the mechanism of ionic regulation of apoptosis: would the Na+/K+-ATPase please stand up? *Acta Physiol (Oxf)*. 2006 May-Jun;187(1-2):205-15.

Papadaki C, Sfakianaki M, Ioannidis G, Lagoudaki E, Trypaki M, Tryfonidis K, Mavroudis D, Stathopoulos E, Georgoulias V, Souglakos J. ERCC1 and BRAC1 mRNA expression levels in the primary tumor could predict the effectiveness of the second-line Cisplatin-based chemotherapy in pretreated patients with metastatic non-small cell lung cancer. *J Thorac Oncol.* 2012 Apr;7(4):663-71.

Papsai, P.; Snygg, A.S.; Aldag, J.; Elmroth, S.K. Platination of full length tRNA(Ala) and truncated versions of the acceptor stem and anticodon loop. *Dalton Trans*, 2008, (38), 5225-5234.

Pasetto LM, D'Andrea MR, Rossi E, Monfardini S (August 2006). "Oxaliplatin-related neurotoxicity: how and why?". Crit. Rev. *Oncol. Hematol*. 59 (2): 159–68.

Patt S, Preussat K, Beetz C, Kraft R, Schrey M, Kalff R, Schönherr K, Heinemann SH. Expression of ether à go-go potassium channels in human gliomas. *Neurosci Lett.* 2004 Sep 30;368(3):249-53.

Pedersen SF, Kapus A, Hoffmann EK. Osmosensory mechanisms in cellular and systemic volume regulation. *J Am Soc Nephrol*. 2011 Sep; 22(9):1587-97.

Pegram MD, Pauletti G, Slamon DJ. HER-2/neu as a predictive marker of response to breast cancer therapy. *Breast Cancer Res Treat*. 1998;52(1-3):65-77.

Peretti M, Angelini M, Savalli N, Florio T, Yuspa SH, Mazzanti M. Chloride channels in cancer: Focus on chloride intracellular channel 1 and 4 (CLIC1 AND CLIC4) proteins in tumor development and as novel therapeutic targets. *Biochim Biophys Acta.* 2015 Oct;1848(10 Pt B):2523-31.

Pillozzi S, Brizzi MF, Balzi M, Crociani O, Cherubini A, Guasti L, Bartolozzi B, Becchetti A, Wanke E, Bernabei PA, Olivotto M, Pegoraro L, Arcangeli A. HERG potassium channels are constitutively expressed in primary human acute myeloid

leukemias and regulate cell proliferation of normal and leukemic hemopoietic progenitors. *Leukemia.* 2002 Sep;16(9):1791-8.

Pillozzi S, Brizzi MF, Bernabei PA, Bartolozzi B, Caporale R, Basile V *et al*. VEGFR-1 (FLT-1), beta1 integrin, and hERG K+ channel for a macromolecular signaling complex in acute myeloid leukemia: role in cell migration and clinical outcome. *Blood* 2007; 110: 1238–1250.

Pillozzi S, Masselli M, De Lorenzo E, Accordi B, Cilia E, Crociani O, Amedei A, Veltroni M, D'Amico M, Basso G, Becchetti A, Campana D, Arcangeli A. Chemotherapy resistance in acute lymphoblastic leukemia requires hERG1 channels and is overcome by hERG1 blockers. *Blood.* 2011 Jan 20;117(3):902-14.

Planells-Cases R, Lutter D, Guyader C, Gerhards NM, Ullrich F, Elger DA, Kucukosmanoglu A, Xu G, Voss FK, Reincke SM, Stauber T, Blomen VA, Vis DJ6 Wessels LF, Brummelkamp TR, Borst P, Rottenberg S, Jentsch TJ. Subunit composition of VRAC channels determines substrate specificity and cellular resistance to Pt-based anti-cancer drugs. *EMBO J.* 2015 Dec 14;34(24):2993-3008.

Poulsen KA, Andersen EC, Hansen CF, Klausen TK, Hougaard C, Lambert IH, Hoffmann EK. Deregulation of apoptotic volume decrease and ionic movements in multidrug-resistant tumor cells: role of chloride channels. *Am J Physiol Cell Physiol*. 2010 Jan;298(1):C14-25.

Prevarskaya N, Ouadid-Ahidouch H, Skryma R, Shuba Y. Remodelling of Ca2+ transport in cancer: how it contributes to cancer hallmarks? *Philos Trans R Soc Lond B Biol Sci.* 2014 Feb 3;369(1638):20130097. doi: 10.1098/rstb.2013.0097. Print 2014 Mar 19.

Prevarskaya N, Skryma R, Shuba Y Ion channels and the hallmarks of cancer. *Trends Mol Med.*2010 Mar; 16(3):107-21.

Qu Y, Xia P, Zhang S, Pan S, Zhao J. Silencing XIAP suppresses osteosarcoma cell growth, and enhances the sensitivity of osteosarcoma cells to doxorubicin and Cisplatin. *Oncol Rep*. 2015 Mar;33(3):1177-84.

Rabjerg M, Oliván-Viguera A, Hansen LK, Jensen L1, Sevelsted-Møller L, Walter S, Jensen BL, Marcussen N, Köhler R. High expression of KCa3.1 in patients with clear cell renal carcinoma predicts high metastatic risk and poor survival. *PLoS One*. 2015 Apr 7;10(4):e0122992.

Radtke J, Schmidt K, Wulff H, Köhler R, de Wit C. Activation of KCa3.1 by SKA-31 induces arteriolar dilatation and lowers blood pressure in normo- and hypertensive connexin40-deficient mice. *Br J Pharmacol*. 2013 Sep;170(2):293-303.

Ragnhammar P, Hafström L, Nygren P, Glimelius B; SBU-group. Swedish Council of Technology Assessment in Health Care. (2001)

Ridereau-Zins C. Imaging in colonic cancer Diagn. Interv. Imaging, 95 (2014), pp. 475–483

Ro TH, Mathew MA, Misra S. Value of screening endoscopy in evaluation of esophageal, gastric and colon cancers. *World J Gastroenterol*. 2015 Sep 7;21(33):9693-706.

Robbins & Cotran Pathologic Basis of Disease, 9th Edition By Vinay Kumar, MBBS, MD, FRCPath, Abul K. Abbas, MBBS and Jon C. Aster, MD, PhD Saunders;

Robbins CM, Tembe WA, Baker A, Sinari S, Moses TY, Beckstrom-Sternberg S, Beckstrom-Sternberg J, Barrett M, Long J, Chinnaiyan A, Lowey J, Suh E, Pearson JV, Craig DW, Agus DB, Pienta KJ, Carpten JD Copy number and targeted mutational analysis reveals novel somatic events in metastatic prostate tumors. *Genome Res*. 2011 Jan; 21(1):47-55.

Roderick HL, Cook SJ Ca2+ signalling checkpoints in cancer: remodelling Ca^{2+} for cancer cell proliferation and survival. *Nat Rev Cancer*. 2008 May; 8(5):361-75.

Roy J, Vantol B, Cowley EA, Blay J, Linsdell P. Pharmacological separation of hEAG and hERG K+ channel function in the human mammary carcinoma cell line MCF-7. *Oncol Rep*. 2008 Jun;19(6):1511-6.

Russo A, Bazan V, Iacopetta B, Kerr D, Soussi T, Gebbia N. The TP53 colorectal cancer international collaborative study on the prognostic and predictive significance of p53 mutation: influence of tumor site, type of mutation, and adjuvant treatment. *J Clin Oncol*. 2005;23:7518–7528.

Ryan KM, Phillips AC, Vousden KH. Regulation and function of the p53 tumor suppressor protein. *Curr Opin Cell Biol*. 2001;13:332–337.

Rybalchenko V, Prevarskaya N, Van Coppenolle F, Legrand G, Lemonnier L, Le Bourhis X, Skryma R. Verapamil inhibits proliferation of LNCaP human prostate cancer cells influencing K+ channel gating. *Mol Pharmacol*. 2001 Jun;59(6):1376-87.

Samuels Y, Wang Z, Bardelli A, Silliman N, Ptak J, Szabo S, Yan H, Gazdar A, Powell SM, Riggins GJ, Willson JK, Markowitz S, Kinzler KW, Vogelstein B, Velculescu VE High frequency of mutations of the PIK3CA gene in human cancers. *Science*. 2004 Apr 23; 304(5670):554.

Sancho-Martínez SM, Prieto-García L, Prieto M, López-Novoa JM, López-Hernández FJ Subcellular targets of Cisplatin cytotoxicity: an integrated view. *Pharmacol Ther*. 2012 Oct; 136(1):35-55.

Sanguinetti MC, Tristani-Firouzi M (March 2006). "hERG potassium channels and cardiac arrhythmia". *Nature* 440 (7083): 463–9.

Sankaranarayanan A, Raman G, Busch C, Schultz T, Zimin PI, Hoyer J, Köhler R, Wulff H. Naphtho[1,2-d]thiazol-2-ylamine (SKA-31), a new activator of KCa2 and KCa3.1 potassium channels, potentiates the endothelium-derived hyperpolarizing factor response and lowers blood pressure. *Mol Pharmacol*. 2009 Feb;75(2):281-95. doi: 10.1124/mol.108.051425.

Santin AD, Bellone S, Roman JJ, McKenney JK, Pecorelli S Trastuzumab treatment in patients with advanced or recurrent endometrial carcinoma overexpressing HER2/neu. *Int J Gynaecol Obstet*. 2008 Aug;102(2):128-31.

Sawers L, Ferguson MJ, Ihrig BR, Young HC, Chakravarty P, Wolf CR, Smith G. Glutathione S-transferase P1 (GSTP1) directly influences platinum drug chemosensitivity in ovarian tumour cell lines. *Br J Cancer*. 2014 Sep 9;111(6):1150-8. doi: 10.1038/bjc.2014.386.

Scata KA, El-Deiry WS. p53, BRCA1 and breast Cancer chemoresistance. *Adv Exp Med Biol*. 2007;608:70-86.

Schindler AE Long-term use of progestogens: colon adenoma and colon carcinoma. *Gynecol Endocrinol*. 2007 Oct;23 Suppl 1:42-4.

Servais H., Ortiz A., Devuyst O., Denamur S., Tulkens P.M., Mingeot-Leclercq M.P. Renal cell apoptosis induced by nephrotoxic drugs: cellular and molecular mechanisms and potential approaches to modulation *Apoptosis,* 13 (2008), pp. 11–32

Sharaf el dein O, Gallerne C, Brenner C, Lemaire C. Increased expression of VDAC1 sensitizes carcinoma cells to apoptosis induced by DNA cross-linking agents. *Biochem Pharmacol*. 2012 May 1;83(9):1172-82.

Shi S, Chen L, Huang G. Antiangiogenic therapy improves the antitumor effect of adoptive cell immunotherapy by normalizing tumor vasculature. *Med Oncol*. 2013;30:698

Shi X, Wu S, Yang Y, Tang L, Wang Y, Dong J, Lü B, Jiang G, Zhao W. AQP5 silencing suppresses p38 MAPK signaling and improves drug resistance in colon cancer cells. *Tumour Biol*. 2014 Jul;35(7):7035-45.

Shimizu T, Numata T, Okada Y. A role of reactive oxygen species in apoptotic activation of volume-sensitive Cl(-) channel. *Proc Natl Acad Sci U S A.* 2004 Apr 27;101(17):6770-3. Epub 2004 Apr 19.

Shimizu T, Lee EL, Ise T, Okada Y. Volume-sensitive Cl(-) channel as a regulator of acquired Cisplatin resistance. *Anticancer Res. 2008* Jan-Feb;28(1A):75-83.

Sibileau E., Ridereau-Zins C., Vanel D., Pavageau A.H., Bertrais S., Metivier-Cesbron E. Accuracy of water-enema multidetector computed tomography (WE-MDCT) in colon cancer staging: a prospective study *Abdom.* Imaging, 39 (2014), pp. 941–948

Siddik ZH Cisplatin: mode of cytotoxic action and molecular basis of resistance. *Oncogene.* 2003 Oct 20;22(47):7265-79.

Smith GA, Tsui HW, Newell EW, Jiang X, Zhu XP, Tsui FW, Schlichter LC. Functional up-regulation of HERG K+ channels in neoplastic hematopoietic cells. *J Biol Chem.* 2002 May 24;277(21):18528-34. Epub 2002 Mar 13.

Smith J, Tho LM, Xu N, Gillespie DA The ATM-Chk2 and ATR-Chk1 pathways in DNA damage signaling and cancer. *Adv Cancer Res*. 2010; 108():73-112.

Spitzner M, Ousingsawat J, Scheidt K, Kunzelmann K, Schreiber R. Voltage-gated K+ channels support proliferation of colonic carcinoma cells. *FASEB J*. 2007 Jan;21(1):35-44. Epub 2006 Nov 29.

Splettstoesser F1, Florea AM, Büsselberg D. IP(3) receptor antagonist, 2-APB, attenuates Cisplatin induced Ca2+-influx in HeLa-S3 cells and prevents activation of calpain and induction of apoptosis. *Br J Pharmacol*. 2007 Aug;151(8):1176-86. Epub 2007 Jun 25.

Spreckelmeyer S, Orvig C, Casini A. Cellular transport mechanisms of cytotoxic metallodrugs: an overview beyond Cisplatin. *Molecules.* 2014 Sep 29;19(10):15584-610.

Srivastava R.C. Froehlich J., Eichhorn G. L. (1978): The effect of platinum binding on the structure of DNA and its functionin RNA synthesis. *Biochimie* 60, 879—891

Strøbaek D, Teuber L, Jørgensen TD, Ahring PK, Kjaer K, Hansen RS, Olesen SP, Christophersen P, Skaaning-Jensen B. Activation of human IK and SK Ca2+ -activated K+ channels by NS309 (6,7-dichloro-1H-indole-2,3-dione 3-oxime). *Biochim Biophys Acta*. 2004 Oct 11;1665(1-2):1-5.

Tajeddine N, Galluzzi L, Kepp O, Hangen E, Morselli E, Senovilla L, Araujo N, Pinna G, Larochette N, Zamzami N, Modjtahedi N, Harel-Bellan A, Kroemer G Hierarchical involvement of Bak, VDAC1 and Bax in Cisplatin-induced cell death. *Oncogene*. 2008 Jul 10; 27(30):4221-32.

Tamburro AM, Celotti L, Furlan D, Guantieri V. Interaction of Pt(II) complexes with DNAs from various sources. A circular dichroism study. *Chem Biol Interact*. 1977 Jan;16(1):1-11.

Torkzad M.R., Kamel I., Halappa V.G., Beets-Tan R.G. Magnetic resonance imaging of rectal and anal cancer *Magn. Reson. Imaging Clin*. N. Am., 22 (2014), pp. 85–112

Trigueros-Motos L, Pérez-Torras S, Casado FJ, Molina-Arcas M, Pastor-Anglada M. Aquaporin 3 (AQP3) participates in the cytotoxic response to nucleoside-derived drugs. *BMC Cancer*. 2012 Sep 27;12:434.

Tsang RY, Al-Fayea T, Au HJ. Cisplatin overdose: toxicities and management. *Drug Saf.* 2009;32(12):1109-22.

Turner KL, Honasoge A, Robert SM, McFerrin MM, Sontheimer H. A proinvasive role for the Ca(2+) -activated K(+) channel KCa3.1 in malignant glioma. *Glia.* 2014 Jun;62(6):971-81.

Van Petegem F, Minor DL Jr. The structural biology of voltage-gated calcium channel function and regulation. *Biochem Soc Trans.* 2006 Nov;34(Pt 5):887-93.

Videira M, Reis RL, Brito MA Deconstructing breast cancer cell biology and the mechanisms of multidrug resistance. *Biochim Biophys Acta*. 2014 Dec;1846(2):312-25. doi: 10.1016/j.bbcan.2014.07.011.

Viet CT, Dang D, Achdjian S, Ye Y, Katz SG, Schmidt BL. Decitabine rescues Cisplatin resistance in head and neck squamous cell carcinoma. *PLoS One.* 2014 Nov 12;9(11):e112880.

Vogel CL, Cobleigh MA, Tripathy D, Gutheil JC, Harris LN, Fehrenbacher L, Slamon DJ, Murphy M, Novotny WF, Burchmore M, Shak S, Stewart SJ, Press M. Efficacy and safety of trastuzumab as a single agent in first-line treatment of HER2-overexpressing metastatic breast cancer. *J Clin Oncol*. 2002 Feb 1;20(3):719-26.

Wang D, Lippard SJ. Cellular processing of platinum anticancer drugs. *Nat Rev Drug Discov*. 2005 Apr;4(4):307-20.

Wang Y, Li G, Hu F, Bi H, Wu Z, Zhao X, Li Y, Li S, Li D, Cui B, Dong X, Zhao Y. The prognostic significance of polymorphisms in hMLH1/hMSH2 for colorectal cancer. *Med Oncol*. 2014 Jun;31(6):975

Wang Y, Duan H, Yang H, Lin J. A pooled analysis of alcohol intake and colorectal cancer. *Int J Clin Exp Med*. 2015 May 15;8(5):6878-89. eCollection 2015.

West NP, Hohenberger W, Weber K, Perrakis A, Finan PJ, Quirke P. Complete mesocolic excision with central vascular ligation produces an oncologically superior specimen compared with standard surgery for carcinoma of the colon. *J Clin Oncol*. 2010;28:272–278.

Wheate NJ, Walker S, Craig GE, Oun R. The status of platinum anticancer drugs in the clinic and in clinical trials. *Dalton Trans*. 2010 Sep 21;39(35):8113-27.

Wilson JJ, Lippard SJ. Synthetic methods for the preparation of platinum anticancer complexes. *Chem Rev*. 2014 Apr 23;114(8):4470-95.

World Health Organization *World Cancer Report 2014*. International Agency for Research on Cancer, 2014.

Wulff H, Kolski-Andreaco A, Sankaranarayanan A, Sabatier JM, Shakkottai V. Modulators of small- and intermediate-conductance calcium-activated potassium channels and their therapeutic indications. *Curr Med Chem*. 2007;14(13):1437-57.

Xiao X, Melton DW, Gourley C. Mismatch repair deficiency in ovarian cancer -- molecular characteristics and clinical implications. *Gynecol Oncol*. 2014 Feb;132(2):506-12.

Xuejun C, Weimin C, Xiaoyan D, Wei Z, Qiong Z, Jianhua Y. Effects of aquaporins on chemosensitivity to Cisplatin in ovarian cancer cells. *Arch Gynecol Obstet*. 2014 Sep;290(3):525-32.

Yang H, Li G, Li WF. Association between ERCC1 and XPF polymorphisms and risk of colorectal cancer. *Genet Mol Res*. 2015 Jan 30;14(1):700-5.

Yokoo S, Yonezawa A, Masuda S, Fukatsu A, Katsura T, Inui K. Differential contribution of organic cation transporters, OCT2 and MATE1, in platinum agent-induced nephrotoxicity. *Biochem Pharmacol*. 2007 Aug 1;74(3):477-87.

Yonezawa A, Masuda S, Yokoo S, Katsura T, Inui K. Cisplatin and oxaliplatin, but not carboplatin and nedaplatin, are substrates for human organic cation transporters (SLC22A1-3 and multidrug and toxin extrusion family). *J Pharmacol Exp Ther*. 2006 Nov;319(2):879-86.

Yousef M.I., Saad A.A., El-Shennawy L.K.. Protective effect of grape seed proanthocyanidin extract against oxidative stress induced by Cisplatin in rats *Food Chem*. Toxicol., 47 (2009), pp. 1176–1183

Yu H, Su J, Xu Y, Kang J, Li H, Zhang L, Yi H, Xiang X, Liu F, Sun L p62/SQSTM1 involved in Cisplatin resistance in human ovarian cancer cells by clearing ubiquitinated proteins. *Eur J Cancer*. 2011 Jul; 47(10):1585-94.

Yuan S., Yu X., Topf M., Ludtke S.J., Wang X., Akey C.W. Structure of an apoptosome–procaspase-9 CARD complex *Structure*, 18 (2010), pp. 571–583

Zhang H, Li H, Yang L, Deng Z, Luo H, Ye D, Bai Z, Zhu L, Ye W, Wang L, Chen L. The ClC-3 chloride channel associated with microtubules is a target of paclitaxel in its induced-apoptosis. *Sci Rep*. 2013;3:2615.

Zhang R, Tian P, Chi Q, Wang J, Wang Y, Sun L, Liu Y, Tian S, Zhang Q. Human ether-à-go-go-related gene expression is essential for Cisplatin to induce apoptosis in human gastric cancer. *Oncol Rep*. 2012 Feb;27(2):433-40.

Zhang WM, Zhou J, Ye QJ. Endothelin-1 enhances proliferation of lung cancer cells by increasing intracellular free Ca^{2+}. *Life Sci.* 2008 Mar 26;82(13-14):764-71.

Zhou XP, Loukola A, Salovaara R, Nystrom-Lahti M, Peltomäki P, de la Chapelle A, Aaltonen LA, Eng C. PTEN mutational spectra, expression levels, and subcellular localization in microsatellite stable and unstable colorectal cancers. *Am J Pathol.* 2002 Aug; 161(2):439-47.

Zimmermann, T., Chval, Z., Burda, J.V. Cisplatin interaction with cysteine and methionine in aqueous solution: computational DFT/PCM study. J Phys Chem B, 2009, 113 (10), 3139-3150.